# Chemical Biological Studies on the Regulatory Mechanism of Tumor Cell Migration

March 2013

Shigeyuki Magi

# 主　論　文　要　旨

| 報告番号 | ㊙ 乙 第　　号 | 氏 名 | 間木 重行 |
|---|---|---|---|

主 論 文 題 目 :

Chemical Biological Studies on the Regulatory Mechanism of Tumor Cell Migration

（ケミカルバイオロジー研究によるがん細胞遊走制御機構の解析）

（内容の要旨）

ある表現型を特異的に生み出す低分子化合物や、ある特定の分子を阻害する化合物を利用することで生物学的な新たな知見が得られるケミカルバイオロジー研究は、様々な生命現象を理解するにあたり非常に有用な手法である。一方、細胞遊走とは細胞が能動的に移動する現象であり、がん治療の大きな障害となっているがん転移に必須の生命現象である。本学位論文研究では、ケミカルバイオロジーの手法にもとづいてがん細胞の遊走制御機構を解析することで、その制御機構の一端を明らかにした。

１．新規アクラシノマイシン(ACM)誘導体が誘導する H-Ras のファルネシル化阻害を介した細胞遊走の阻害効果

抗がん剤として知られる ACM の新規誘導体 N-benzyl-ACM および N-allyl-ACM は、*in vitro* のスクリーニング系においてファルネシルトランスフェラーゼ(FTase)の阻害活性を持つことが見出された。これら２化合物は、FTase の類似酵素であるゲラニルゲラニルトランスフェラーゼや、ゲラニルゲラニル二リン酸合成酵素に殆ど影響を与えなかった。また、両化合物はヒト扁平上皮がん A431 細胞において H-Ras の細胞膜への移行、H-Ras 依存的な PI3K/Akt シグナルの活性化、EGF 依存的細胞遊走の全てを阻害することを見出した。

２．ケミカルシステムバイオロジーによるがん細胞遊走制御機構の普遍性および多様性の解析

細胞遊走制御機構の普遍性および多様性を担う分子群を明らかにするため、34 種類の低分子化合物の影響を、10 種類の遊走細胞において創傷治癒アッセイにより定量的に評価した。続いて、各細胞における化合物の遊走阻害プロファイルに対して階層的クラスタリングを行った。その結果、化合物は階層的クラスタリングによってそれらの標的分子にもとづいて的確に分類された。さらに、本研究で用いたがん細胞は 3 つのクラスターに分類され、化合物は 4 つのクラスターにグループ分けされた。JNK 阻害剤はすべてのタイプの細胞遊走を抑制したが、ROCK、GSK-3、p38MAPK の阻害剤は、一部の細胞株の遊走のみを抑制した。このように、本解析システムによって、細胞遊走に対する共通なシグナル応答と細胞型特異的なシグナル応答を容易に区別することに成功した。続いて、前述のケミカルゲノミクス研究で明らかになった細胞遊走制御機構の普遍性および多様性を担う分子群のパスウェイ関係を明らかにするため、EGF 刺激依存的に遊走する 3 種類のがん細胞株において、EGF が誘導する 9 種類の情報伝達分子のリン酸化および発現上昇に対して、15 種類の細胞遊走阻害剤が与える影響を網羅的かつ定量的に評価した。続いて得られたデータをもとに、各がん細胞株における EGF 依存的細胞遊走を制御するシグナル伝達図を描画した。その結果、MAPK 経路や JNK/cJun 経路などは 3 細胞において普遍的であるが、他の多くのパスウェイが各細胞に特徴的に存在することが示唆された。特に、CysLT1 経路が TT 細胞では MAPK 経路を制御するが、EC109 細胞では PI3K/Akt 経路のみを制御するという結果は、これまでの研究からは予期出来ない興味深い結果であった。即ち、CysLT1 経路は EGF が引き起こすがん細胞遊走制御機構において細胞依存的なシグナル伝達を制御する分子であることが見出された。

# SUMMARY OF Ph.D. DISSERTATION

| School | Student Identification Number | SURNAME, First name |
|---|---|---|
| Science and Technology | 80947574 | MAGI, Shigeyuki |

Title

Chemical Biological Studies on the Regulatory Mechanism of Tumor Cell Migration


Abstract

Chemical biology is a remarkable approach in which small molecular compounds are used as probes to elucidate protein functions within signaling pathways. On the other hand, tumor cell migration is a required step for cancer metastasis which remains the greatest obstacle for anti-cancer therapy. In this thesis, the author researched the regulatory mechanism of tumor cell migration based on chemical biological approach.

1. **Novel Aclacinomycin A (ACM) derivatives suppressed tumor cell migration through the inhibition of the farnesylation of H-Ras.** N-benzyl-ACM and N-allyl-ACM, which are new derivatives of ACM, were identified as farnesyl transferase (FTase) inhibitors. There two compounds inhibited FTase activity specifically rather than geranylgeranyl transferase or geranylgeranyl pyrophosphate synthase. In addition, both compounds also blocked the membrane localization of H-Ras, activation of the H-Ras-dependent PI3K/Akt pathway, as well as epidermal growth factor (EGF)-induced migration of epidermal carcinoma A431 cells.

**2. A combination study of chemical and systems biology identifying novel features of signaling pathway in cancer cell migration.** To analyze the diversity and consistency of regulatory signaling in cancer cell migration, the author assessed quantitatively the effects of 34 small molecular compounds on ten types of migrating cells by wound healing assay. Hierarchical clustering was performed on the subsequent migration inhibition profile of the compounds and cancer cell types. The author found that the cancer cells tested in this study were classified into three clusters, and the compounds were grouped into four clusters. An inhibitor of JNK suppressed all types of cell migration; however, inhibitors of ROCK, GSK-3 and p38MAPK only inhibited the migration of a subset of cell lines. Next, to explore the diversity and consistency of EGF-induced cell migration pathway, the author quantified the effect of the 15 inhibitors on the levels of expression or phosphorylation of nine proteins induced by EGF stimulation in three cancer cell lines. Based on obtained data and chemical biological assumptions, the author deduced cell migration pathway in each cancer cell, and compared them. As a result, the author found that MEK/ERK-, and JNK/c-Jun-pathway are activated in migrating all three cells. Moreover, CysLT1 was found to regulate only MEK/ERK pathway in T.T cells, whereas it regulates only PI3K/Akt pathway in EC109 cells. These results indicate that the CysLT1 signaling is related to the diversity of regulatory mechanisms in cancer cells.

A Thesis for the Degree of Ph.D. in Science

# Chemical Biological Studies on the Regulatory Mechanism of Tumor Cell Migration

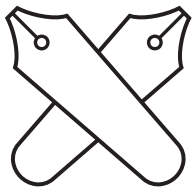

March 2013

Graduate School of Science and Technology
Keio University

Shigeyuki Magi

# Contents

**1 General Introduction** **1**

**2 Novel derivatives of aclacinomycin A block cancer cell migration through inhibition of farnesyl transferase** **10**

2.1 Introcudtion . . . . . 10

2.2 Results and Discussion . . . . . 11

2.3 Experimental Procedures . . . . . 19

**3 A chemical genomic study identifying diversity in cell migration signaling in cancer cells** **35**

3.1 Introduction . . . . . 35

3.2 Results . . . . . 38

3.3 Discussion . . . . . 51

3.4 Experimental Procedures . . . . . 58

**4 A combination study of chemical and systems biology identifying novel**

**features of signaling pathway in cancer cell migration** **63**

4.1 Introduction . . . . . 63

4.2 Results . . . . . 65

4.3 Discussion . . . . . 81

4.4 Experimental Procedures . . . . . 89

**5 Conclusion** **92**

**References** **98**

**Acknowledgement** **108**

# Chapter 1

# General Introduction

## The history of cancer research

In the latter half of the 20th century, biology has advanced rapidly, and many responsible genes of life-threatening diseases were uncovered. Particularly, a lot of oncogenes and proto-oncogenes have been identified. An oncogene is a gene that contributes to converting a normal cell into a cancer cell when it mutated or overexpressed. The first oncogene was discovered in 1979 and was named *Src* by Dr. Bishop and Dr. Varmus[1]. It is a family of tyrosine-specific protein kinase, that associates with the cytoplasmic face of the plasma membrane. *Src* mediates cell migration and proliferation through various signal-transducting proteins. Also, one of the most classic oncogene includes *Ras*, which was defined in 1982[2–4]. It is

a family of small GTPase that is known as regulator of signal transduction. Activation of Ras signaling causes cell growth, differentiation, and survival through several pathways, such as mitogen-activated protein kinase (MAPK) cascade. *Ras* gene mutations are found in 20% to 30% of all human tumors[5]. As oncogenes were uncovered gradually, it was considered that oncogenes could be potential targets for cancer chemotherapy. Some of the oncogene-targeted durgs have been depeloped, and are going on the market. For example, Herceptin® (Trastuzumab, Roche), an anti-HER2 monoclonal antibody which has efficacy only in HER2-positive tumors, and Greevec® (Imatinib, Novartis), a small molecule inhibitor of the non-receptor tyrosine kinase of BCR/ABL which takes effect for chronic myeloid leukaemia, are currently known as the major powerful anticancer drugs.

## Cancer metastasis and cell migration

However, infallible medical treatment against all types of cancer was not still established, possibly, at least in part, due to cancer metastasis. Metastases are the major cause of death from cancer, and are the biggest obstacles to treatment. Even now, the doctors cannot trace the process of metastasizing tumor in clinical practice, though some kind of *in vivo* experiments for metastasis are well established. The biological cascade of metastasis is understood as following[6–8]:

A) loss of cellular adhesion

B) increased migratory capacity and invasiveness

C) entry and survival in the circulation

D) exit into new tissue

E) eventual colonization of distant site

Especially, cell migration which is a required step for B), C) and D) have widely attracted attention as a central process in cancer metastasis. Cell migration involoves dynamic morphological change. At the beginning, actin polymerization are caused at leading edge, and cells acquire a spatial asymmetry. Subsequently, extended cellular membrane attaches to extra cellular matrix (ECM), and formed focal adhesion (FA). Then, actin stress fiber bridges between FA at front and at rear, which provides contractile forces. By myosin ATPase activity, cytoplasm is contracted and cells are moved forward. Finally, rear attachments are released. In this way, cell migration is commonly believed to repeat these morphological processes[9]. Cell migration is induced by various extracellular stimuli, such as growth factors and chemokines. These molecules bind and activate each specific receptors, which activate small GTPase proteins locally. The local activation of Rac1 and/or Cdc42, in concert with other regulators such as WAVE/WASP family proteins and the arp2/3 complex, stimulates the formation of a branching actin filament network at the leading edge, which in tern induces a protrusion in the

direction of migration[6].

Recent investigations for migration have demonstrated core elements of regulatory mechanism, but little is known about precise details. In addition, regulatory mechanisms of cancer cells migration are more diverse and complicated than normal cells because of accumulation of genetic mutations. Therefore, tissue or cell line specific analysis on regulatory mechanism for cancer cell migration is required for an anti-metastatic therapy.

## Rapid progress of systems biology

From year 2000 onwards, systems biology has developed as a new approach for the systems-level understanding of biology. Systems biology requires to understand four key properties: system structures, system dynamics, the control method, and the design method[10]. At present most of system biologist in basic science have mainly focused on the first two properties.

System structures is variously categorised in terms of metabolic pathways, gene regulatory networks, protein interactions, and signaling pathways. The conventional methods for creating the pathway map fall into two broad approaches. One is conducting extensive literature surveys, and the other is performing molecular biological experiments. The former approach is to integrate the information

about interactions of biological molecules using text data mining. Many of preceding studies are based on this method[11–13]. On the latter approach, microarray and yeast two-hybrid system are usually used[14–16]. The studies on biological system structures are largely analysed on the basis of the clustering, network motif, and topology[17,18]. Now, several type of databases that aim to integrate pathway structures, such as KEGG[19] (www.genome.jp/kegg/), Reactome[20] (www.reactome.org/), are available.

The researches on system dynamics requires creating its model. The first quantitative modeling system of cellular metabolism is E-Cell, published in 1999[21]. This system can simulate cell behavior by integrating the ordinary differential equations described in these reaction rules. Several mathematical models of cellular signaling pathways have been constructed about a few years ago[22,23]. In addition, a study of cell migration using time-series measurements of DNA microarray data and network analysis is made in public[24]. In this way, systems biology is used for various study regions, and the utility of systems biology has begun to be recognized.

Systems-biological approach also has been applied to cancer research. For example, the B-cell interactome, a genome-wide compendium of human B-cell molecular interactions cellular network is used in the study for B-cell lymphoma[25]. This study reveals genes whose function within the cellular network of gene

products in a given B-cell lymphoma phenotype is significantly altered. In another case, prognostic markers for the pattern of metastatic breast cancer is identified[26]. This study is based on the quantitative methodology consist of a statical analysis. It clarifies several subnetworks that can provide as markers to distinguish between metastatic and non-metastatic cancer.

## Chemical biology meets systems biology

Chemical biology has been advocated during the past few decades by Prof. Schreiber. He revealed that immunosuppresant FK506 forms a complex with novel protein FKBP12 (FK506 binding protein 12), and the complex suppresses immune systems on the molecular level[27]. Afterwards, various biological active compounds have been discovered or synthesized, and new biological molecules involved intracellular signaling have been identified. These compounds have been used to identify biological systems as small molecule inhibitors which can mimic loss-of-function. Small molecule inhibitors act more quickly than RNA interference. RNA interference involves the time delay between siRNA transfection and protein repression[28], but the most of small-molecule inhibitors react to target protein on a time scale of anything between a few seconds to a couple of minutes. In addition, the inhibitory effects of small molecule are often tunable

and reversible by controlling the dose of molecule and the duration of activity. Thus, small molecule inhibitor can become a powerful tool for real-time analysis of dynamic biological systems.

Recent years, chemical biology and systems biology have begun to intersect. The disciplines of chemical biology and systems biology encompass a great deal of progressive, cutting-edge science[29]. Chemical biological approach for understanding entire biological systems will lead to new exciting knowledge. For example, *Hughes et al.* conducted gene expression profiling to functionally characterize 300 genetic mutations and small molecules in yeast[30]. *Lamb et al.* extended this work to mammalian cells and constructed a 'Connectivity map' based on gene expression profiles and pattern matching analysis following small molecule treatment. The Connectivity map is a useful resource to classify drugs with common mechanisms of action, discover novel mode-of-action of compounds, and find small molecules that mimic or suppress a disease state[31]. These approach have (i) expanded the number of pathways that can be probed with small molecules, (ii) allowed for a more comprehensive understanding of how compounds alter larger networks of pathways by generating phenotypic profiles based on these changes, and (iii) enabled compound clustering to shed light on new mechanisms of action, including identifying the target proteins of previously uncharacterized compounds. Not only is the 'chemical systems biology' approach applied to

the research for gene expression, but it has also applied to phosphoproteomics. *Pan et al.* performed global phosphoproteomics to analyse the effects of U0126, a MEK1/2 inhibitor, and SB202190, a p38$\alpha$ inhibitor, on EGFR signaling in HeLa cells[32]. In this way, the combination of chemical genetics and system biology is a powerful and unbiased strategy for discovering biological network topologies.

However, the consciousness of researchers is a little different between chemical biologist and systems biologist. Chemical biology in general is still dominated by the mindset of pairing individual compounds and targets. By contrast, systems biology seeks to compare the effect of compounds as a means of understanding relationships, revealing higher order network structure and modeling the complexity[29]. Although 'chemical systems biology' is emerging frontier, and has a huge potential for development, there are a number of challenges to be considered.

## The purpose of this study

In this thesis, the author reported a study on the regulatory mechanism for tumor cell migration based on the both of chemical biological approach and systems biological approach. In **chapter 2**, the novel inhibitors of farnesyl transferase (FTase) were screened, and cell migration mechanism in epidermal carcinoma was

partially identified using the novel compounds. In **chapter 3** and **4**, the consistency and diversity of regulatory signaling for cell migration in several cancer cell line were proposed based on the combination approach between chemical biology and systems biology. These studies would open up new insight into the research field of tumor cell motility, and also open up the potential for 'chemical systems biology'.

# Chapter 2

# Novel derivatives of aclacinomycin A block cancer cell migration through inhibition of farnesyl transferase

## 2.1 Introcudtion

Cell migration is not only a central feature of a range of physiological processes, but also a crucial event in the spread of cancer and, consequently, the metastatic process[6]. Ras protein, a guanine nucleotide (GTP) binding protein, plays an important role in signal transduction and regulation of cell migration[33,34]. A series of post-translational modifications are essential for the cell membrane association of

Ras protein. One key modification is farnesylation of Ras by farnesyl transferase (FTase) on the C-terminus cystein residue of the CAAX motif[35]. Previously, *Takemoto et al.* screened for inhibitors of cancer cell migration and obtained moverastin A and B, new members of the cylindrol family, from *Aspergillus* sp. F7720[36]. Furthermore, they found that moverastin A and B inhibited FTase, and demonstrated that moverastins inhibited the migration of tumor cells by inhibiting the farnesylation of H-Ras. However, the inhibitory activity of moverastins for FTase was rather modest ($IC_{50}$ value of 14.7 $\mu$M). Thus the author started screening of potent inhibitors of FTase as part of the project in Screening Committee of Anticancer Drugs (SCADS). In this study, the author found new inhibitors of FTase, N-benzyl-ACM and N-allyl-ACM, which are chemically synthesized derivatives of aclacinomycin A (aclarubicin), and described the anti-migrative effect of these compounds.

## 2.2 Results and Discussion

### Screening for inhibitors of FTase

The author evaluated the inhibitory activity of compounds against FTase in the project of the SCADS. SCADS is offering several biological activity evaluation of synthesized or isolated compounds for Japanese chemists. For the *in vitro* FTase

assay, FTase was partially purified from human esophageal tumor EC17 cells, and recombinant GST-H-Ras and [$^3$H]-farnesyl pyrophosphate (FPP) were used as the substrates. We firstly investigated the effect of compounds on FTase activity at the concentration of 10 $\mu$M. As a result, two compounds were found to have inhibitory activity against FTase. As shown in **Figure 2–1a**, these are novel derivatives of aclacinomycin A (ACM), and were named N-benzyl-ACM and N-allyl-ACM, respectively. ACM was discovered from a culture of *Streptomyces galilaeus*, and it showed potent antitumor activity[37,38].

## Effect of N-benzyl-ACM and N-allyl-ACM on FTase activity

In the next step, the author examined the inhibitory activities of these ACM derivatives to give $IC_{50}$ values. As shown in **Figure 2–2**, N-benzyl-ACM and N-allyl-ACM inhibit FTase activity in a dose-dependent manner, and the $IC_{50}$ values of N-benzyl-ACM and N-allyl-ACM were 0.86 and 2.93 $\mu$M, respectively (**Table 2–1**). On the other hand, ACM did not inhibit FTase activity at the concentration of 10 $\mu$M in the process of the screening project of SCADS. Interestingly, neither the C-10 epimer of N-benzyl-ACM (10-epi-N-benzyl-ACM, **Figure 2–1b**) nor the C-10 epimer of N-allyl-ACM (10-epi-N-allyl-ACM, **Figure 2–1b**) also showed an inhibitory effect against FTase activity at the concentration of 10 $\mu$M. These results indicated that both modification of the N-dimethyl group and the configuration

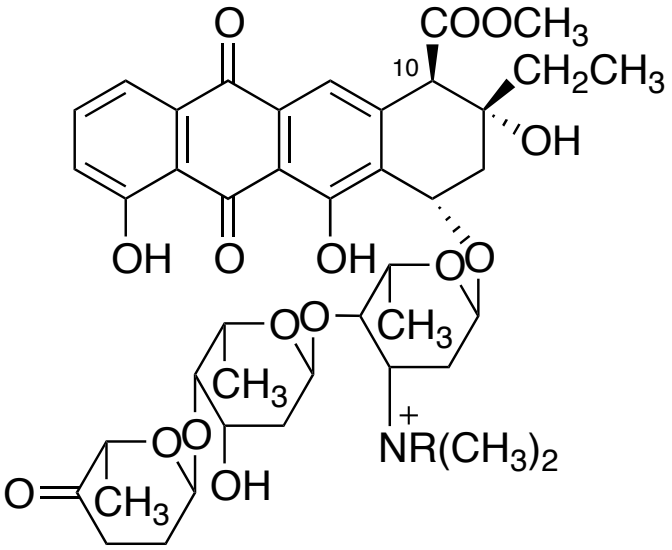


Aclacinomycin A (ACM): R = H
N-benzyl-ACM: R = $CH_2C_6H_5$
N-allyl-ACM: R = $CH_2CH{=}CH_2$

**Figure 2–1. Structures of aclacinomycin A derivatives.** (**a**) Structures of ACM, N-benzyl-ACM, and N-allyl-ACM.

of C-10 are critical for the inhibitory activity of N-benzyl-ACM and N-allyl-ACM toward FTase. Like FTase, geranylgeranyl transferase (GGTase) catalyzes the geranylgeranylation of proteins terminating with a CAAX motif where X is restricted to leucine, isoleucine or phenylalanine. FTase and GGTase have been shown to be heterodimers that share a common $\alpha$ subunit with a different $\beta$ subunit; therefore, the author examined the effect of N-benzyl-ACM and N-allyl-ACM on the inhibitory activity against GGTase and found that they failed to inhibit GGTase up to 100 $\mu$M. Geranylgeranyl pyrophosphate (GGPP) synthase is an enzyme that

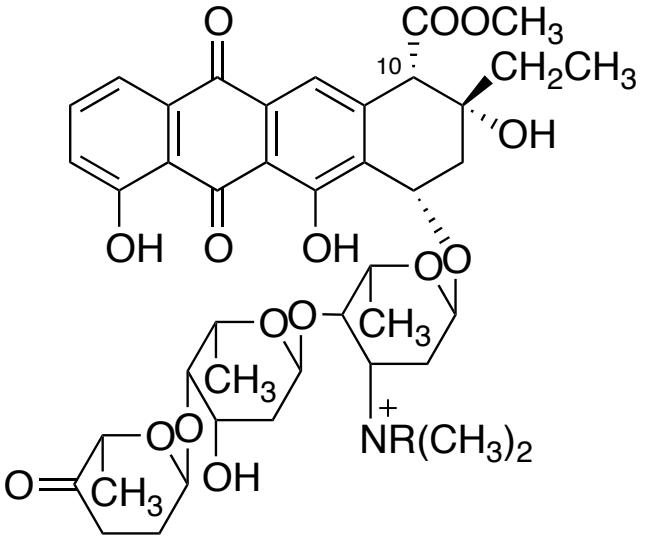


10-epi-N-benzyl-ACM: R = $CH_2C_6H_5$
10-epi-N-allyl-ACM: R = $CH_2CH{=}CH_2$

**Figure 2–1. Structures of aclacinomycin A derivatives (*continued*).** (**b**) Structures of 10-epi-N-benzyl-ACM and 10-epi-N-allyl-ACM.

catalyzed the synthesis of GGPP from isopentenyl pyrophosphate (IPP) and FPP; thus, because both FTase and GGPP synthase use FPP as a substrate, the effect of N-benzyl-ACM and N-allyl-ACM on GGPP synthase activity was examined. However, neither FTase inhibitor could inhibit GGPP synthase up to 100 $\mu$M (**Table 2–1**). So far, although several anthraquinones have been reported as FTase inhibitors[39,40], none of the anthracycline family has been identified as an FTase inhibitor; thus, N-benzyl-ACM and N-allyl-ACM are the first examples in a series of the anthracycline family, demonstrating that the compounds inhibit FTase.

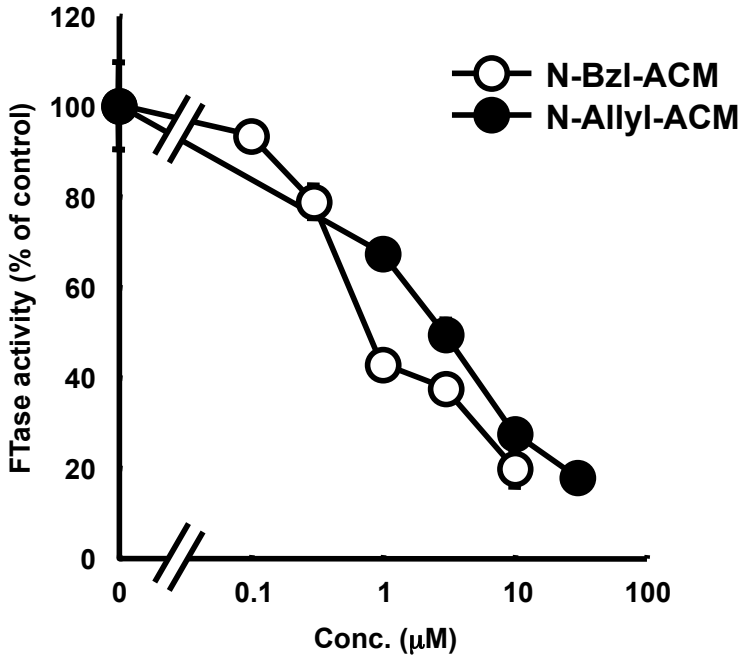


**Figure 2–2. Effect of N-benzyl-ACM and N-allyl-ACM on FTase activity *in vitro*.** Partially purified FTase from EC17 cells was incubated with [$^3$H]-FPP plus recombinant GST-H-Ras in the presence or absence of N-benzyl-ACM (N-Bzl-ACM) or N-allyl-ACM (N-Allyl-ACM). The reaction was terminated by the addition of TCA. The radioactivity of the TCA-insoluble fraction was measured. The results are the mean ±SD of two independent experiments.

**Table 2–1.** Biological activities of N-benzyl-ACM and N-allyl-ACM in A431 cells.

| $IC_{50}$ ($\mu$M) | N-benzyl-ACM | N-allyl-ACM |
|---|---|---|
| FTase | 0.86 | 2.93 |
| GGTase | 100 | >100 |
| GGPP synthase | >100 | >100 |
| Cell migration | 0.65 | 1.55 |
| Cell viability (-EGF) | >10 | >30 |
| Cell viability (+EGF)[a)] | 9.09 | 22.0 |

a) The concentration of EGF was 30 ng/ml.

## Effect of N-benzyl-ACM and N-allyl-ACM on localization of H-Ras

Because N-benzyl-ACM and N-allyl-ACM selectively inhibited FTase *in vitro*, next the author examined whether these compounds could inhibit FTase in a cultured cell system. A431 cells were well-known EGF receptor-overexpressing cells that displayed a sufficient level of H-Ras protein[41]. As shown in **Figure 2–3a**, the amount of H-Ras in the membrane fraction was not changed in the presence or absence of EGF; however, treatment of cells with N-benzyl-ACM and N-allyl-ACM reduced the amount of H-Ras in the membrane fraction. On the other hand, N-benzyl-ACM and N-allyl-ACM did not increase the amount of unprenylated Rap1A which is mainly prenylated by GGTase I in the same condition (**Figure 2–3b**), suggesting that both compounds did not inhibit GGTase I in A431 cells. These results suggested that N-benzyl-ACM and N-allyl-ACM inhibited the membrane localization of H-Ras protein through the selective inhibition of FTase in A431 cells.

## Effect of N-benzyl-ACM and N-allyl-ACM on PI3K signaling

The activation of H-Ras was reported to further activate the PI3K pathway[42,43]. Indeed, *Takemoto et al.* previously reported that other FTase inhibitors, moverastin

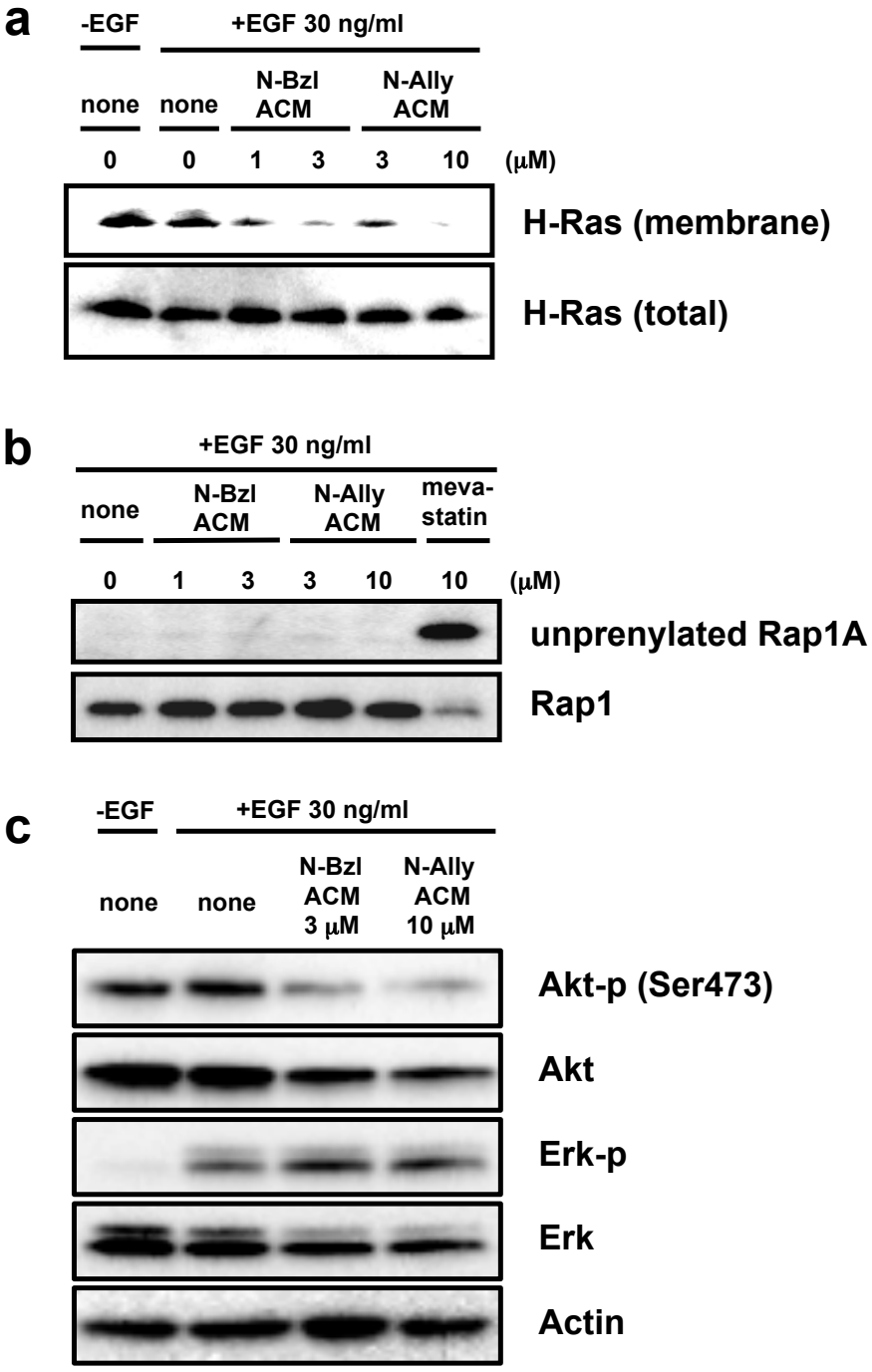


**Figure 2–3. Effect of N-benzyl-ACM and N-allyl-ACM on H-Ras translocation, Rap1 prenylation, and phosphorylation of Akt and Erk in A431 cells.** A431 cells were pretreated with drugs for 15 min and stimulated with EGF. Following 24 h of incubation, cells were collected and the membrane fraction was extracted (**a**). All samples were subjected to immunoblotting.

A and B, inhibited the PI3K/Akt pathway but not the Raf/MEK/Erk pathway[36]. To confirm whether N-benzyl-ACM or N-allyl-ACM also could inhibit the PI3K pathway selectively, the author examined the effect of these compounds on the phosphorylation of Akt or Erk in A431 cells. As shown in **Figure 2–3c**, the phosphorylation of Akt (Ser473) was significantly decreased in the presence of either N-benzyl-ACM or N-allyl-ACM, whereas these compounds did not affect the phosphorylation level of Erk. These results suggested that N-benzyl-ACM and N-allyl-ACM inhibited PI3K activation through the suppression of H-Ras farnesylation.

## Effect of N-benzyl-ACM and N-allyl-ACM on cell migration

Since the activation of H-Ras through the farnesylation by FTase was involved in cell migration[36], the author examined the effect of N-benzyl-ACM or N-allyl-ACM on EGF-induced cell migration in A431 cells. As a result, N-benzyl-ACM or N-allyl-ACM inhibited EGF-induced cell migration in a dose-dependent manner (**Figure 2–4a, b**). These inhibitory effects were not due to the toxic effect of the drugs because their $IC_{50}$ values for A431 cell viability were at least seven times higher than those for cell migration (**Table 2–1**). Importantly, the dose of N-benzyl-ACM or N-allyl-ACM required to inhibit cell migration was consistent with that for inhibition of the membrane localization of H-Ras. Moreover, accord-

ing to the inhibitory activity against FTase, the $IC_{50}$ value for the cell migration of N-benzyl-ACM was lower than that of N-allyl-ACM (**Table 2–1**). Neither 10-epi-N-benzyl-ACM nor 10-epi-N-allyl-ACM, which failed to inhibit FTase, suppressed EGF-induced migration of A431 cells (**Figure 2–4c**). Taken together, these findings suggest that N-benzyl-ACM and N-allyl-ACM inhibited the EGF-induced migration of A431 cells by inhibiting H-Ras farnesylation (**Figure 2–5**).

## 2.3 Experimental Procedures

### General experimental procedures

Centrifugal partition chromatography (CPC) was performed using a Centrifugal Partition Chromatograph-L.L.N. (Model-NMF, 250 ml cell; Sanki Engineering). High-resolution mass spectra (HRMS) were recorded on an Accu TOF-T100LC (JEOL) mass spectrometer. $^{1}$H-NMR and $^{13}$C-NMR data were measured on a JEOL ECX-600 spectrometer. Chemical shifts for proton are reported in parts per million downfield from tetramethylsilane. For $^{13}$C-NMR, chemical shifts were reported in the scale relative to NMR solvent ($CDCl_3$: 77.0 ppm) as an internal reference. Optical rotations were measured with a P-1030 polarimeter (JASCO). IR spectra were recorded on a FT/IR-4100 fourier transform infrared spectrometer (JASCO).

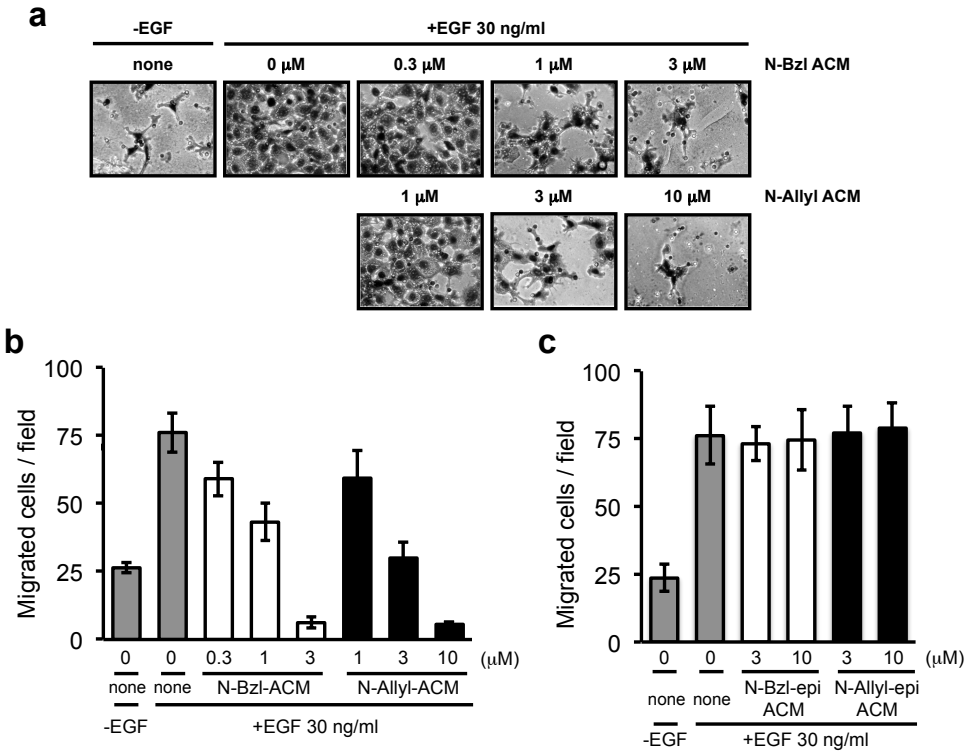


**Figure 2–4. Effect of N-benzyl-ACM and N-allyl-ACM on EGF-induced cell migration in A431 cells.** A431 cells suspended in DMEM supplemented with 0.2% CS were incubated in the upper chamber; the lower chamber contained DMEM supplemented with 0.2% CS in the presence or absence of EGF (30 ng/ml). Drugs were added to both chambers. After 24 h, the cells that migrated through the filter to the lower surface were photographed (**a**), and the number of migrated cells was counted (**b, c**). The results are the mean ±SD of five different fields.

## Preparation of N-benzyl-ACM

Aclacinomycin A hydrochloride (255.9 mg, 0.301 mM) in dry dimethylformamide (DMF) (5.2 ml) was treated with benzyl bromide (0.108 ml, 3.0 equiv.) in the presence of diisopropylethylamine (0.315 ml, 6.0 equiv.) at room temperature for 19 h. After removal of the solvent, the residue was dissolved in $CHCl_3$, washed

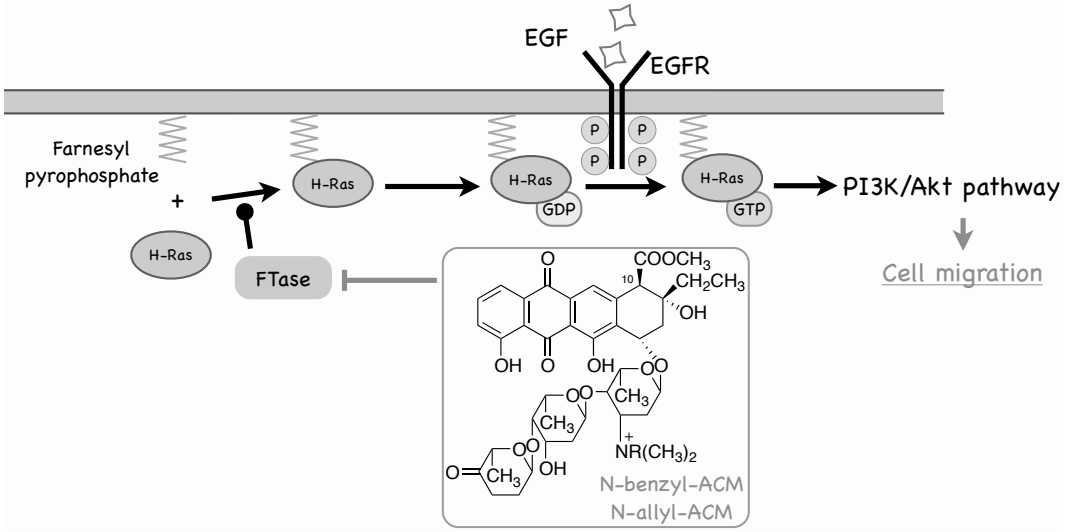


**Figure 2–5. Schematic illustration of findings in this chapter.** N-benzyl-ACM and N-allyl-ACM inhibit FTase, and thereby suppress H-Ras/PI3K/Akt signaling and cell migration in A431 cells.

with $H_2O$, and then continuously with aqueous $Na_2SO_4$. The $CHCl_3$ layer was dried over $Na_2SO_4$ and evaporated. The oily residue was washed with hexane-diethyl ether (4 : 1) three times and the remaining residue (crude material 1) (328.4 mg) was purified by CPC ($CHCl_3$ : $CH_3OH$ : $H_2O$ = 5 : 6 : 4, ascending mode), to give mixtures containing N-benzyl-ACM (151.28 mg). The portion (118.6 mg) of obtained crude materials was passed through a Dowex 1 × 2, (chloride form, $CH_3OH$ : $H_2O$ = 1 : 4), and finally purified by silica gel column chromatography ($CHCl_3$ : $CH_3OH$ : $H_2O$ = 10 : 1 : 0.1), to give pure N-benzyl-ACM (71.4 mg, yield 32%) as an orange powder. HRMS ($ESI^+$ mode): m/z 902.39627 (observed), m/z 902.39575 (calcd. for $C49H60NO15^+$); $^1$H-NMR of rhodosamine and D-ring

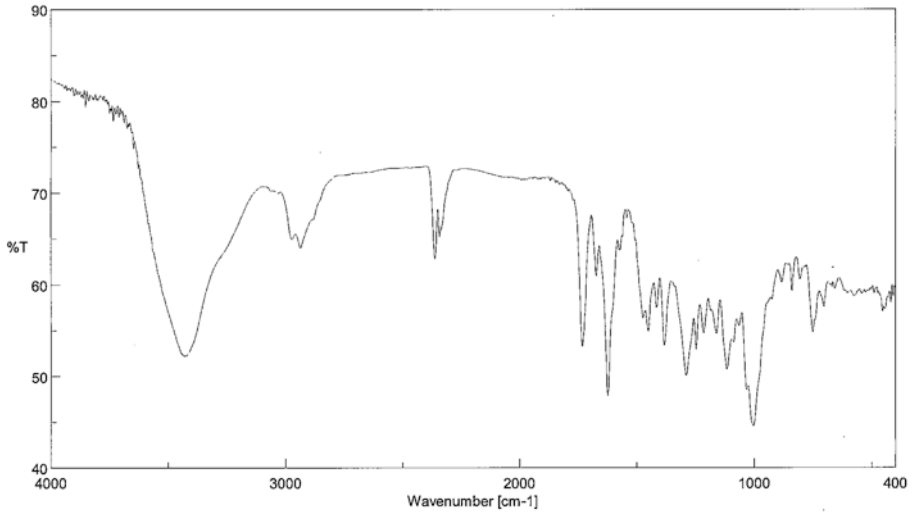


**Figure 2–6. IR spectrum of N-benzyl-ACM**

moieties (chemical shift in ppm, splitting pattern, J in Hz) in $CDCl_3$ : H-7 (5.18, d, 5.5), H-8a (2.20, d, 15.0), H-8b (2.61, dd, 5.5 & 15.0), 9-OH (4.57, br s), H-10 (4.12, s), H-13a (1.69, dq, 7.5 & 15.0), H-13b (1.79, dq, 7.5 & 15.0), H-14 (1.15, t, 7.5), -COOMe (3.69, s), H-1′ (5.81, br d, 2.0), H-2′a (overlapping at around 2.1ppm), H-2′b (overlapping at around 2.4 ppm), H-3′ (5.13, br d, 14.0), H-4′ (4.45, br s), H-5′ (overlapping at around 4.55ppm), H-6′ (1.38, d, 7.0). Optical rotation: $[\alpha]_D^{26}$ +23 (*c* 0.1, $CHCl_3$) NMR table of N-benzyl-ACM is presented in **Table 2–1a**. IR spectrum of N-benzyl-ACM is presented in **Figure 2–6**.

## Table 2–2. $^{13}$C- and $^{3}$H-NMR data for N-benzyl-ACM and N-allyl-ACM

(**a**) N-benzyl-ACM

| *Number* | $\delta_C$ *(p.p.m.)* | $\delta_H$ *(p.p.m.)* |
|---|---|---|
| 1 | 120.1 | 7.75 (1H, dd, J = 1.5, 7.5) |
| 2 | 137.4 | 7.64 (1H, dd, J = 7.5, 8.0) |
| 3 | 124.7 | 7.25 (1H, dd, J = 1.5, 8.0) |
| 4 | 162.4 or 162.5 | — |
| 4a | 115.7 | — |
| 5 | 192.7 | — |
| 5a | 114.4 | — |
| 6 | 162.4 or 162.5 | — |
| 6a | 132.1 or 132.3 | — |
| 7 | 69.25 or 69.33 | 5.18 (1H, d, J = 5.5) |
| 8a | 36.5 | 2.20 (1H, d, J = 15.0) |
| 8b | | 2.61 (1H, dd, J = 5.5, 15.0) |
| 9 | 70.4 | — |
| 10 | 55.6 | 4.12 (1H, s) |
| 10a | 143.9 | — |
| 11 | 121.2 | 7.68 (1H, s) |
| 11a | 132.1 or 132.3 | — |
| 12 | 181.2 | — |
| 12a | 133.4 | — |
| 13a | 32.6 | 1.69 (1H, dq, J = 7.5, 15.0) |
| 13b | | 1.79 (1H, dq, J = 7.5, 15.0) |
| 14 | 6.98 | 1.15 (3H, t, J = 7.5) |
| 1′ | 99.0 | 5.81 (1H, brd, J = 2̃.0) |
| 2′a | 26.5 | 2.02–2.17 (1H, m) |
| 2′b | | 2.35–.245 (1H, m) |
| 3′ | 67.2 | 5.13 (1H, brd, J = 1̃4.0) |
| 4′ | 76.1 | 4.45 (1H, brs) |
| 5′ | 69.25 or 69.33 | 4.52-4.60 (1H, m) |
| 6′ | 18.1 | 1.38 (3H, d, J = 7.0) |
| 1″ | 98.3 | 5.31 (1H, t, J = 4.0) |
| 2″a,b | 34.8 | 2.02–2.17 (2H, m) |
| 3″ | 66.0 | 4.05-4.13 (1H, m) |
| 4″ | 78.5 | 3.80 (1H, t, J = 3.0) |
| 5″ | 69.5 | 4.05–4.13 (1H, m) |
| 6″ | 16.3 | 1.27 (3H, d, J = 7.0) |
| 1‴ | 98.9 | 5.09 (1H, t, J = 6.0) |
| 2‴a | 27.7 | 2.02–2.17 (1H, m) |
| 2‴b | | 2.35–2.45 (1H, m) |
| 3‴ | 33.3 | 2.44–2.53 (2H, m) |
| 4‴ | 209.6 | — |
| 5‴ | 71.7 | 4.44 (1H, q, J = 7.0) |
| 6‴ | 14.8 | 1.31 (3H, d, J = 7.0) |
| 4-OH | — | 11.98 (1H, s) |
| 6-OH | — | 12.78 (1H, brs) |
| 9-OH | — | 4.57 (1H, brs) |
| 3″-OH | — | 3.45 (1H, d, J = 6.0) |
| COO**Me** | 52.4 | 3.69 (3H, s) |
| **C**OOMe | 171.3 | — |
| Bzl-1 | 127.1 | — |
| Bzl-2 | 133.2 | 7.41 (2H, d, J = 7.8) |
| Bzl-3 | 129.0 | 7.19 (2H, t, J = 7.8) |
| Bzl-4 | 130.6 | 7.32 (1H, t, J = 7.8) |
| Bzl-CH2a | 66.6 | 4.60 (1H, d, J = 12.5) |
| Bzl-CH2b | | 5.11 (1H, d, J = 12.5) |
| N-Mea | 47.2 | 3.08 (3H, s) |
| N-Meb | 46.6 | 3.27 (3H, s) |

(**b**) N-allyl-ACM

| *Number* | $\delta_C$ *(p.p.m.)* | $\delta_H$ *(p.p.m.)* |
|---|---|---|
| 1 | 120.1 | 7.68 (1H, d, J = 8.0) |
| 2 | 137.5 | 7.60 (1H, dd, t = 8.0) |
| 3 | 124.8 | 7.20 (1H, d, J = 8.0) |
| 4 | 162.4 or 162.5 | — |
| 4a | 115.6 | — |
| 5 | 181.1 | — |
| 5a | 114.3 | — |
| 6 | 162.4 or 162.5 | — |
| 6a | 132.1 or 132.3 | — |
| 7 | 69.1 | 5.12 (1H, d, J = 5.5) |
| 8a | 36.4 | 2.15 (1H, d, J = 15) |
| 8b | | 2.58 (1H, dd, J = 5.5, 15) |
| 9 | 70.3 | — |
| 10 | 55.7 | 4.06 (1H, s) |
| 10a | 144.0 | — |
| 11 | 121.2 | 7.50 (1H, s) |
| 11a | 132.1 or 132.3 | — |
| 12 | 192.6 | — |
| 12a | 133.2 | — |
| 13a | 32.7 | 1.69 (1H, dq, J = 7.5, 15) |
| 13b | | 1.76 (1H, dq, J = 7.5, 15) |
| 14 | 7.1 | 1.15 (3H, t, J = 7.5) |
| 1′ | 98.9 | 5.78 (1H, brd, J = 2̃) |
| 2′a | 26.2 | 2.03–2.16 (1H, m) |
| 2′b | | 2.22–.236 (1H, m) |
| 3′ | 67.8 | 5.08–5.14 (1H, m) |
| 4′ | 76.2 | 4.44 (1H, brs) |
| 5′ | 69.1 | 4.61 (1H, q, J = 7.0) |
| 6′ | 18.1 | 1.36 (3H, d, J = 7.0) |
| 1″ | 98.7 | 5.28 (1H, t, J = 3.5) |
| 2″a,b | 34.8 | 2.03–2.16 (2H, m) |
| 3″ | 66.0 | 4.06-4.13 (1H, m) |
| 4″ | 78.6 | 3.81 (1H, t, J = 2.5) |
| 5″ | 69.5 | 3.97——4.06 (1H, m) |
| 6″ | 16.5 | 1.28 (3H, d, J = 7.0) |
| 1‴ | 98.9 | 5.10 (1H, t, J = 6.0) |
| 2‴a | 27.8 | 2.03–2.16 (1H, m) |
| 2‴b | | 2.38–2.54 (1H, m) |
| 3‴a,b | 33.3 | 2.38–2.54 (2H, m) |
| 4‴ | 209.8 | — |
| 5‴ | 71.8 | 4.46 (1H, q, J = 7.0) |
| 6‴ | 14.9 | 1.32 (3H, d, J = 7.0) |
| 4-OH | — | 11.93 (1H, s) |
| 6-OH | — | 12.73 (1H, brs) |
| 9-OH | — | 4.76 (1H, brs) |
| 3″-OH | — | 3.50 (1H, brd, J = 6.0) |
| COO**Me** | 52.4 | 3.67 (3H, s) |
| **C**OOMe | 171.3 | — |
| Allyl-1a | 64.5 | 3.97–4.06 (1H, m) |
| Allyl-1b | | 4.39 (1H, dd, J = 6.0, 13.0) |
| Allyl-2 | 124.5 | 5.88–5.97 (1H, m) |
| Allyl-3a | 129.8 | 5.59 (1H, d, J = 17.0) |
| Allyl-3b | | 5.62 (1H, d, J = 10.0) |
| N-Mea | 47.6 | 3.15 (3H, s) |
| N-Meb | 47.4 | 3.24 (3H, s) |

## Preparation of 10-epi-N-benzyl-ACM

Crude material 1, obtained in the process to synthesize N-benzyl-ACM (328.4 mg) was purified by CPC ($CHCl_3$ : $CH_3OH$ : $H_2O$ = 5 : 6 : 4, ascending mode), to give mixtures containing 10-epi-N-benzyl-ACM (60.6 mg). The portion (43.2 mg) of obtained crude materials was passed through a Dowex 1 × 2 (chloride form, $CH_3OH$: $H_2O$ = 1 : 4) and finally purified by silica gel column chromatography ($CHCl_3$ : $CH_3OH$ : $H_2O$ = 10 : 1 : 0.1 — 6 : 1 : 0.1) to give pure 10-epi-N-benzyl-ACM (29.1 mg, yield 14%) as an orange powder. NMR and CD spectrum of 10-epi-N-benzyl-ACM is presented in **Figure 2–7 and 2–8**, respectively.

## Preparation of N-allyl-ACM

Aclacinomycin A hydrochloride (259.2 mg, 0.305 mM) in dry DMF (5.2 ml) was treated with allyl iodide (0.042 ml, 1.5 equiv.) in the presence of diisopropylethylamine (0.16 ml, 3.0 equiv.) at room temperature for 24 h. The reagents, allyl iodide (0.028 ml, 1.0 eauiv.) and diisopropylethylamine (0.053 ml, 1.0 equiv.) were added and the reaction mixtures were maintained for a further 7 h. After removal of the solvent, the residue was dissolved in $CHCl_3$, washed with $H_2O$ and then continuously with aqueous $Na_2SO_4$. The $CHCl_3$ layer was dried over $Na_2SO_4$ and evaporated. The oily residue was washed with hexane-diethyl ether (4 : 1) three times and the remaining residue (crude material 2) (302.8 mg) was purified

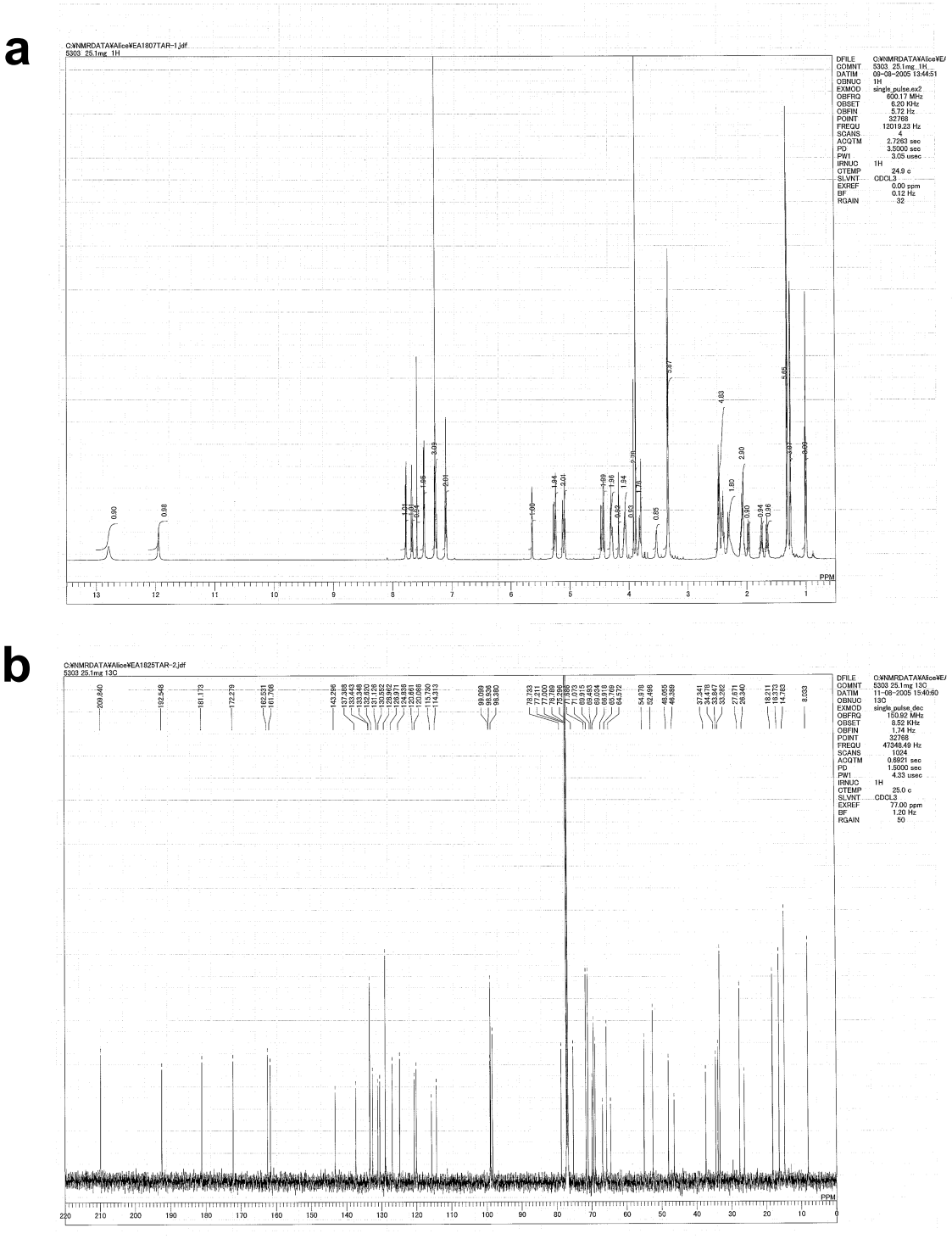


**Figure 2–7. NMR Spectra of 10-epi-N-benzyl-ACM** (**a**) $^{1}$H-NMR spectrum of 10-epi-N-benzyl-ACM in $CDCl_3$ (600 MHz). (**b**) $^{13}$C-NMR spectrum of 10-epi-N-benzyl-ACM in $CDCl_3$ (75 MHz).

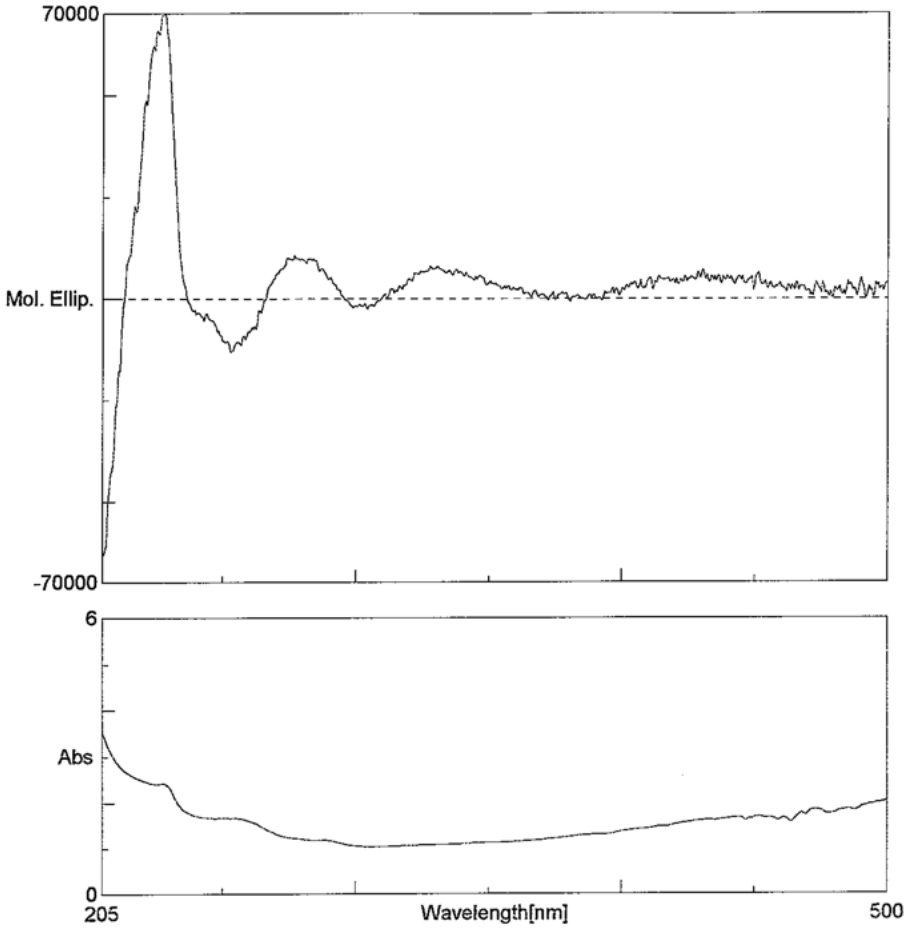


**Figure 2–8. CD Spectra of 10-epi-N-benzyl-ACM**

by CPC ($CHCl_3$ : $CH_3OH$ : $H_2O$ = 5 : 6 : 4, ascending mode), to give mixtures containing N-allyl-ACM (108.2 mg). The crude materials were passed through a Dowex 1 × 2, (chloride form, $CH_3OH$ : $H_2O$ = 1 : 4), and finally purified by silica gel column chromatography ($CHCl_3$ : $CH_3OH$ : $H_2O$ = 10 : 1 : 0.1), to give pure N-allyl-ACM (71.0 mg, yield 26%) as an orange powder. HRMS ($ESI^+$ mode): m/z 852.38267 (observed), m/z 852.38010 (calcd. for $C45H58NO15^+$); $^1$H-NMR of rhodosamine and D-ring moieties (chemical shift in ppm, splitting pattern, J in Hz)

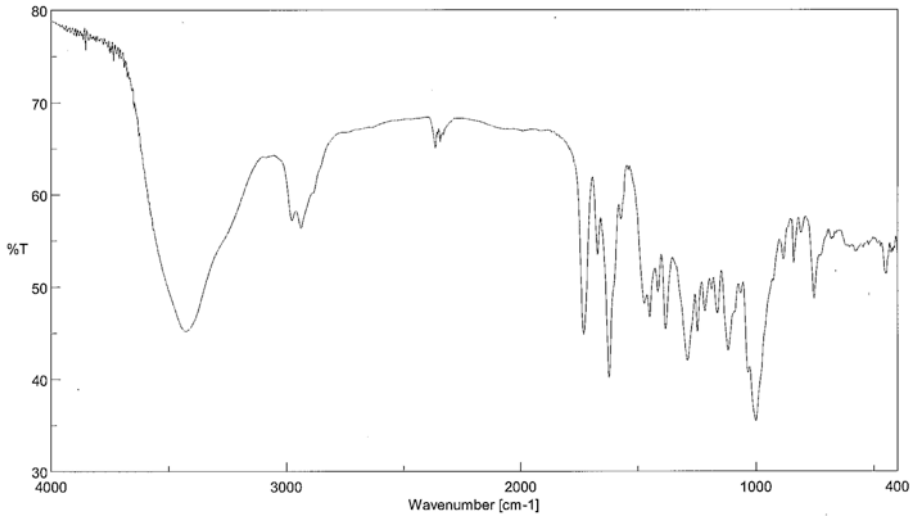


**Figure 2–9. IR spectrum of N-allyl-ACM**

in $CDCl_3$: H-7 (5.12, d, 5.5), H-8a (2.15, d, 15.0), H-8b (2.58, dd, 5.5 & 15.0), 9-OH (4.76, br s), H-10 (4.06, s), H-13a (1.69, dq, 7.5 & 15.0), H-13b (1.76, dq, 7.5 & 15.0), H-14 (1.15, t, 7.5), -COOMe (3.67, s), H-1′ (5.78, br d, 2.0), H-2′a (overlapping at around 2.1ppm), H-2′b (overlapping at around 2.3ppm), H-3′ (5.08-5.14, m), H-4′ (4.44, br s), H-5′ (4.61, q, 7.0), H-6′ (1.36, d, 7.0). Optical rotation: $[\alpha]_D^{27}$ -1.7($c$ 0.1, $CHCl_3$) NMR table of N-allyl-ACM is presented in **Table 2–1b**. IR spectrum of N-benzyl-ACM is presented in **Figure 2–9**.

## Preparation of 10-epi-N-allyl-ACM

Crude material 2, obtained in the process to synthesize N-allyl-ACM (302.8 mg) was purified by CPC ($CHCl_3$ : $CH_3OH$ : $H_2O$ = 5 : 6 : 4, ascending mode),

to give mixtures containing 10-epi-N-allyl-ACM (32.3 mg). The crude materials were passed through a Dowex 1 × 2 (chloride form, $CH_3OH : H_2O = 1 : 4$) to give pure 10-epi-N-allyl-ACM (27.8 mg, yield 10%) as an orange powder. NMR and CD spectrum of 10-epi-N-allyl-ACM is presented in **Figure 2–10 and 2–11**, respectively.

## Cell culture

A431 cells were maintained in Dulbecco's modified Eagle's medium (DMEM) supplemented with 5% calf serum (CS), 0.1 g/l kanamycin, 100 units/ml penicillin G, 0.6 g/l L-glutamine, and 2.5 g/l $NaHCO_3$. For routine culture, cells were incubated in a standard humidified incubator at 37 °C with 5% $CO_2$.

## Reagents

Epidermal growth factor (EGF) and mevastatin were purchased from Sigma.

## Cell viability assay

A431 cells ($7.5 \times 10^4$) were seeded in 48-well plate and cultured overnight. After the culture supernatant was replaced with DMEM with 0.2% CS, the cells were treated with drugs in the presence or absence of 30 ng/ml EGF for 24 h. After the cells were trypsinized and collected, cell viability was determined by trypan blue

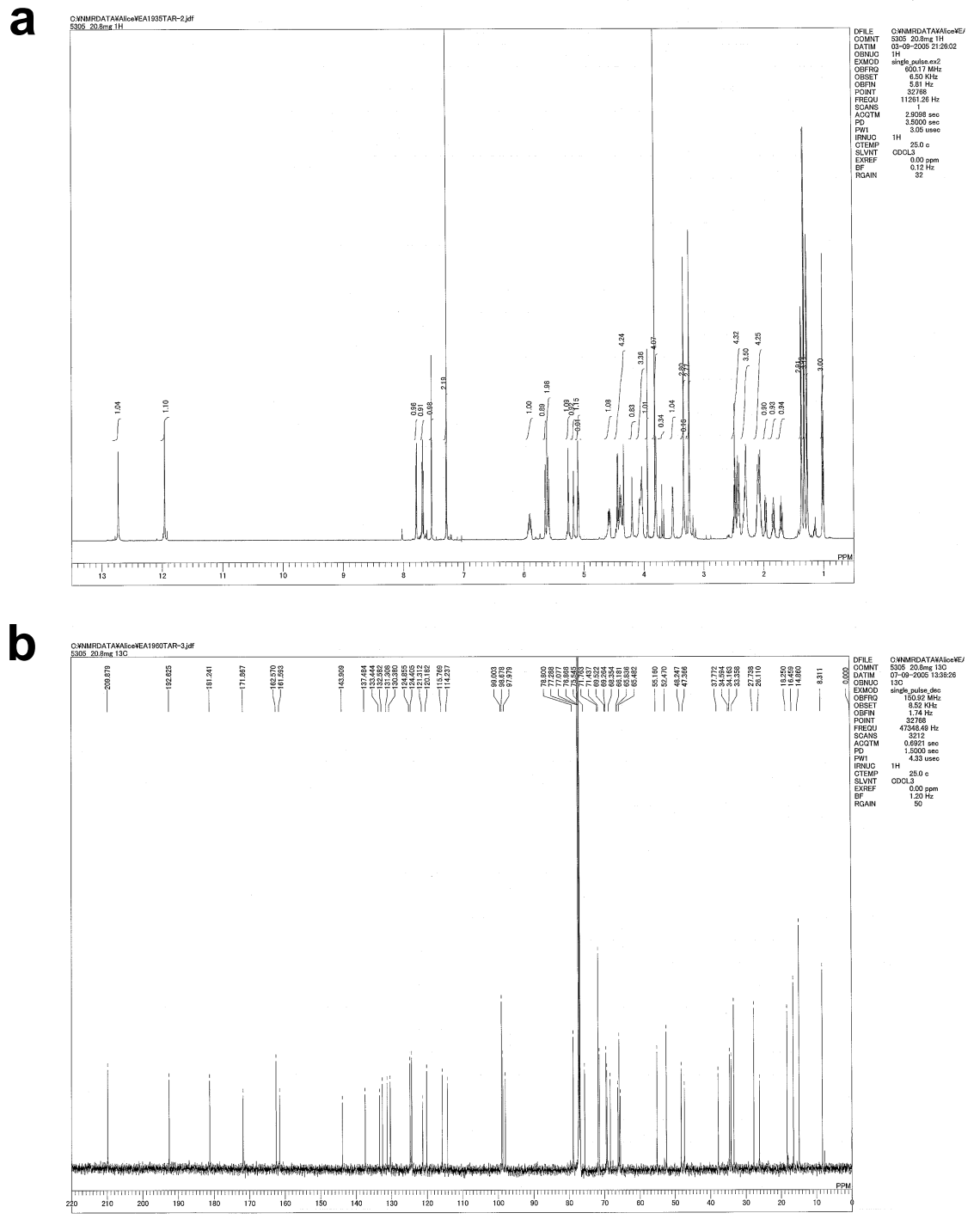


**Figure 2–10. NMR Spectra of 10-epi-N-allyl-ACM** (**a**) $^{1}$H-NMR spectrum of 10-epi-N-allyl-ACM in $CDCl_3$ (600 MHz). (**b**) $^{13}$C-NMR spectrum of 10-epi-N-allyl-ACM in $CDCl_3$ (75 MHz).

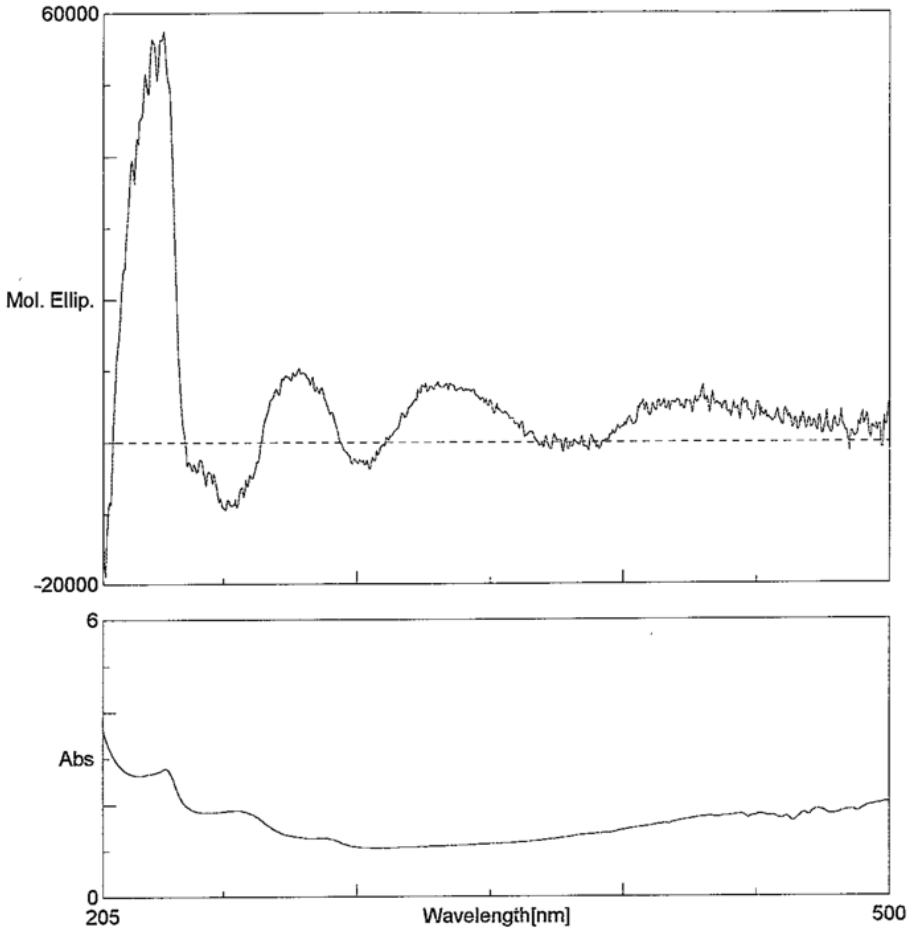


**Figure 2–11. CD Spectra of 10-epi-N-allyl-ACM**

dye exclusion assay.

## *In vitro* FTase assay

*In vitro* FTase assay was carried out according to the procedures previously described[36]. In brief, the standard reaction mixture of FTase contained the following components in a final volume of 60 $\mu$l : 10 $\mu$g of partially purified FTase from

human esophageal tumor EC17 cells, 10 $\mu$g of recombinant GST-H-Ras protein, 0.06 $\mu$M of [$^3$H]-FPP (596 GBq/mmol; New England Nuclear), 50 mM Tris-HCl (pH 7.5, Sigma), 50 $\mu$M $ZnCl_2$ (Kanto Chemical), 4 mM $MgCl_2$ (Wako), and 4 mM DTT (Wako). The reaction was initiated by the addition of enzyme and incubated for 1 h at 37 °C. The reaction was stopped by the addition of 0.5 ml of 1% SDS (Wako) in MeOH and 0.5 ml of 30% trichloroacetic acid (TCA, Wako). The mixture was then filtered through a Whatman GF/C filter (GE Healthcare), washed with 5 ml of 6% TCA. The dried filter was finally placed in a liquid scintillation counter (Beckman Coulter). A blank value was determined in a parallel incubation with boiled enzymes and was subtracted before calculating percent inhibition.

## *In vitro* GGTase and GGPP synthase assays

*In vitro* GGTase assay was carried out according to the procedures previously described[36]. In brief, the standard reaction mixture contained the following components in a final volume of 60 $\mu$l : 10 $\mu$g of partially purified enzymes from the cytosol of EC17 cells, 8 $\mu$g recombinant GST-Rho A protein, 0.08 $\mu$M of [$^3$H]-GGPP (1.48 TBq/mmol; Amersham Bioscience), 50 mM Tris-HCl (pH 7.5), 50 $\mu$M $ZnCl_2$, 4 mM $MgCl_2$, and 4 mM DTT. The reaction was initiated by the addition of enzyme and incubated for 1 h at 37 °C. The reaction was stopped by the addition of 0.5 ml of 1% SDS in MeOH and 0.5 ml of 30% TCA. The mixture was then filtered

through a Whatman GF/C filter, washed with 5 ml of 6% TCA. The dried filter was finally placed in a liquid scintillation counter. A blank value was determined in a parallel incubation with boiled enzymes and was subtracted before calculating percent inhibition. To measure GGPP synthase activity, the standard mixture contained, in a final volume of 0.2 ml, 0.1 M Tris-HCl buffer (pH 7.5), 0.3 mM $MnCl_2$, 0.2 mM $MgCl_2$, 10 $\mu$g/ml BHT, 47.9 ng/ml FPP, 0.81 nCi [$^{14}$C] isopentenyl diphosphate (IPP) and an appropriate amount of purified GST-GGPP synthase in the presence or absence of test sample. The mixture was incubated at 37 °C for 45 min and the reaction was terminated by the addition of 0.3 ml of 1-BuOH and mixed. Enzyme activity was evaluated for the radioactivity of the 1-BuOH extract of the reaction mixture.

## Detection of H-Ras translocation to plasma membrane

Human epidermoid carcinoma A431 cells ($1 \times 10^6$) were seeded in 100 mm dish and cultured overnight. After the culture supernatant was replaced with DMEM with 0.2% CS, the cells were pretreated with drugs for 15 min and stimulated with 30 ng/ml EGF. Following 24 h of incubation, cells were collected and resuspended in buffer A [20 mM Hepes (Sigma), pH 7.5, 10 mM KCl (Kanto Chemical), 1.5 mM $MgCl_2$, 1 mM EDTA (Kanto Chemcial), 1 mM EGTA (Wako), and 1 mM DTT] containing 250 mM sucrose (Sigma) and 1 mM phenylmethylsulfonyl fluoride

(PMSF, Sigma). The cells were homogenized and unbroken cells were removed by centrifuging the homogenates at 1,000 g for 10 min at 4 °C. The supernatant was centrifuged at 100,000 g for 1 h at 4 °C. The supernatant was removed and the pellets were lysed in RIPA buffer [25 mM Hepes, 1.5% Triton X-100 (Wako), 1% sodium deoxycholate (Wako), 0.1% SDS, 0.5 M NaCl (Wako), 5 mM EDTA, 50 mM NaF (Sigma), 0.1 mM sodium vanadate (Sigma), and 1 mM PMSF, pH 7.8] with sonication. The lysates were centrifuged at 100,000 g for 15 min at 4 °C to give the plasma membrane fraction. The cells were also directly lysed in RIPA buffer with sonication, and the resultant samples were used as the total cell lysate. All samples were subjected to western blotting to detect H-Ras protein.

## Western blotting

A431 cells ($2 \times 10^5$) were seeded in 6-well plate and cultured overnight. After the culture supernatant was replaced with DMEM supplemented with 0.2% CS, the cells were pretreated with drugs for 15 min and stimulated with 30 ng/ml EGF. Following 24 h of incubation, cells were collected and lysed in RIPA buffer. After sampling, the samples were subjected to SDS-PAGE, and proteins were transferred onto a PVDF membrane (Millipore) by electroblotting. After the membranes had been incubated with primary and secondary antibodies, the immune complexes were detected with an Immobilon Western kit (Millipore), and

the luminescence was detected with a LAS-1000 mini (Fujifilm). Antibodies employed for immunoblotting include the following: anti-H-Ras antibody (sc-520), anti-Rap1 antibody (sc-65), anti-Rap1A antibody (sc-1482, the antibody specifically hybridizes to the unprenylated form of Rap1A[44–46]), and horseradish peroxidase (HRP)-conjugated anti-goat antibody (sc-2020) from Santa Cruz Biotechnology; anti-Akt antibody (#9272), anti-phospho-Akt (Ser473) antibody (#9271), anti-p44/42 MAP kinase (Erk 1/2) antibody (#9102), and anti-phospho-p44/42 MAP kinase (Erk 1/2) (Thr202/Tyr204) antibody (#9101) from Cell Signaling Technology; HRP-conjugated anti-mouse IgG (NA931) and anti-rabbit IgG (NA934) secondary antibodies from GE healthcare.

## Transwell migration assay

Cell migration was assayed with a chemotaxis chamber (Becton Dickinson). A431 cells ($7.5 \times 10^4$) suspended in DMEM with 0.2% CS were incubated in the upper chamber; the lower chamber contained DMEM with 0.2% CS in the presence or the absence of 30 ng/ml EGF. Drugs were added to both chambers. Following 24 h of incubation, the filter was fixed with MeOH and stained with hematoxylin (Sigma). The cells attached to the lower side of the filter were counted.

# Chapter 3

# A chemical genomic study identifying diversity in cell migration signaling in cancer cells

## 3.1 Introduction

Cell migration is central to many physiological processes, including development, tissue remodeling, and immune responses, and is also a required step in cancer metastasis. When a cell moves, multiple intracellular signaling networks control cell morphology. Signaling can be initiated through receptor tyrosine kinases, G protein-coupled receptors (GPCRs), integrin, and other receptors. These re-

ceptors are upregulated by extracellular stimuli that induce the activation of one or more intermediate signaling network branches. Finally, this signaling reaches the Rho family of small GTPase proteins. Many molecules and pathways have been implicated in intermediate signaling. For example, the Ras/Raf/MEK/Erk pathway has been reported to enhance cell motility[47–50]. In addition to the Ras/Raf/MEK/Erk pathway, a phosphoinositide 3-OH kinase (PI3K)/Akt pathway is widely known to regulate cell migration. This pathway is considered to be necessary for both Cdc42- and Rac1-induced cell motility and invasiveness[51], and it regulates the expression of Snail, which can increase cell motility[52]. c-Jun NH2-terminal kinase (JNK) and p38 mitogen-activated protein kinase (p38MAPK) have also been reported to play important roles in the signaling mechanisms involved in migration[53,54]. The role of Rho family small GTPase proteins, which is considered to constitute the final stage of the migration-signaling network, is known to regulate actin nucleation and polymerization. In particular, RhoA, Rac1, and Cdc42 are the major regulators of cytoskeletal remodeling. Activation of RhoA increases cell contractility and leads to the formation of focal adhesions and stress fibers[55]. Rac1 and Cdc42 activation induce the lamellipodia and filopodia, respectively[56,57]. Thus, the core elements of the intracellular migration-signaling network have been demonstrated.

However, it is likely that signaling molecules regulating cell migration in one

cancer cell may not regulate cell migration in other genetically distinct cancer cells. Indeed, the PI3K/Akt pathway, but not the MEK/Erk pathway, has been shown to be critical for prostate cancer cell migration[52]. Other studies have reported that the constitutive activation of the MEK/Erk pathway by oncogenic mutations of BRafV600E significantly induced cell migration through activation of RhoA GTPase[58]. In addition, the role of the Rho family of proteins in cell migration depends on specific cellular circumstances. The migration of several types of cancer cell is based on reorganization of the actin cytoskeleton, but their requirements for Rho and Rac signaling differ. With respect to a particular subset of cancer cells, cells migrated in a Rac-dependent manner, but Rho signaling was not essential. With respect to another subset of cancer cells, the inhibition of Rho/Rock signaling inhibited cell migration. Thus, although the same basic process of cell migration is induced, each type of cancer cell brings about migration in different contexts using distinct molecular repertoires. Therefore, understanding the diversity and commonality of signaling pathways that regulate cell migration in various cell types is important not only for basic research into cell migration, but also for the development of anti-metastatic anti-tumor drugs.

To address this issue, the author utilized the chemical genomic approach in which chemical inhibitors were used as probes to mimic loss-of-function phenotypes by inhibiting target protein activity; that is, if a chemical inhibitor suppresses

the cell migration of one type of cancer cell, the target protein of the inhibitor can be considered as being involved in the mechanism of cell migration of that type of cell. This chemical genetic approach is easily applicable to different cell models; therefore, it can determine which signaling molecule is universally involved in the migration mechanism in several types of cancer cells, and which one is specifically involved in each type of cell. In the present study, the author first examined the effects of various chemical inhibitors on cell migration in several cancer cell models, and subsequently obtained chemosensitive migratory profiles and undertook cluster analysis to classify the signaling molecules and their inhibitors as being either common to all cancer cells or specific to certain cell types.

## 3.2 Results

### Determination of appropriate experimental conditions for the wound healing assay

To select the cell models used in this study, sixteen cell lines, including colon carcinoma, esophageal carcinoma and lung cancer, were assessed with regard to their migration ability in response to migration factors using a wound healing assay[59]. The assay conditions of each cell line were optimized by examining migration factors such as growth factors, cell number required to maintain a confluent cell

monolayer, and an assay duration that clearly revealed the extent of motility. The author found out that the eight cell lines were suitable for use in a migration assay under the conditions indicated in **Table 3–1** (see also Experimental Procedure, section 3.4, page 58). The author also confirmed that both number of alive and dead cells in each condition were not clearly increased in optimized assay condition. The other cell lines tested were not affected by migratory stimuli or could not be scratched. Among the eight cell lines selected, EC17 cells migrated without extracellular stimulation, indicating that EC17 cells secrete chemoattractants into the media, and acquire motility by autocrine signaling. Conversely, others required the addition of migration factors, such as epidermal growth factor (EGF), conditioned medium from EC17 cells (EC17-CM), or serum (**Figure 3–1**). A431 cells and EC109 cells migrated in response to both EGF and EC17-CM. **Figure 3–2** shows the morphology of migration in these cell lines. A431 cells and EC109 cells moved together in sheet-like structures (collective migration), whereas the other cell lines showed a fibroblast-like spindle-shaped morphology and migrated individually like mesenchymal cells (mesenchymal migration).

**Table 3–1.** The experimental conditions of the wound healing assays

| Cell line | Origin | Cell number (cells/well) | Migration factor |
|---|---|---|---|
| 3Y1 | Rat fiblobrast | $7.5 \times 10^4$ | FBS 5% |
| A431 | Human epithelial carcinoma | $7.5 \times 10^4$ | EGF 3 ng/ml or EC17-CM |
| B16 | Mouse melanoma | $2.2 \times 10^5$ | EC17-CM |
| EC17 | Human esophageal carcinoma | $7.5 \times 10^4$ | None |
| EC109 | Human esophageal carcinoma | $7.5 \times 10^4$ | EGF 3 ng/ml or EC17-CM |
| HT1080 | Human fibrosarcoma | $7.5 \times 10^4$ | FBS 2% |
| TE8 | Human esophageal carcinoma | $7.5 \times 10^4$ | EGF 3 ng/ml |
| TT | Human medullary thyroid | $7.5 \times 10^4$ | EGF 3 ng/ml |

## Signaling pathway regulating for cell migration differs among three cancer cell lines

Next, to examine whether this analytical system could distinguish between common signals responsible for cell migration in the cancer cells tested and cell type-specific signals, using signal transduction inhibitors, a test was done using A431 cells, EC109 cells or TT cells that were randomly selected to analyze their migration ability. This was conducted following treatment with three kinase inhibitors; PI3K inhibitor, Rho-associated kinase (ROCK) inhibitor and EGF receptor kinase inhibitor. The reason why the author focused on the inhibitors of PI3K and ROCK for this test was that PI3K and ROCK were expected to reveal cell type-specific effects on migration. This is because they have been reported to be involved in

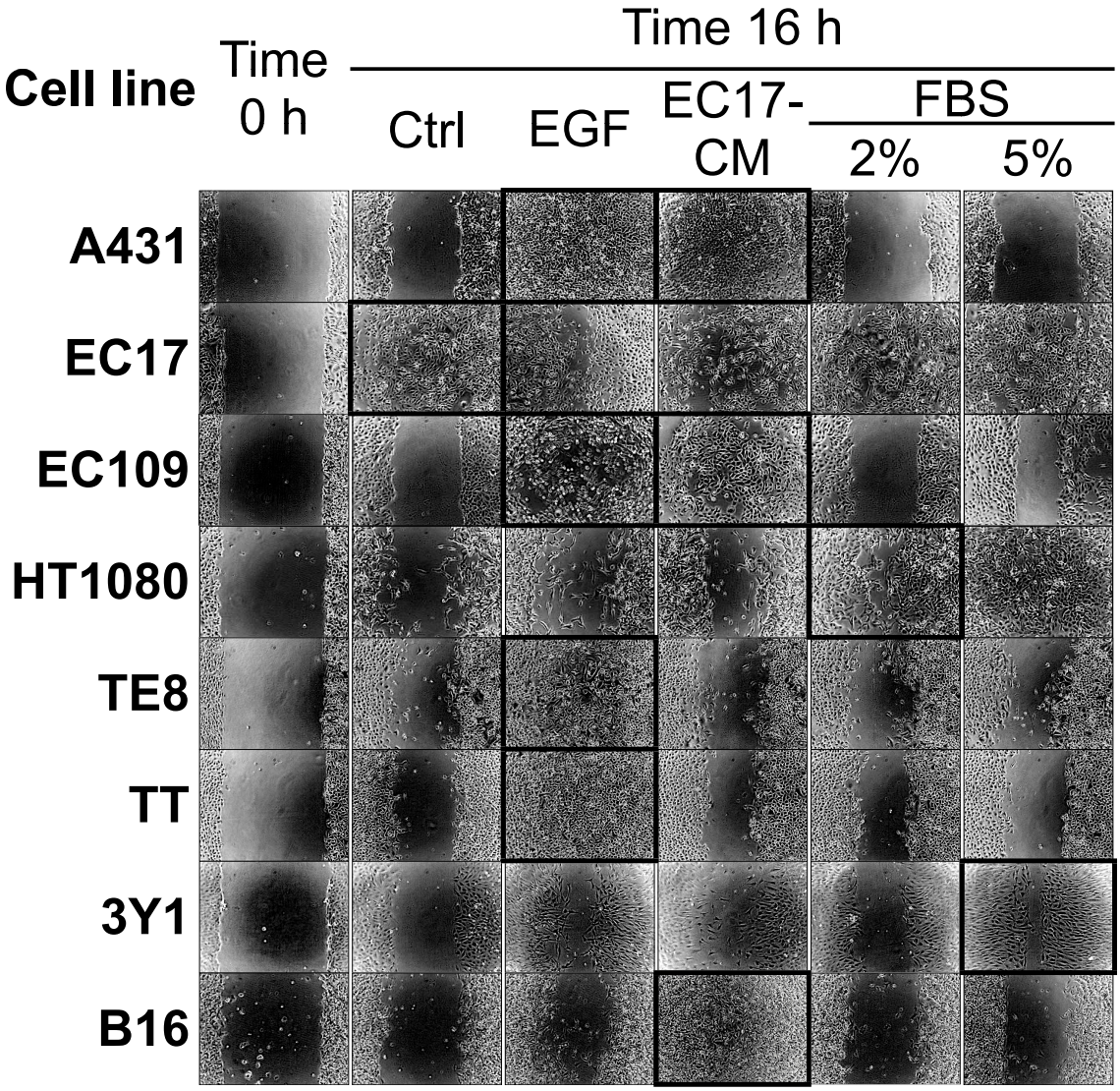


**Figure 3–1. The effect of migratory stimuli on cell migration in various cell lines.** Cells were scratched and then stimulated by EGF (3 ng/ml), serum, or conditioned medium from EC17 cells. After 16 h, wound areas were observed and photographed under microscopy.

regulation mechanisms of cell migration that are initiated downstream to growth factor signaling in a subset of cancer cells[51,60], although they were also reported to be dispensable for migration or membrane ruffling in certain conditions[61,62]. **Fig-**

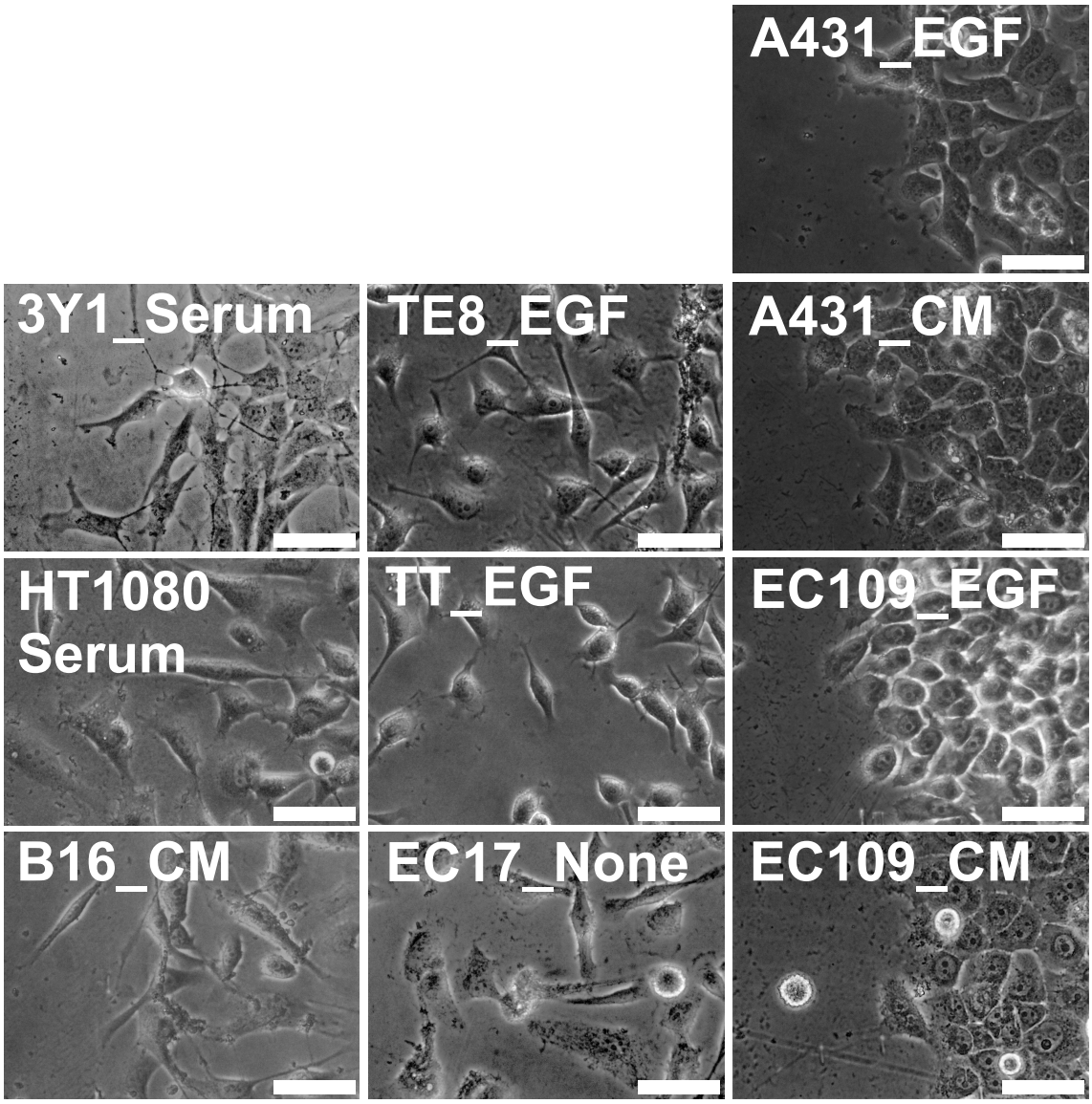


**Figure 3–2. Cell morphology of each migrating cell line.** Images of cell lines treated with migratory stimuli. Cells were photographed 10 h after stimulation. The scale bar represents 50 $\mu$m.

**ure 3–3a** presents the effect of these three inhibitors on the EGF-induced motility of A431 cells, EC109 cells, and TT cells. The extent of the cell motility was quantified by the measurement of the cell-free area in a photograph. The quantified

value was calculated over a fixed period of time, and was termed the 'migration inhibition score (MIS)' (**Figure 3–3b**). These results indicated that the EGF receptor kinase inhibitor, AG1478, inhibited the EGF-induced migration of all three cell lines, as expected. The PI3K inhibitor and LY294002 suppressed the EGF-induced migration of A431 cells and EC109 cells, but not of TT cells, indicating that PI3K plays a critical role in EGF-induced cell migration in A431 cells and EC109 cells. In contrast, the ROCK inhibitor, Y27632, suppressed migration only in A431 cells and TT cells, indicating that ROCK is indispensable for EGF-induced cell migration in A431 cells and TT cells but not in EC109 cells. Thus, this analytical system using chemical inhibitors of signal transduction easily distinguished between common and cell type-specific signals responsible for cell migration.

## Two-way cluster analysis of migration inhibition score

To reveal the diversity and generality of regulatory signaling in cancer cell migration, the author tested the effect of 34 different signal transduction inhibitors on the migration of ten types of cells, as shown in **Table 3–1**. **Table 3–2** lists the names of the chemical inhibitors of signal transduction used in this study, the experimental concentrations of each inhibitor, and their modes of action. Each inhibitor was used at three concentrations, the highest one being a concentration

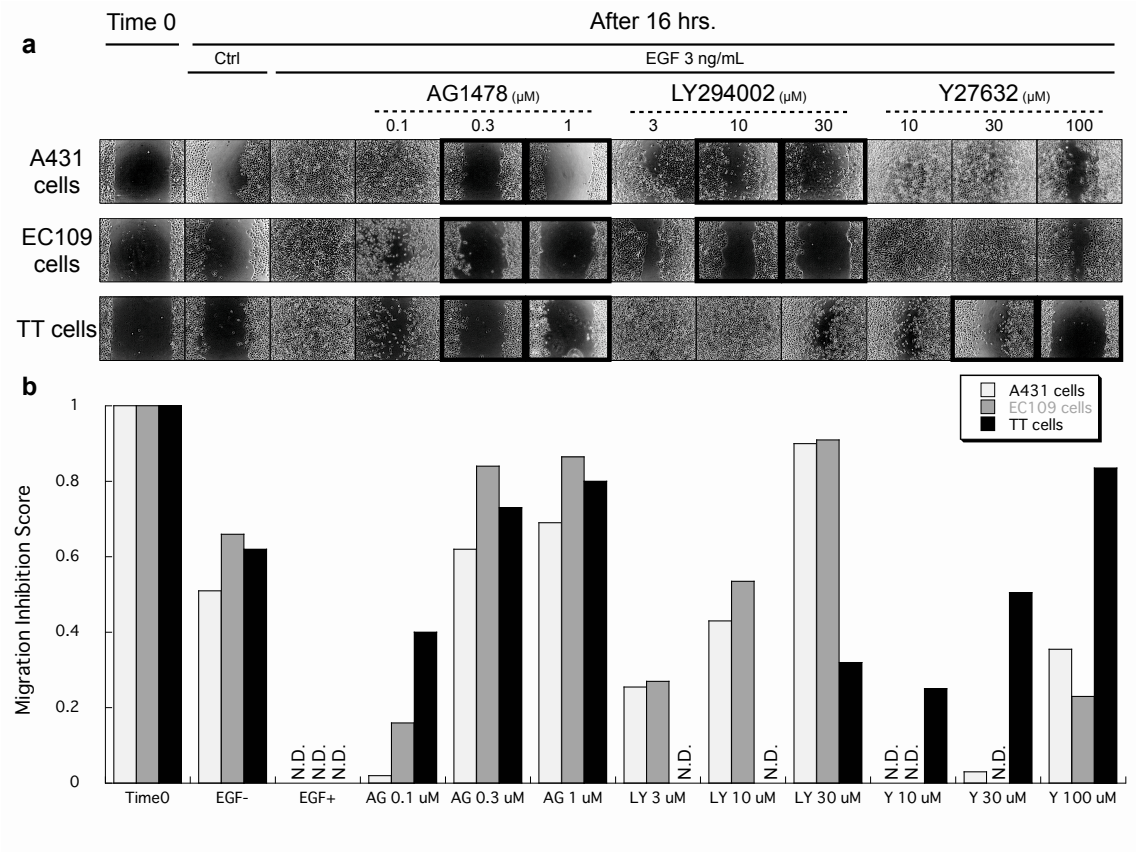


**Figure 3–3. The inhibitory pattern of cell migration was dependent on the types of cancer cell line.** A confluent monolayer of A431 cells, EC109 cells, and TT cells were scratched, treated with AG1478, LY294002, or Y27632, and stimulated with EGF as described in the Experimental Procedures. (**a**) Wound areas were photographed just after scratching (time zero). After 16 h, wound areas were photographed again (others). Black boxes indicate the inhibitory effects of chemicals on cell migration. The data were representative of two independent studies. (**b**) Migration inhibition score (MIS) of each experimental condition. MIS was quantified by measurement of the cell-free area in the picture. The quantified value was normalized against the value at time zero. The data were the average of two independent studies. N.D.; Not detected.

just below the level that would affect cell viability. Using these chemical inhibitors under the stated concentrations, the author carried out two highly reproducible, independent experiments on each cell line ($r = 0.94$, $p\text{-}value < 2.2 \times 10^{-16}$, **Fig-**

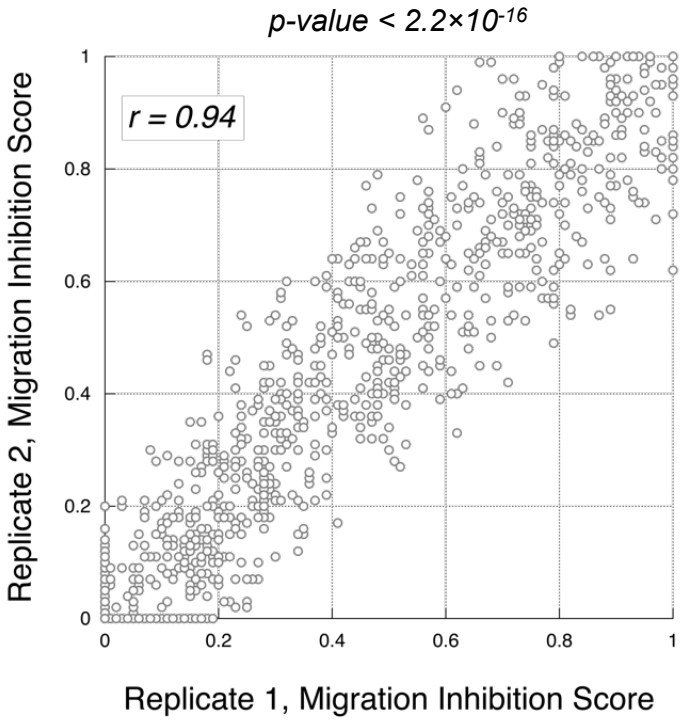


**Figure 3–4. Reproducibility of the migration inhibition score.** Before averaging, two independent data sets were checked for high correlation ($r = 0.94$, *p-value* $< 2.2 \times 10^{-16}$)

**ure 3–4**), and provided a final dataset by averaging the data points from the two experiments. Then a hierarchical cluster analysis was performed. The results are displayed in the form of a heat map and a tree diagram (**Figure 3–5**). The heat map employs a gradient color scale from green, indicating MIS = 0, to magenta, indicating MIS = 1.0, interpolated over black indicating MIS = 0.5.

As a result of these experiments, the characteristic features of cell migration affected by chemical inhibitors in cancer cells were classified into three general clusters (**Figure 3–5a**). Cluster A consisted of three types of cells and cell migration

**Table 3–2.** Compound concentrations and targets of inhibition used in this study

| Compound name | Concentration | Target / Mode of action | References |
|---|---|---|---|
| A23187 | 30, 100, 300 nM | $Ca^{2+}$ ionophore | 63 |
| AA861 | 3, 10, 30 $\mu$M | 5-Lipoxygenase | 64 |
| AG1478 | 0.1, 0.3, 1 $\mu$M | EGFR | 65 |
| Alendronate | 10, 30, 100 $\mu$M | FPP synthetase | 66 |
| ALLN | 1, 3, 10 $\mu$M | Calpain | 67 |
| Bafilomycin A | 0.3, 1, 3 nM | V-ATPase | 68 |
| Cytochalasin D | 0.1, 0.3, 1 $\mu$M | Actin filament | 69 |
| Herbimycin A | 1, 3, 10 $\mu$g/ml | HSP90 | 70 |
| Leptomycin B | 0.1, 0.3, 1 ng/ml | CRM1 | 71 |
| LY294002 | 3, 10, 30 $\mu$M | PI3K | 72 |
| Mevastatin | 3, 10, 30 $\mu$M | HMG-CoA reductase | 73 |
| Moverastin | 3, 10, 30 $\mu$M | Farnesyl transferase | 36 |
| MG132 | 10, 30, 100 nM | Proteasome | 74 |
| MK571 | 3, 10, 30 $\mu$M | CysLT1 | 75 |
| MK886 | 1, 3, 10 $\mu$M | FLAP | 76 |
| Okadaic acid | 3, 10, 30 nM | PP2A | 77 |
| Pacritaxel | 30, 100, 300 ng/ml | Tubulin depolymeration | 78 |
| PD169316 | 1, 3, 10 $\mu$M | p38 | 79 |
| Radicicol | 1, 3, 10 $\mu$g/ml | HSP90 | 80 |
| Rapamycin | 3, 10, 30 $\mu$g/ml | mTOR | 81 |
| Risedronate | 30, 100, 300 $\mu$M | FPP synthetase | 66 |
| SB203580 | 3, 10, 30 $\mu$M | p38 | 82 |
| SB218078 | 30, 100, 300 nM | Chk1 | 83 |
| SB415286 | 3, 10, 30 $\mu$M | GSK-3 | 84 |
| SP600125 | 1, 3, 10 $\mu$M | JNK | 85 |
| Thapsigargin | 3, 10, 30 nM | $Ca^{2+}$-ATPase | 86 |
| Trichostatin A | 30, 100, 300 ng/ml | Histone deacetylase(HDAC) | 87 |
| Tunicamycin | 30, 100, 300 ng/ml | Glycosylation | 88 |
| U0126 | 3, 10, 30 $\mu$M | MEK | 89 |
| UTKO1 | 1, 3, 10 $\mu$M | 14-3-3 | 90 |
| Vinblastin | 3, 10, 30 ng/ml | Tubulin polymeration | 91 |
| Wortmanin | 0.3, 1, 3 $\mu$M | PI3K | 92 |
| Xanthohumol | 0.3, 1, 3 $\mu$g/ml | Valosin-containing protein | 93 |
| Y27632 | 10, 30, 100 $\mu$M | ROCK | 94 |

properties: B16 cells, HT1080 cells, and 3Y1 cells; their cell migration displayed lower sensitivities to the inhibitors tested in this study than the others (**Figure 3–5b**). Cluster B consisted of cell migration of A431 cells and EC109 cells stimulated with either EGF or EC17-CM. The EGF-induced chemosensitive migratory profile of these cells was similar to that induced by EC17-CM. Cluster C consisted of three types of cells: EC17 cells, TE8 cells and TT cells.

It was expected that the chemical inhibitors that targeted the same molecule would be clustered into the same tree. Indeed, PD169316 and SB203580 as p38MAPK inhibitors, herbimycin A and radicicol (Hsp90 inhibitors), LY294002 and wortmannin (PI3K inhibitors), paclitaxel and vinblastine (tubulin binders), and alendronate and risedronate (farnesyl diphosphate (FPP) synthase inhibitors), were all clustered into the same position (indicated by gray boxes). These results indicate that the chemical genomic approach was able to classify the chemical inhibitors based on their respective modes of action, similar to previous studies on the chemosensitivities of cancer cells[95–97].

Furthermore, the chemical inhibitors used in this study were classified into four general clusters (**Figure 3–5b**), and each inhibitor in **Figure 3–5b** can be linked to its target molecule. The author also displayed the relationships of the targets of the inhibitors as a non-root phylogenetic tree (**Figure 3–5c**). The inhibitors grouped into cluster 1 contained the 5-lipoxygenase-activating protein

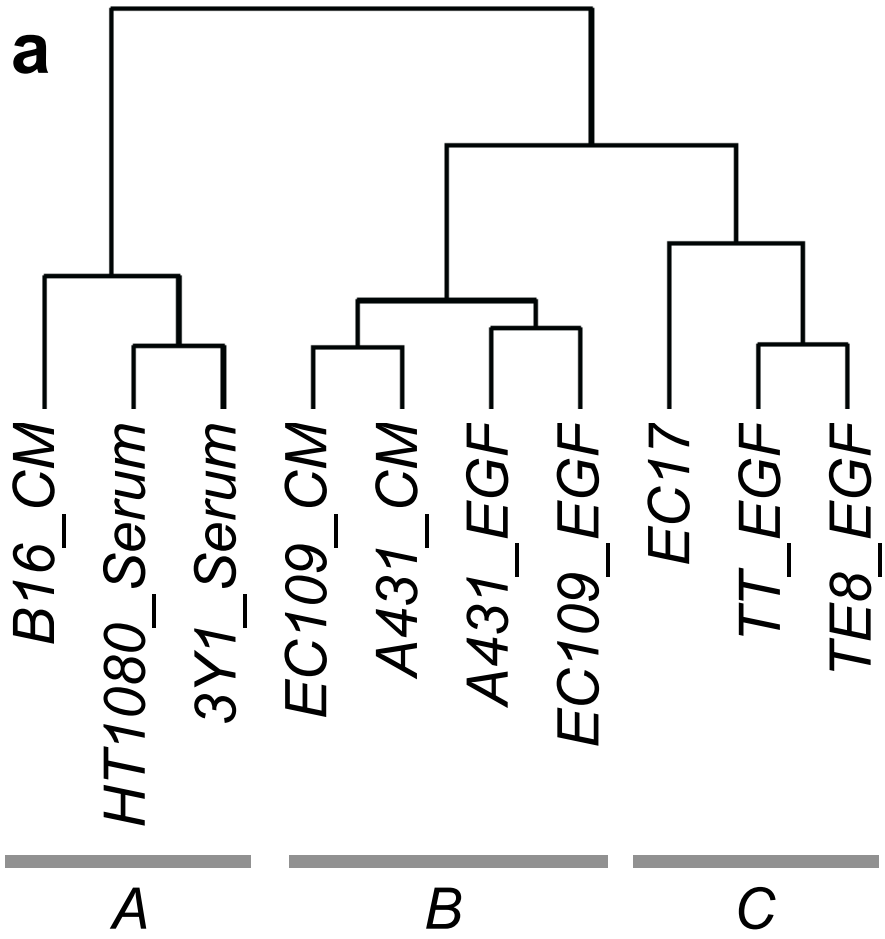


**Figure 3–5. Cluster analysis of the chemosensitivity profile of migration inhibition.** Cluster analysis was performed using Euclidean distance and Ward's method. (**a**) The MIS dataset was clustered into ten types of cell migration. Cell migration types were classified into three general clusters; clusters A, B, and C.

(FLAP) inhibitor, MK886, the vacuolar-type proton-ATPase (V-ATPase) inhibitor, bafilomycin A, and the FPP synthase inhibitors, the bisphosphonates. These inhibitors showed little inhibitory effect on cell migration in almost all cell types, thus the target molecules of these compounds had little bearing on the regulating mechanisms of cell migration tested in this study. Cluster 2 contained Y27632,

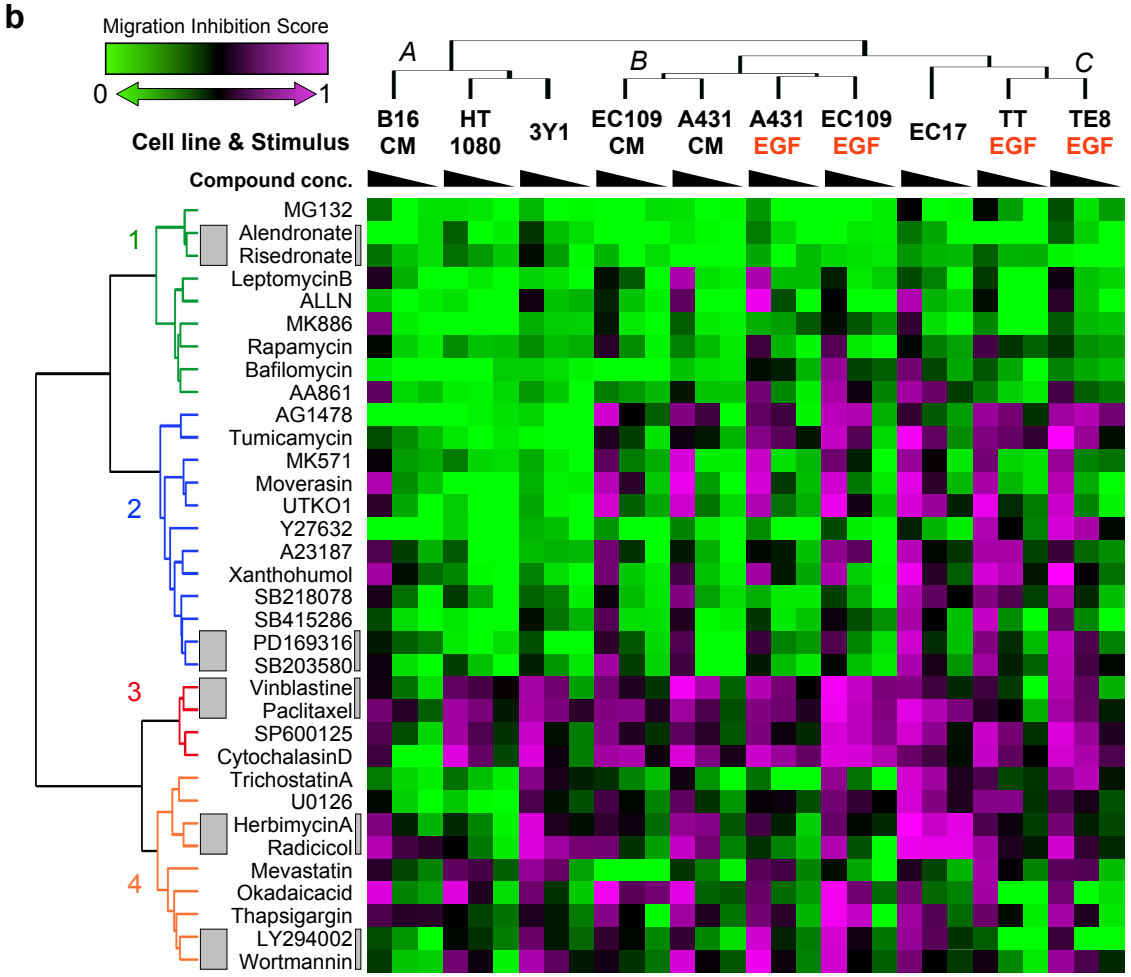


**Figure 3–5. Cluster analysis of the chemosensitivity profile of migration inhibition (*continued*).** (**b**) The MIS dataset was hierarchically clustered using data from 34 compounds. Rows indicate 34 different small molecular compounds. Columns indicate the ten migration types, including the three different compound concentrations. The heat map shows a gradient color scale from green, indicating MIS = 0, to magenta, indicating MIS = 1, interpolated over black for MIS = 0.5. Gray boxes beside the heat map indicate that two labeled compounds have almost the same molecular target. The 34 compounds were clustered into four general groups.

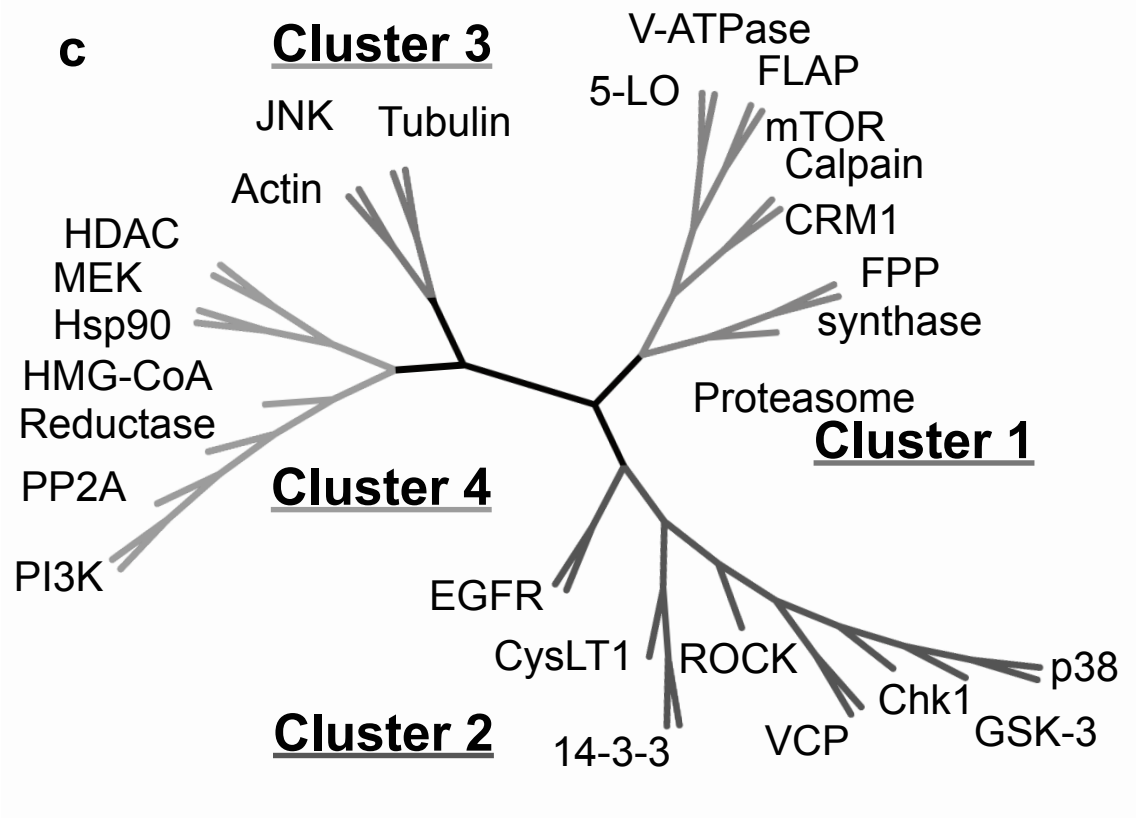


**Figure 3–5. Cluster analysis of the chemosensitivity profile of migration inhibition (*continued*).** (**c**) The non-rooted phylogenetic tree classifies the target molecules of the small molecular compounds tested in this study. Each small compound inhibitor used in this study can be replaced with its target molecule because most targets have already been identified. This phylogenetic tree presents the distances between molecules on the signaling network contributing to cell migration.

AG1478, the p38MAPK inhibitors, the Chk1 inhibitor, SB218078 and so on. Most of these compounds showed a stronger inhibitory effect on cell migration, classified into migration type clusters B and C, in contrast to cluster A. Therefore, the target molecules of these compounds were not involved in the migration of HT1080 cells and 3Y1 cells but they did regulate cell migration in the subset of cell lines grouped

into clusters B and C. Cluster 3 contained SP600125 and the cytoskeleton-affecting compounds. This group of inhibitors affected all types of cell migration, indicating that not only cytoskeletal molecules, but also JNK, are common regulators of cell migration, irrespective of cell type. Cluster 4 contains the Hsp90 inhibitors, the MEK inhibitor, U0126, and the PI3K inhibitors. These inhibitors also suppressed migration in all types of cell with different potencies depending on cell type. Thus the target molecules of these inhibitors also played a common role in all types of cell migration.

## 3.3 Discussion

In the present study, the author investigated some general and specific regulatory mechanisms of cell migration. To accomplish the objective, the author assessed the effects of 34 different kinds of chemical inhibitors on the migration of ten types of cells using a wound healing assay, and subsequently performed a cluster analysis on the dataset. One significant aspect of this work is that each compound showed a characteristic cell type-specific inhibitory pattern on migration, and hierarchical clustering precisely classified the compounds according to their respective targets, such as p38, Hsp90, PI3K, tubulin and FPP synthase (**Figure 3–5b, c**). Therefore, this research could be applied to predict the mode

of action of each compound. For example, moverastin and its derivative UTKO1 were classified into same cluster, in spite of the different functions of these two compounds, which have similar structures. The author previously reported that moverastin was an inhibitor of farnesyltransferase[36], and it inhibited cell migration by inhibiting farnesylation in H-Ras. On the other hand, UTKO1 was reported not to inhibit farnesyltransferase[41], but it directly bound to 14-3-3ζ, and inhibited the interaction between the 14-3-3 proteins and Tiam1, a protein that has been reported to be a Rac-specific GEF. This resulted in the inhibition of Rac1[90]. Therefore, it has been demonstrated that the migration of epithelial cells requires Taim1-mediated Rac1 activation. However, because the profiling data demonstrated that moverastin and UTKO1 were classified in the same cluster, Mr. Kei Takano, one of the author's collegue, examined the possibility that moverastin could bind to 14-3-3ζ, and obtained similar results (unpublished data). Therefore it is likely that moverastin might inhibit cell migration not only by inhibiting protein farnesylation, but also by inhibiting Tiam1-mediated Rac1 activation. In addition, because the CysLT1 antagonist MK571 was classified into the same cluster as moverastin and UTKO1, this raised the possibility that CysLT1 signaling might be closely related to Tiam1-mediated Rac1 activation. The author therefore confirmed the possibility by RNAi experiments. The successful knockdown of CysLT1 by siRNA was confirmed by western blotting (**Figure 3–6a**). Silencing

of CysLT1 expression consequently suppressed not only EGF-induced Tiam1 expression at protein level, but also EGF-induced Rac1 activation (**Figure 3–6b, c**). These results indicate that EGF-induced Rac1 activation was actually regulated by CysLT1 signaling. Thus, the author's profiling data appeared to be helpful in the mechanistic study of cell migration. At the same time, the author's clustering data indicated that xanthohumol was grouped in the same category as the $Ca^{2+}$ ionophore, A23187. Recently, xanthohumol was reported to bind to and inhibit valosin-containing protein (VCP)[93], resulting in the induction of ER stress. Although A23187 is also a well-known inducer of ER stress[98,99], other ER stress-inducing compounds such as tunicamycin and thapsigargin were classified into different clusters from xanthohumol and A23817. Therefore, an interpretation of the clustering data must be made with great caution.

The characteristics of cell migration based on chemical inhibitor-sensitivity profiles were grouped into three clusters (clusters A, B and C), and chemical inhibitors were classified into four general groups (clusters 1 to 4, **Figure 3–5**). Although the motilities of several cell lines the author tested are upregulated by extracellular stimuli such as EGF, they migrated a little without stimulation (**Figure 3–1**). Additionally, EC17 cells did not require extracellular stimulation to migrate. Thus the author just has to evaluate and discuss chemical inhibitor-sensitivity profiles as total effects on 'basal' and 'stimulated' motility. JNK in-


**Figure 3–6. Knockdown of CysLT1 suppressed EGF-induced Tiam1 expression and Rac1 activation.** (**a**) A431 cells were transfected with control or CysLT1 siRNA and cultured for 72 h. Then the cells were collected and subjected to western blotting using the indicated antibodies. (**b**) The effect of silencing CysLT1 on the protein level of Tima1. Control or CysLT1 siRNA-transfected A431 cells were stimulated with EGF for 6 h. Then the cells were subjected to western blotting using indicated antibodies. (**c**) The effect of silencing CysLT1 on Rac1 activation. Control or CysLT1 siRNA-transfected A431 cells were stimulated with EGF for 12 h. Then Rac1-GTP were examined by pulldown assay.

hibitor, tubulin and actin polymerization inhibitors in cluster 3 showed a potent inhibitory effect on migration of all cell types, indicating that JNK is a common and crucial signaling molecule regulating cell migration. Indeed, JNK was reported to modulate migration in a broad range of cell types[100], such as keratinocytes[53], neuronal cells[101], and many cancer cell lines[102,103]. Because dynamic reorganization of the actin cytoskeleton is considered to be key to the cell's capacity to migrate[104], JNK may be indispensable for the phosphorylation of paxillin and F-actin polymerization[53,54].

In contrast, some of the chemical inhibitors classified into cluster 2 (AG1478, tunicamycin, the CysLT1 antagonist MK571, Moverastin and UTKO1) affected the

migration of cell lines of epithelial origin (EC109 cells, A431 cells, EC17 cells, TT cells, TE8 cells) in clusters B and C, but did not affect the migration of cell lines of mesenchymal origin (HT1080 cells and 3Y1 cells) placed in cluster A. This suggests that there is an essentially different regulatory mechanism of cell migration between cells of these two origins. The regulatory mechanism of cell migration of B16 cells appeared somewhat similar to that of cell lines of mesenchymal origin when compared to those with an epithelial origin.

Moreover, although EGF did induce migration of cells of epithelial origin (TT cells, TE8 cells, A431 and EC109 cells), differential sensitivities to several inhibitors was observed in A431 and EC109 cells in cluster B and TT cells and TE8 cells in cluster C. These results suggest that the EGF signaling pathway leading to migration of A431 and EC109 cells in cluster B was not identical to that of TT cells and TE8 cells in cluster C. Furthermore, EC17-CM also induced migration of A431 and EC109 cells with a similar chemosensitive profile to that seen in EGF-induced migration, indicating that EC17-CM might activate almost the same signaling pathway as the EGF-signaling pathway in the context of the migration of these cells. One exception is AA861, an inhibitor of 5-lipoxygenase (5-LO). AA861 inhibited the EGF-induced migration of A431 cells and EC109 cells, but not EC17-CM-induced migration. Therefore, production of leukotriene(s) catalyzed by 5-lipoxygenase is required for EGF-induced cell migration, whereas EC17-CM

may already contain leukotriene(s), so EC17-CM-induced cell migration was not inhibited by inhibition of 5-LO. In addition, a specific inhibitor of EGF-receptor tyrosine kinase (AG1478) potently inhibited the EC17-CM-induced migration of A431 and EC109 cells, but weakly inhibited migration of EC17 cells, indicating that EC17 cells might produce and secrete EGF, whereas EC17 cells underwent cell migration in response to migration factors other than EGF.

Interestingly, the mode of EGF-induced cell migration based on cell morphology can also be classified into clusters B and C. As shown in **Figure 3–2**, A431 cells and EC109 cells in cluster B showed collective migration, whereas TT, TE8 and EC17 cells in cluster C showed a mesenchymal migration. With respect to collective migration, cells moved in groups and a leading cell at the tip of the group generated the migratory traction and the cells in the middle and at the back of the group were predominantly dragged passively. In contrast, mesenchymal migration required the formation of protrusions at the leading edge and actomyosin-mediated retraction of the trailing edge. This raises the possibility that the difference in the mode of cell migration of epithelial cells might be correlated with the differences in sensitivity to chemical inhibitors between clusters B and C. The ROCK inhibitor, Y27632, is a representative example; it inhibited mesenchymal migration of TT cells and TE8 cells more potently than collective migration of A431 and EC109 cells. Indeed, Rho-ROCK signaling is proposed

to induce actomyosin-mediated retraction at the trailing edge in mesenchymal migration[61]. As an exception, the ROCK inhibitor Y27632 failed to inhibit mesenchymal migration of EC17 cells. At present, although the author do not know why inhibition of ROCK did not suppress the migration of EC17 cells, one possible explanation is that another Rho effector, citron kinase or mDia, could regulate mesenchymal migration if used instead of ROCK. Moreover, the GSK-3 inhibitor (SB415286) and the p38MAPK inhibitors (PD169316 and SB203580) also inhibited the EGF-induced migration of TE8, TT, and EC17 cells more potently than they did in A431 and EC109 cells. This indicates that GSK-3 and p38MAPK might be involved in the Rho-ROCK signaling responsible for mesenchymal migration. These ideas can be supported by other findings. GSK-3 phosphorylated and inactivated p190A RhoGAP, which is a key Rho regulatory protein in the context of cell migration. This resulted in the activation of Rho-ROCK signaling[105]. Furthermore, the phosphorylation of protein substrates by GSK-3 often requires the "priming" of a neighboring residue by a distinct kinase, leading to subsequent phosphorylation by GSK-3[106]. p38MAPK could effectively prime the C-terminal fragment of p190A RhoGAP for subsequent phosphorylation by GSK-3. The Chk1 inhibitor SB218078 also inhibited EGF-induced migration of TE8, TT, and EC17 cells more potently than it did in A431 and EC109 cells. However, at present the author do not know how Chk1 is involved in mesenchymal migration. Moreover,

the author cannot exclude the possibility that Chk1 is important in mechanisms other than the mode of cell migration. Contrastingly, although PI3K, PP2A and HMG-CoA reductase somewhat selectively inhibited EGF-induced collective migration, the role of these enzymes on cell migration remains unclear.

In summary, the author has shown that JNK is a signaling molecule common to all types of cell migration, and many molecules have diverse functions in the migration of particular types of cancer cells. The author determined this using a chemical genomic approach. This approach can be used as a tool for understanding the diversity and similarities in cancer cell migration signaling, opening up the potential for revealing novel molecular targets in cancer therapy.

## 3.4 Experimental Procedures

### Cell culture

3Y1 and HT1080 cells were maintained in Dulbecco's modified Eagle's medium (DMEM) supplemented with 10% fetal bovine serum (FBS), 0.1 g/l kanamycin, 100 units/ml penicillin G, 0.6 g/l L-glutamine, and 2.5 g/l $NaHCO_3$. A431 cells were maintained in DMEM supplemented with 5% calf serum (CS), 0.1 g/l kanamycin, 100 units/ml penicillin G, 0.6 g/l L-glutamine, and 2.5 g/l $NaHCO_3$. B16 cells were maintained in DMEM supplemented with 8% FBS, 0.1 g/l kanamycin, 100 units/ml

penicillin G, 0.6 g/l L-glutamine, and 2.5 g/l $NaHCO_3$. EC17, EC109, TE8, and TT cells were maintained in Roswell Park Memorial Institute (RPMI)1640 supplemented with 5% FBS, 0.1 g/l kanamycin, 100 units/ml penicillin G, 0.6 g/l L-glutamine, and 2.5 g/l $NaHCO_3$. For routine culture, cells were incubated in a standard humidified incubator at 37 °C with 5% $CO_2$.

## Reagents

A23187, AG1478, ALLN, cytochalasin D, okadaic acid, rapamycin, and Y27632 were purchased from Calbiochem. MK571 was purchased from Cayman. Thapsigargin was purchased from Santa Cruz Biotechnology. AA861, bafilomycin A, LY294002, mevastatin, MG132, MK886, PD169316, SB203580, SB218078, SB415286, SP600125, tunicamycin, U0126, wortmannin, and epidermal growth factor were purchased from Sigma. Paclitaxel, radicicol, and vinblastine were purchased from Wako. Herbimycin A, moverastin, and xanthohumol was purified from cultures of *Streptomyces* sp. in our own laboratory. Leptomycin B and trichostatin A were kind gifts from Dr. Minoru Yoshida at RIKEN. Compound UTKO1 was synthesized and kindly donated by Dr. Hidenori Watanabe of the University of Tokyo. Alendronate and risedronate were kind gifts from Astellas Pharma Inc. (formerly Yamanouchi Pharmaceutical Co., Ltd).

## Preparation of conditioned medium (CM) from EC17 cells

EC17 cells were seeded at a density of $1.0 \times 10^6$ / 100 mm dish. The next day, the medium was replaced with 10 ml of RPMI1640 containing 1% FBS. After 24 h, the medium were recovered and sterilized by filtration.

## Wound healing assay

A confluent monolayer of cells in a 48-well plate was scratched with a micropipette tip to create a cell-free zone in each well, about 1 mm in width. The medium was replaced with RPMI1640 with 1% FBS with or without test compound, and cells were either treated with the migratory stimulus or not treated with it so as to serve as controls. After a fixed period of time, cells were observed and photographed under a microscope. The experimental conditions for each cell line are described as **Table 3–1**. Wound areas were quantified using ImageJ software (rsbweb.nih.gov/ij/). After photographing, cells were trypsinized and collected, and cell viability was determined by trypan blue dye exclusion assay. Average migration inhibition scores were calculated from two independent experiments.

## siRNA transfecion

siRNA double-stranded oligonucleotides designed to interfere with the expression of CysLT1 (sense "5'-UGU UUG UUG GCU UUA UCA UCC CUU U-3'",

HSS116670, Invitrogen), and Stealth™ RNAi Negative Control (Invitrogen) as a negative control were used. Reverse transfection was demonstrated by using Lipofectamine RNAiMAX reagent (Invitrogen) according to the manufacturer's instructions. Briefly, after being trypsinized, cells were resuspended in antibiotic-free medium, and mixed with OPTI-MEM (Gibco) including 50 nM siRNA and Lipofectamine RNAiMAX. After incubation for 20 min at room temperature, cells were diluted with cultured medium and seeded into a 100 mm dish. siRNA-transfected cells were reseeded into a 6-well plate for the detection of Tiam1 protein, or 150 mm dish for the detection of active Rac1 at 72 h after transfection. The silencing of CysLT1 was detected by measuring the expression of each protein just before drug treatment.

## Western blotting

Cells were seeded in 6-well plate or 150 mm dish and cultured overnight. After the culture supernatant was replaced with DMEM supplemented with 0.2% CS, the cells were pretreated with drugs for 15 min and stimulated with 30 ng/ml EGF for indicated time. Cells were collected, lysed, and subjected to western blotting as indicated in **chapter 2**, page 33. Antibodies employed for immunoblotting include the following: anti-CysLT1 antibody (ab93481) from Abcam, anti-CysLT2 antibody (120550) form Cayman, anti-Rac1 antibody (05-389) from Millipore, anti-

Tiam1 antibody (C-16) from Santa Cruz Biotechnology, and anti-$\beta$-actin antibody (AC-74) from Sigma, HRP-conjugated anti-mouse IgG (NA931) and anti-rabbit IgG (NA934) secondary antibodies from GE healthcare.

## Rac1 pulldown assay

Cells were lysed with magnesium-containing lysis buffer [MLB: 25 mM HEPES (pH 7.5), 150 mM NaCl, 1% NP-40, 0.25% sodium deoxycholate, 10% glycerol, 25 mM NaF, 10 mM $MgCl_2$, 1 mM EDTA, 1 mM $Na_3VO_4$, and a protease inhibitor cocktail (Roche)]. The cell lysates were centrifuged at 15,000 g for 10 min at 4 °C. Recombinant protein binding domain of Pak1 (Pak1-PDB) was conjugated with GSH-agarose beads (GE healthcare), and the Pak1-PDB-conjugated beads were incubated with the supernatant at 4 °C for 1 h. The beads were washed three times with MLB, then active Rac1 was eluted by boiling in SDS sample buffer for 5 min. The resultant samples were subjected to western blotting.

## Cluster analysis

The value of migration inhibition was ordered according to the experimental conditions of cell migration or the compounds used. These profiles were analyzed by hierarchical clustering (Ward's linkage based on Euclidean distance) and visualized a heat map using the R project package (www.r-project.org/).

# Chapter 4

# A combination study of chemical and systems biology identifying novel features of signaling pathway in cancer cell migration

## 4.1 Introduction

In previous study described in **chapter 3**, the author investigated the effect of small molecule inhibitors on ten types of cell migration activity, and distinguished between the common and cell type-specific signals responsible for cell migration[107].

This research showed the molecules which are actually involved in each cancer cell migration, however, signaling network of these molecules for regulating cell migration remains unclear. To address this issue, the author utilized the combination approach between chemical genetics and systems biology. In the present study, the author focused on the three cancer cell lines, epidermal carcinoma A431 cells, esophageal carcinoma EC109 cells, and thyroid carcinoma TT cells; which were divided into different cell migration types whereas all of these cell lines acquired the motility by EGF stimulation. Firstly, the author experimentally measured the time course of protein phosphorylation and expression of signaling molecules induced by EGF in three cancer cell lines, and next examined the effect of several small molecule inhibitors, which could suppress motility, on EGF signaling. Based on obtained chemosensitive profiles, the author undertook deduction of cell migration pathway in each cancer cell line, and compare the pathway map to reveal the network topology as being either common to all cancer cells or specific to certain cell types.

## 4.2 Results

### The different activation pattern of EGF signaling among three cancer cell lines

The purpose of this study is to analyze cell migration signaling in several cancer cells by the combination approach of chemical biology and network biology, and to reveal diversity and unity of cell migration signaling in cancer cells. Firstly, the author investigated which signaling pathways are activated, and when signaling pathways are activated in three cancer cell lines by EGF stimulation. **Figure 4–1** shows the time course of protein phosphorylation and expression of signaling molecules induced by EGF in three cancer cell lines. The reason why the author set the time course from 5 min (short-time) to 12 h (long-time) is that there are several reports concluded the activation of signaling molecules in long-time course but not in short-time course is essential for cell fate, such as cell growth[108], migration[90], and differentiation[109,110].

As a result, EGF phosphorylated its receptor, EGFR at 5 min after stimulation, and subsequently several signal transduction molecules such as Erk, p38, and c-Jun, were activated. The protein expression level of p38, Erk, and Akt are almost constant in the presence of EGF in three cancer cell lines; p38 was phosphorylated at 5 min after EGF stimulation in all cell lines; the increase of c-Fos protein

expression and the phosphorylation of c-Jun were induced at 1 h after EGF stimulation in all cell lines. While some of activation or protein expression pattern of signaling molecules are similar between three cancer cell lines, several other molecules showed different activation pattern between three cancer cell lines. For example, the phosphorylation level of Akt (p-Akt)(S473) and p-Akt(T308) were induced at 5 min ~ 1 h after EGF stimulation in EC109 cells and TT cells, however these phosphorylation level were not dramatically increased in A431 cells (**Figure 4–2a**). In addition, the relative intensity of p-Akt(T308) hit a peak at 5 min in TT cells (**Figure 4–2c**), but at 1 h in EC109 cells (**Figure 4–2b**). The pattern of Erk phosphorylation (p-Erk) is also different between three cancer cell line. The relative intensity of p-Erk hit a peak at 5 min in A431 cells and EC109 cells (**Figure 4–2a, b**), but at 1 h in TT cells (**Figure 4–2c**). In addition, relative level of sustained p-Erk is little different: lower level in EC109 cells; middle level in A431 cells; high level in TT cells. The protein expression level of EGFR is constant in the presence of EGF in A431 cells, whereas it decreased in EC109 cells and TT cells. In this way, there are some differences in the time course pattern of EGF-induced signaling among three cancer cell lines.

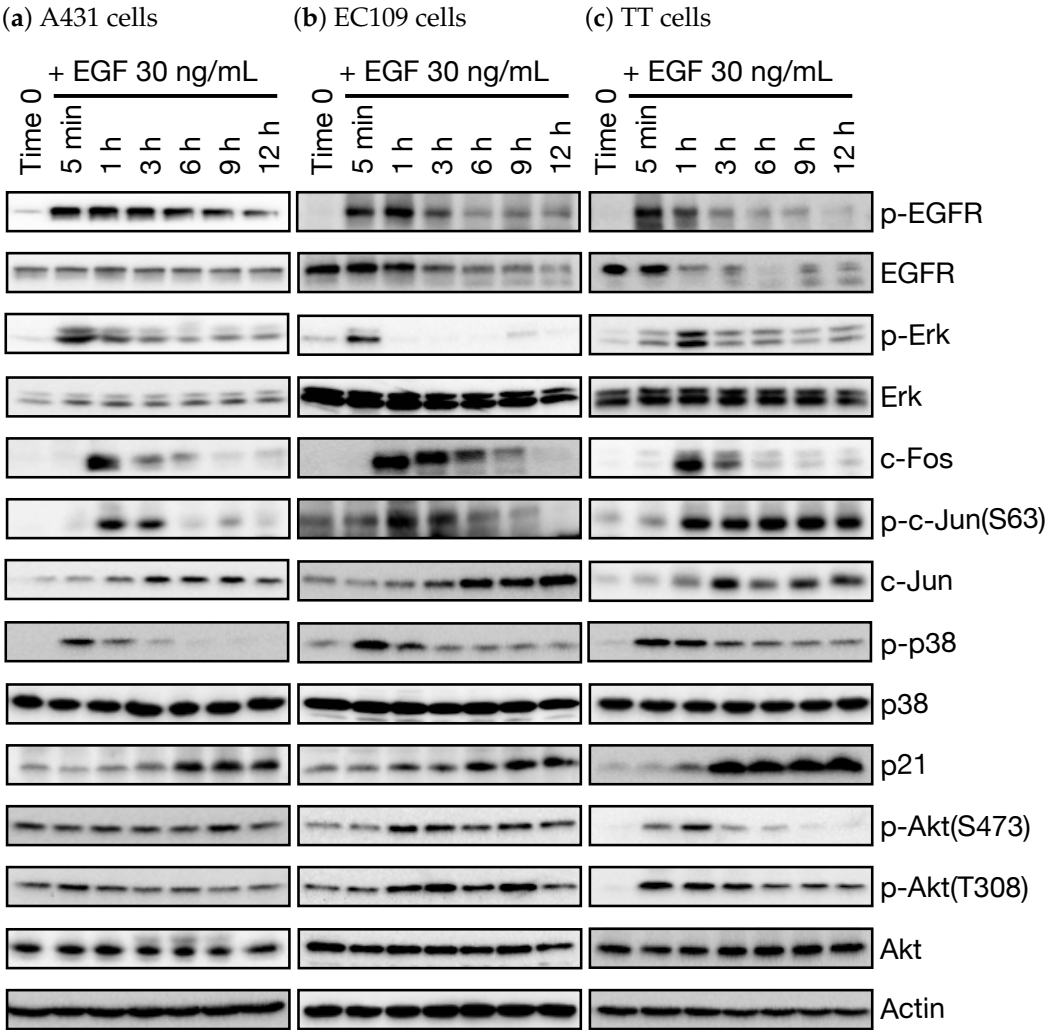


**Figure 4–1. EGF-induced time course of protein phosphorylation and expression in three cancer cell lines.** (**a**) A431 cells, (**b**) EC109 cells, (**c**) TT cells were stimulated by EGF (30 ng/ml) for indicated time and total cell lysates were subjected into western blotting.

## The effects of migration inhibitors on EGF-induced migration signaling

To analyze which protein regulates the EGF-induced migration signaling in each cancer cell, the author next examined the effects of 15 compounds, which affect cell

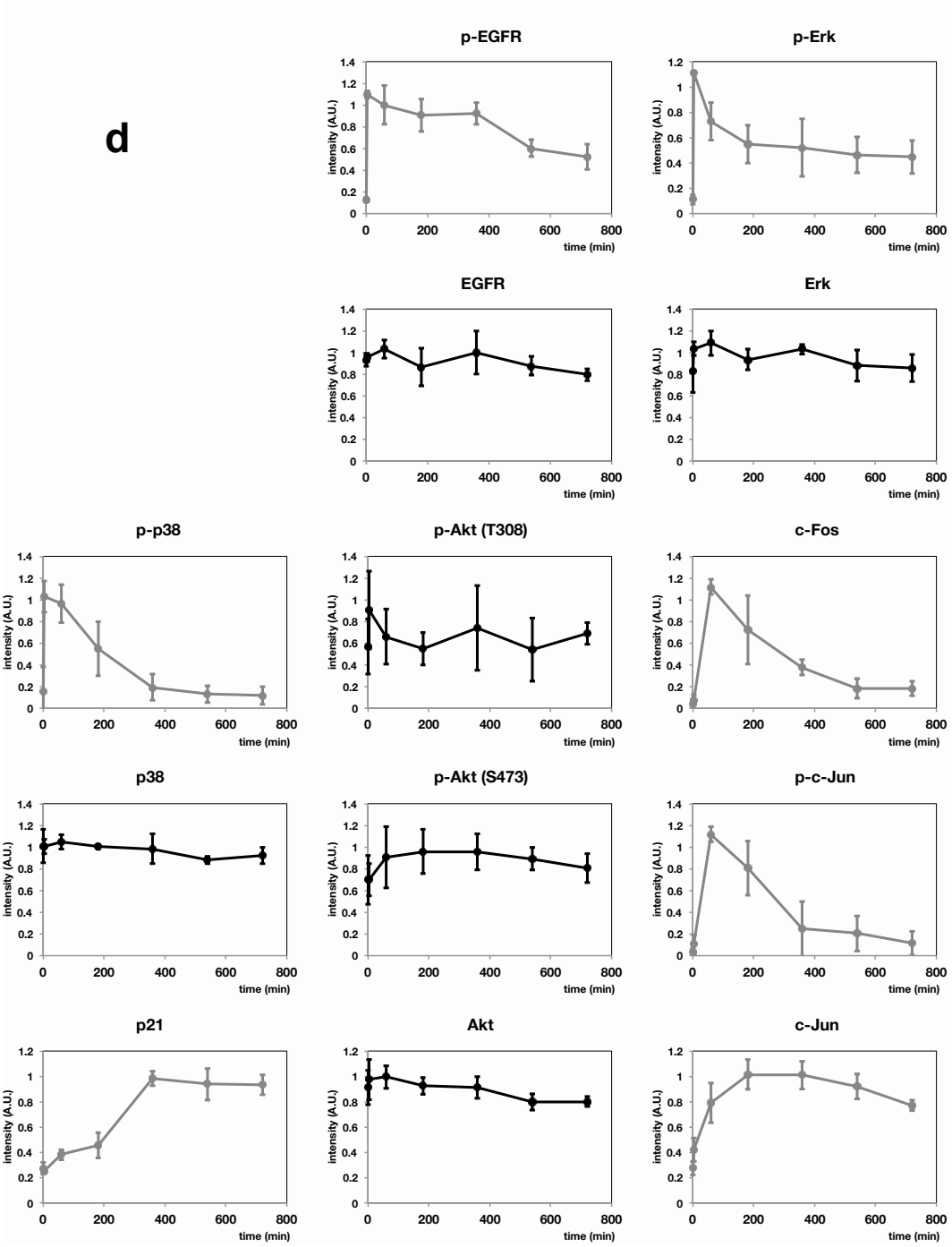


**Figure 4–2. Quantitative data of EGF-induced protein phosphorylation and expression.** (**a**) Quantitative data of **Figure 4–1a**; A431 cells. A.U., arbitrary unit. The means and SDs of three independent experiments are shown. Gray plots mean that EGF stimulation causes significant change of A.U. of each molecule (One-way ANOVA).

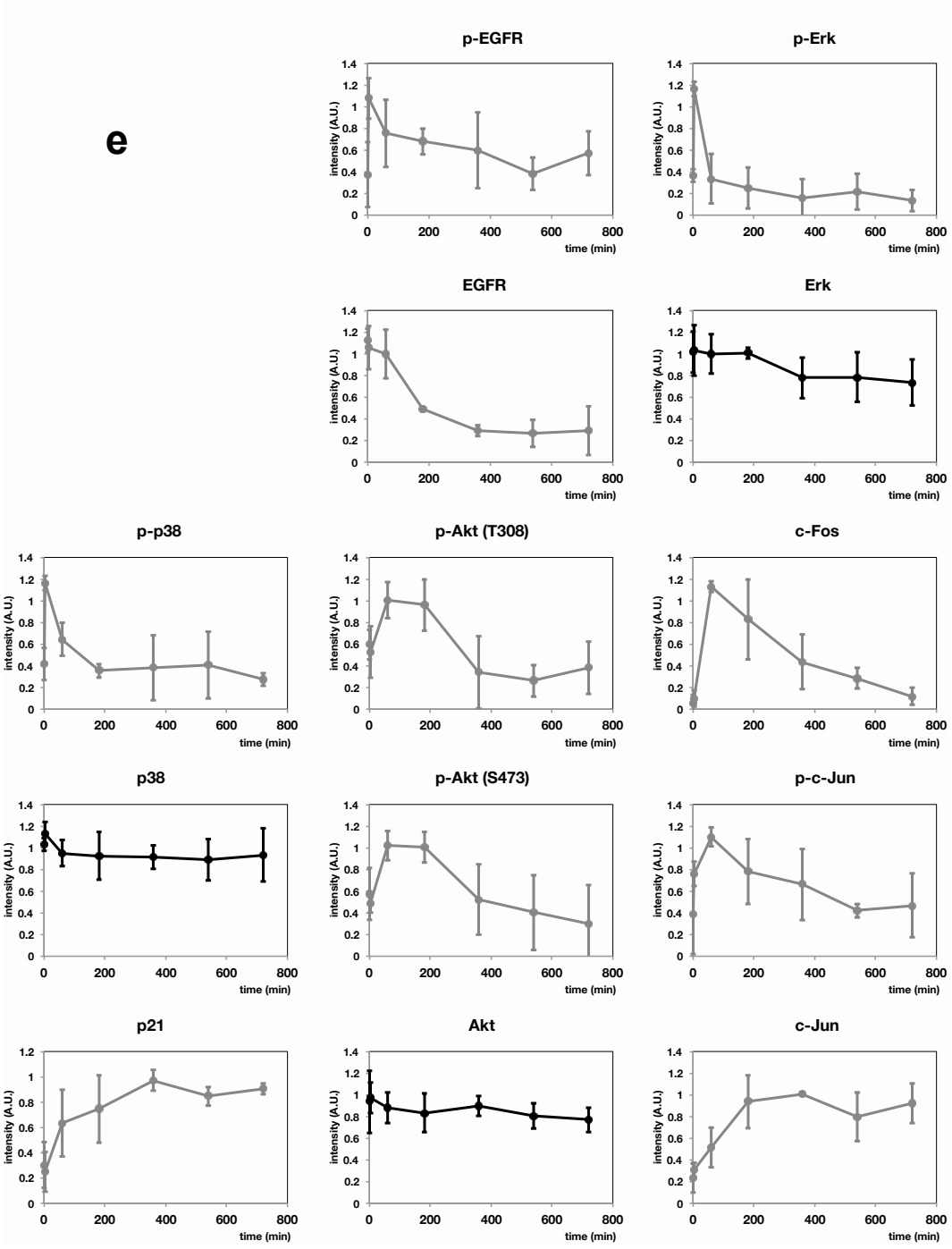


**Figure 4–2. Quantitative data of EGF-induced protein phosphorylation and expression (*continued*).** (**b**) Quantitative data of **Figure 4–1b**; EC109 cells. A.U., arbitrary unit. The means and SDs of three independent experiments are shown. Gray plots mean that EGF stimulation causes significant change of A.U. of each molecule (One-way ANOVA).

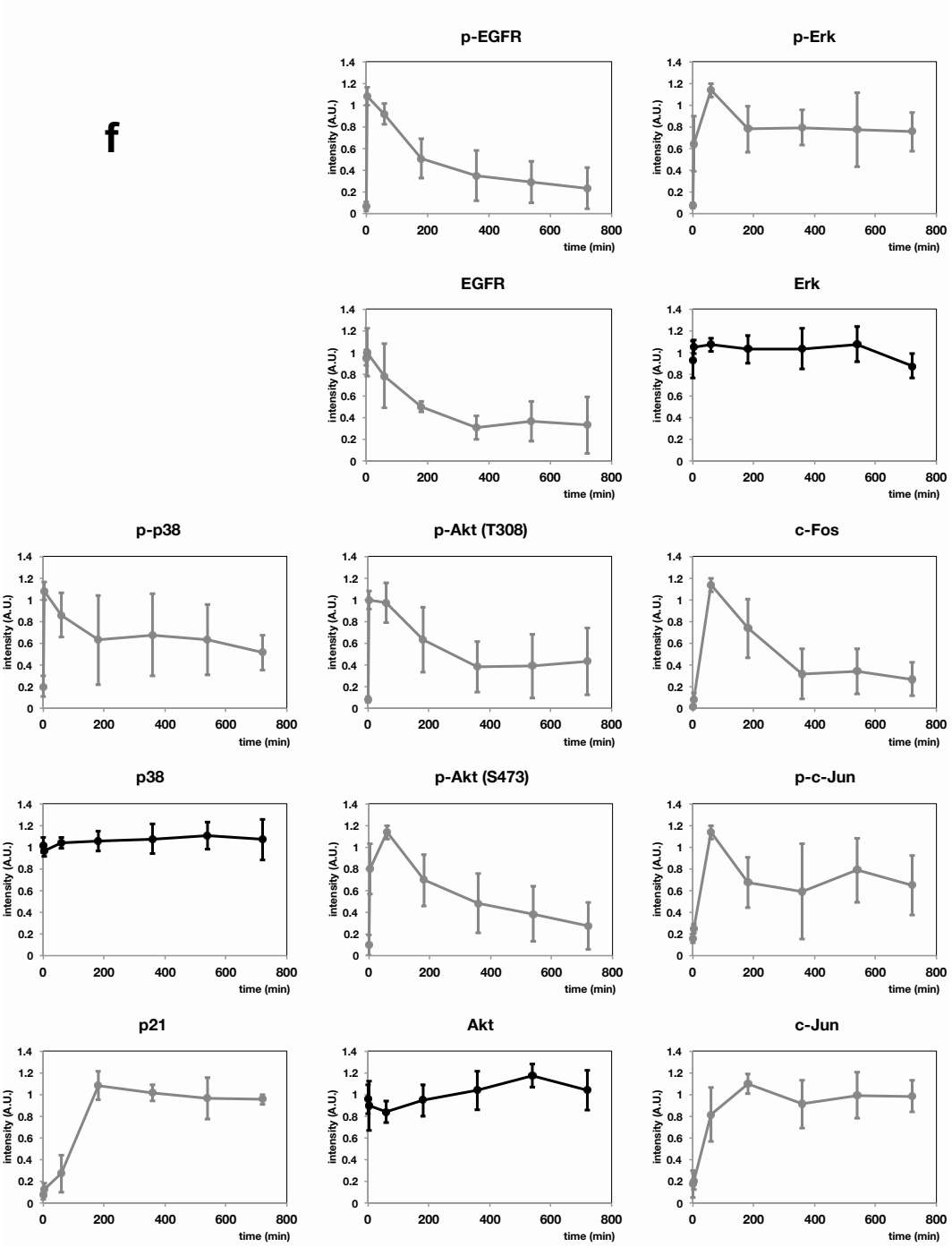


**Figure 4–2. Quantitative data of EGF-induced protein phosphorylation and expression (*continued*).** (**c**) Quantitative data of **Figure 4–1c**; TT cells. A.U., arbitrary unit. The means and SDs of three independent experiments are shown. Gray plots mean that EGF stimulation causes significant change of A.U. of each molecule (One-way ANOVA).

migration ability, on EGF-induced intercellular signaling in each cancer cell line. The author then determined that the effects of inhibitors on EGF-induced signaling are assessed at the time when each relative intensity of signaling molecule hit a peak in time course data (**Table 4–1**), because the effects of inhibitors will be able to be detected clearly. **Table 4–2** lists the names of the chemical inhibitors of signal transduction used in this study, the experimental concentrations of each inhibitor, and their modes of action. Using these chemical inhibitors under the stated concentrations, the author examined the effect of compounds on EGF-induced signaling (**Figure 4–3a, b, c**). These results include four conditions of bands; negative control (EGF − and inhibitor −, left), positive control (EGF + and inhibitor −, the second bands from the left), both EGF and inhibitor-treated condition (EGF + and inhibitor +, the third bands from the left), and inhibitor-treated condition (EGF − and inhibitor +, right). To quantify the effect of inhibitors, we then normalized the signal intensity so that the intensity of the left band (means non-treated condition) as 0, and the intensity of the next band (means EGF-treated condition) as 1. Based on the standards, we relatively quantified the signal intensity of other right two bands. In this way, the author carried out two highly reproducible, independent experiments on each cell line ($r = 0.89$, *p-value* $< 2.2 \times 10^{-16}$, **Figure 4–4**), and provided a final dataset by averaging the data points from the two experiments.

**Table 4–1.** The evaluation timeline of the effects of inhibitors

| Proteins | Cell line | | |
|---|---|---|---|
| | A431 | EC109 | TT |
| p-EGFR | 5 min | 5 min | 5 min |
| p-p38 | 5 min | 5 min | 5 min |
| p-Erk | 5 min | 5 min | 1 h |
| c-Fos | 1 h | 1 h | 1 h |
| p-Akt(T308) | — | 1 h | 5 min |
| p-Akt(S473) | — | 1 h | 1 h |
| p-c-Jun | 1 h | 1 h | 1 h |
| c-Jun | 3 h | 6 h | 3 h |
| p21 | 6 h | 6 h | 3 h |

**Table 4–2.** Compound concentrations and mode of action used in this study

| Compound name | Concentration | Target / Mode of action | References |
|---|---|---|---|
| AA861 | 30 $\mu$M | 5-Lipoxygenase (5-LO) | [64] |
| AG1478 | 1 $\mu$M | EGFR | [65] |
| Herbimycin A | 10 $\mu$g/ml | HSP90 | [70] |
| LY294002 | 30 $\mu$M | PI3K | [72] |
| Mevastatin | 30 $\mu$M | HMG-CoA reductase | [73] |
| MG132 | 300 nM | Proteasome | [74] |
| MK571 | 30 $\mu$M | CysLT1 | [75] |
| Rapamycin | 10 $\mu$g/ml | mTOR | [81] |
| SB203580 | 30 $\mu$M | p38 | [82] |
| SB415286 | 30 $\mu$M | GSK-3 | [84] |
| SP600125 | 10 $\mu$M | JNK | [85] |
| U0126 | 30 $\mu$M | MEK | [89] |
| Y27632 | 30 $\mu$M | ROCK | [94] |
| Actinomycin D | 100 ng/ml | Transcription | [111] |
| Cycloheximide | 1 $\mu$M | Translation | [112] |

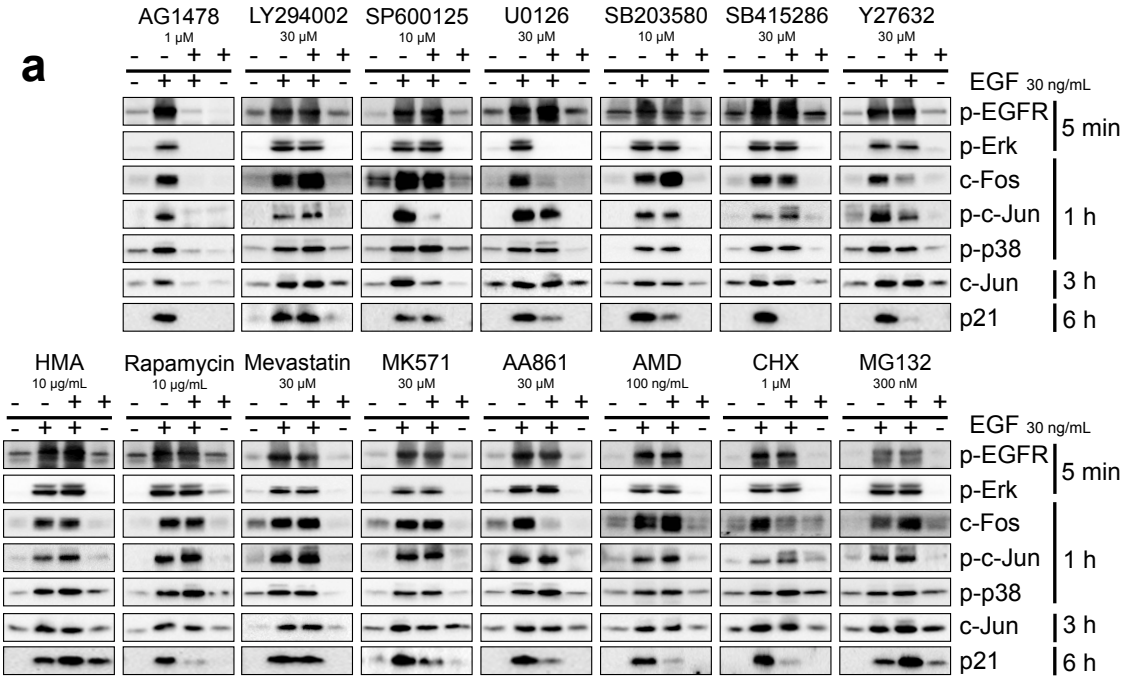


**Figure 4–3. Effects of small molecule inhibitors on EGF-induced migration signaling in three cancer cell lines.** (**a**) A431 cells, (**b**) EC109 cells, and (**c**) TT cells were treated with EGF after the pre-treatment of inhibitors for 15 min. After indicated time, the cells were collected and subjected to western blotting. HMA; herbimycin A, AMD; actinomycin D, CHX; cycloheximide.

## Deduction of migration signaling in three cancer cell lines

Next, the author attempted to deduct the signaling network regulating cell migration in each cancer cell lines based on the obtained chemosensitivity profiles on EGF-induced protein up-regulation. In the region of chemical biology, signaling pathway is deduced using the concept described in **Figure 4–5** (and see also Experimental Procedures, page 77). In this approach, two signaling pathways are generated when a compound affects the relative level of protein bands. To

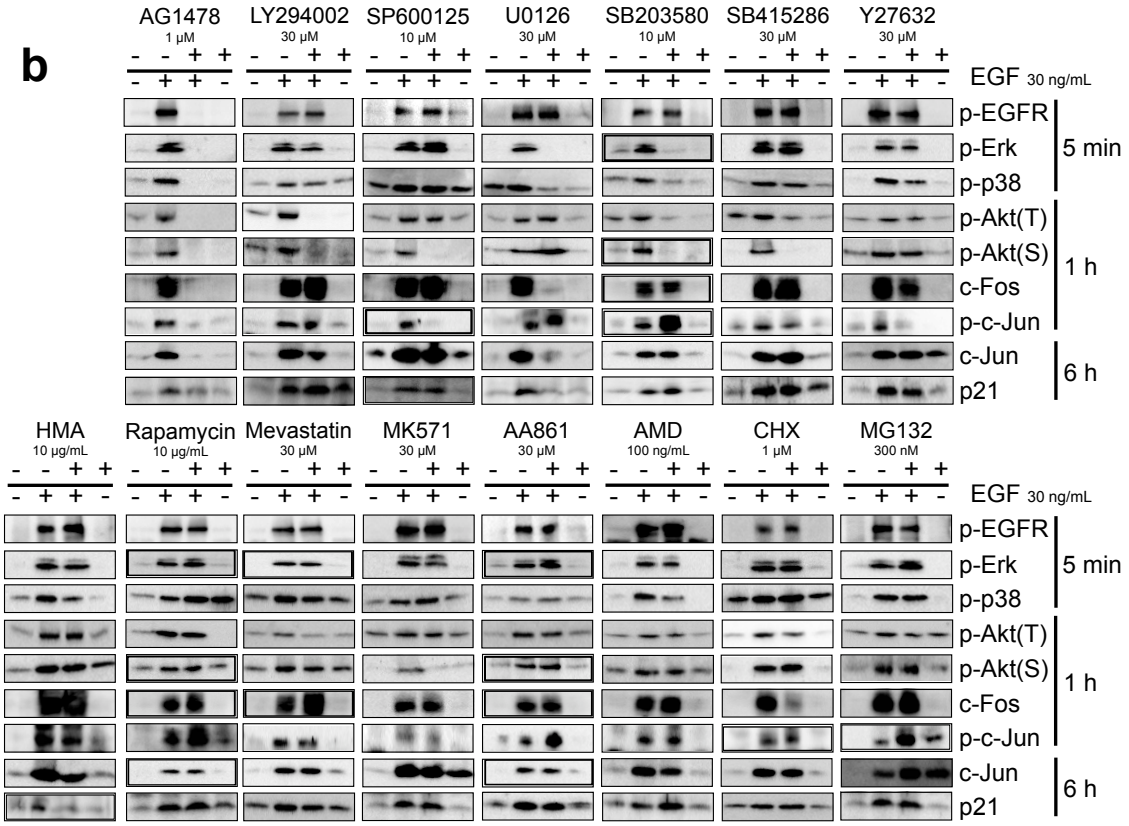


**Figure 4–3. Effects of small molecule inhibitors on EGF-inducecd migration signaling in three cancer cell lines (*continued*).** (**b**), EC109 cells.

determine whether compounds perturbed the signaling molecules or not, the author defined ±0.5 as a threshold. In the case of **Figure 4–5a**, MEK inhibitor U0126 suppressed EGF-induced p-Erk by more than 50%. In such a case, two positive regulations, from EGFR to MEK, and from MEK to p-Erk, were generated. In the case of **Figure 4–5b**, PI3K inhibitor LY294002 increased EGF-induced c-Fos protein expression by more than 50%. In such a case, a positive regulation from EGFR to c-Fos and a negative regulation from PI3K to c-Fos, were generated. In

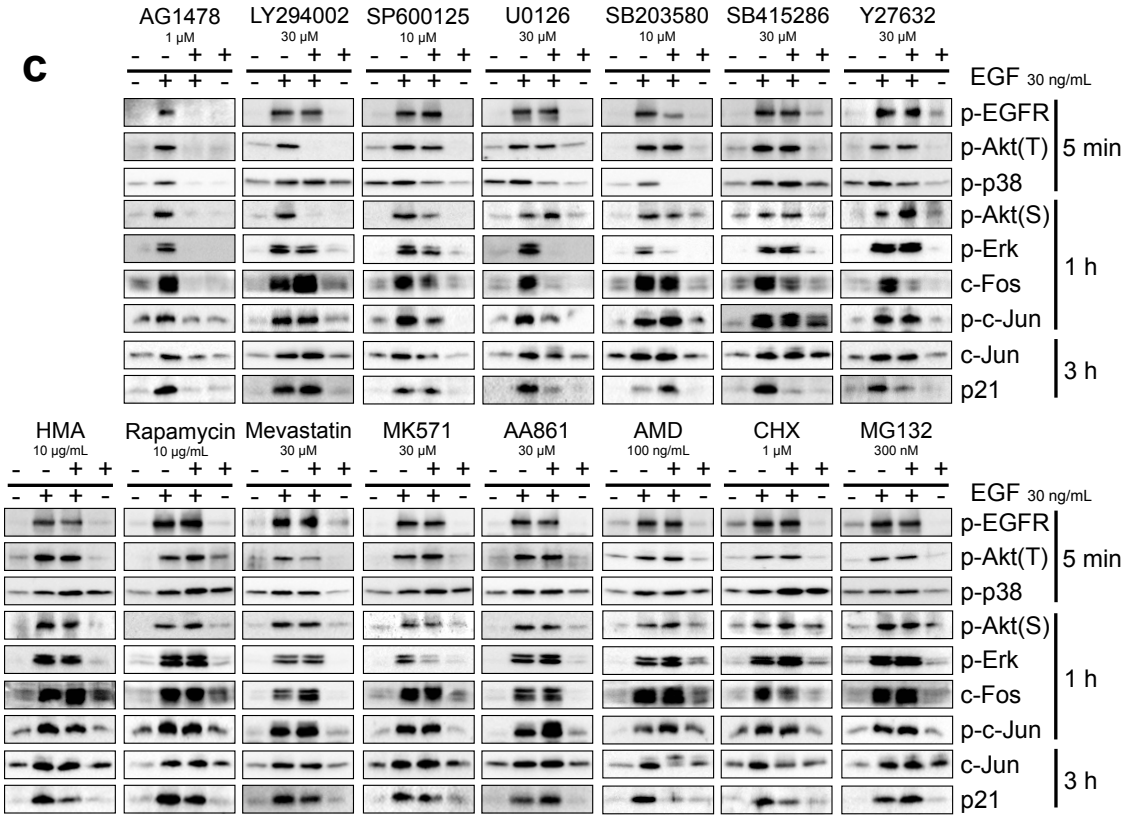


**Figure 4–3. EGF-inducecd time course of protein phosphorylation and expression in three cancer cell lines (*continued*).** (**c**), TT cells.

the case of **Figure 4–5c**, GSK-3 inhibitor SB415286 increased c-Jun protein expression without EGF stimulation. In such a case, a positive regulation from EGFR to c-Jun and a negative regulation from GSK-3 to c-Jun, were generated.

In this way, based on the semi-quantitative profile (**Figure 4–3** and the concept described in **Figure 4–5**), the author deduced signaling network of each cancer cell line as a signed directed graph (**Figure 4–6**). The EGF-induced migration pathway in A431 cells consisted of 19 nodes and 41 edges (**Figure 4–6a**), that in

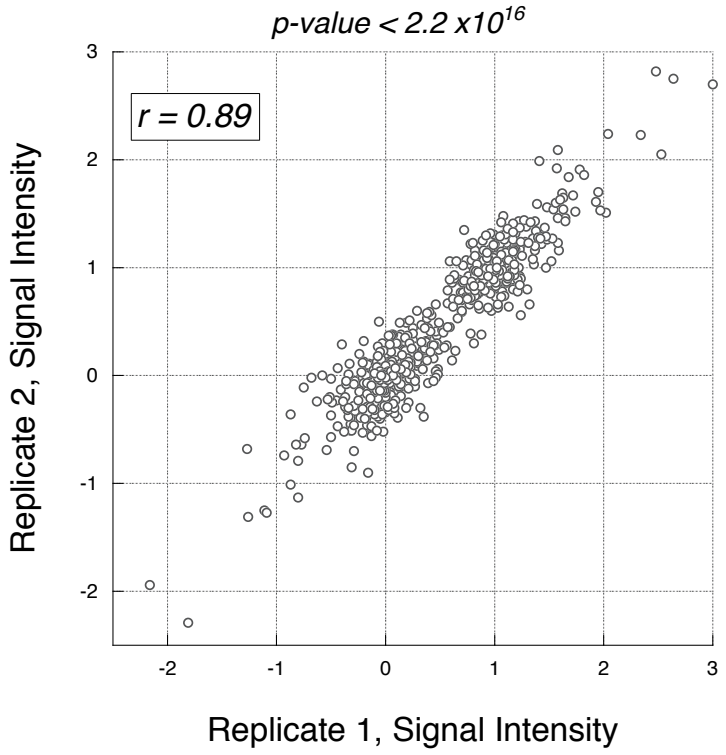


**Figure 4–4. Reproducibility of the quantitative signal intensity.** Before averaging, two independent data sets were checked for high correlation ($r = 0.89$, $p\text{-}value < 2.2 \times 10^{-16}$)

EC109 cells consisted of 22 nodes and 61 edges (**Figure 4–6b**), and that in TT cells consisted of 21 nodes and 53 edges (**Figure 4–6c**). The reason why the number of pathways in A431 cells are fewer than in the other two cell line might be that p-Akt(T308) and p-Akt(S473) could not be evaluated in A431 cells. On the other hand, the number of pathways in EC109 cells and TT cells are close.

(**a**) When a inhibitor canceled the effect of EGF,

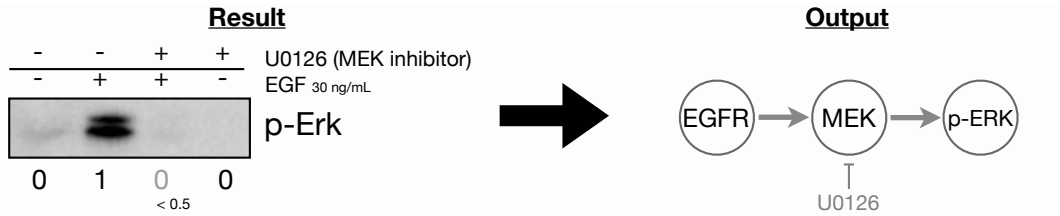


(**b**) When a inhibitor increased the effect of EGF,

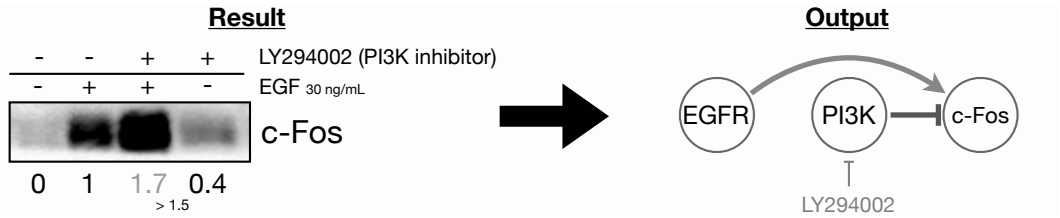


(**c**) When the treatment of inhibitor increased the intensity of protein band,

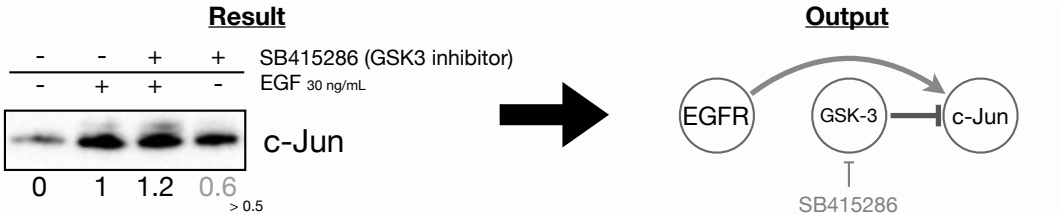


**Figure 4–5. The concept for deduction of signaling pathway.**

## Comparison of signaling pathways in each cancer cell line

Based on these pathway maps, the author firstly investigated the common structure of signaling pathway for cell migration in all three cancer cell lines. **Figure 4–7a** presents the common topology among three cell lines. This pathway map includes MEK/Erk/c-Fos pathway and JNK/c-Jun pathway which have been widely researched in the field of cell migration[102,113]. The author also found that MEK regulated the phosphorylation of p38 (p-p38) and the protein expression level of p21, and PI3K suppressed the protein expression level of c-Fos in all three

caner cell lines. On the other hand, the most of nodes without MEK, JNK, and PI3K, that is such as ROCK and CysLT1, did not have any outdegrees, suggesting that the downstream signals of these molecules are different between three cancer cell lines. Next, the author evaluated the specific structures of signaling pathway for cell migration in each cancer cell lines (**Figure 4–7b, c, d**). Specific pathway in A431 cells includes only eight pathways, such as p-p38 → c-Jun, 5-lipoxygenase (5-LO) → c-Fos, and so on. The number of specific pathway in EC109 cells and in TT cells are 19 and 14, respectively, indicating that about one-fifth to one-third of pathways in these cells are the cell type-specific.

In previous study described in **chapter 3**, the author already predicted that the type of signaling pathway regulating for cell migration induced by EGF might be classified into two groups; collective type includes A431 cells and EC109 cells, and individual type TT cells and TE8 cells. That is, it means that A431 cells and EC109 cells have similar type of regulatory pathway for cell migration, but the pathway in these cell lines may be different from TT cells. To unclear the difference of signaling pathway between two groups, the author then compared the signaling pathway of EC109 cells and TT cells which includes just all the same nodes (**Figure 4–8**). **Figure 4–8a** shows the overlapped pathway topology in both cell lines. The number of interactions in this pathway map is about 1.5 times greater than that in the common pathway between all three cell lines.

This pathway map includes such as PI3K → p-Akt, JNK → p-Akt(S473), ROCK → p-p38 and so on, suggesting that these pathways play a consistent role for cell migration. **Figure 4–8b and 4–8c** present the specific pathway topologies in EC109 cells and TT cells, respectively. 26 pathways such as MEK → c-Jun, GSK-3 → p-Akt(S473), HMG-CoA → pAkt(T308), and so on, are specific in EC109 cells, and 18 pathways such as p-JNK → p-p38, CysLT1 → p-Erk, and ROCK → c-Fos, and so on, are specific in TT cells. The main difference of these specific pathways is the regulation of PI3K/Akt pathway (green nodes) and MAPK pathway (pink nodes). The phosphorylation of p-Akt was up-regulated by p38, GSK-3 and CysLT1 (gray nodes) in EC109 cells, whereas there is no specific positive pathway to p-Akt in TT cells. On the other hand, The MAPK pathway was up-regulated by GSK-3 and CysLT1 in TT cells (GSK-3 → c-Fos, and CysLT1 → p-Erk), whereas these molecules did not regulate MAPK pathway in EC109 cells. These results indicate that the downstream signaling of GSK-3, p38, and CysLT1 might be related to the diversity of regulatory mechanisms for EGF-induced cell migration between two cancer cell lines.

(**a**) A431 cells

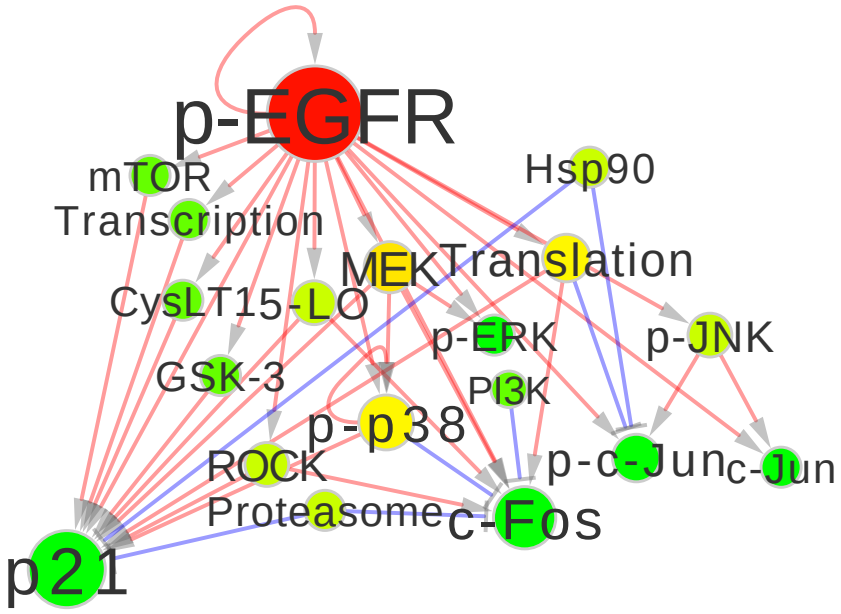


(**b**) EC109 cells

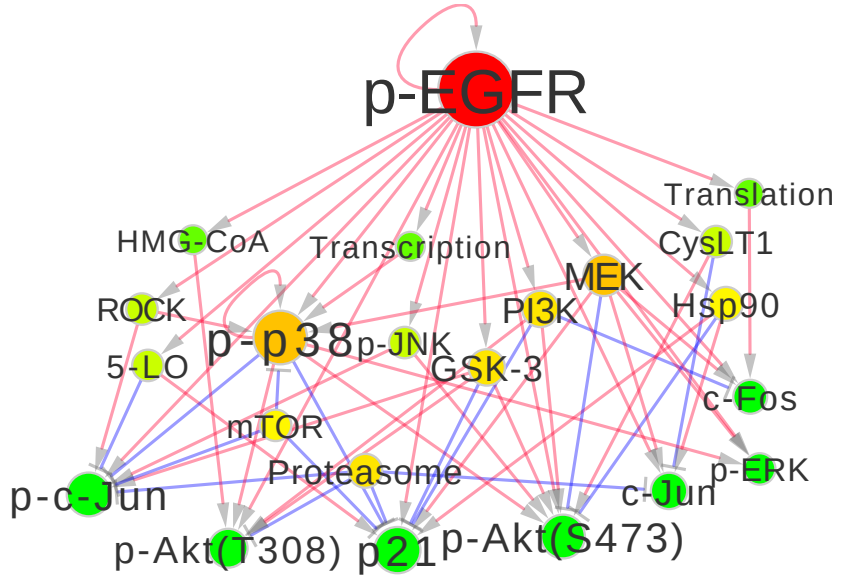


**Figure 4–6. EGF-induced migration signaling network in three cancer cell lines.** EGF-induced migration signaling network in (**a**) A431 cells and (**b**) EC109 cells. The threshold is set ± 50% from positive control. The edge color is decided based on the sign of edges; red means positive signaling, and blue means negative signaling. The size of node indicates the number of connecting edges. The color of node indicates the number of out of edges: a gradient color scale from green to red.

(**c**) TT cells

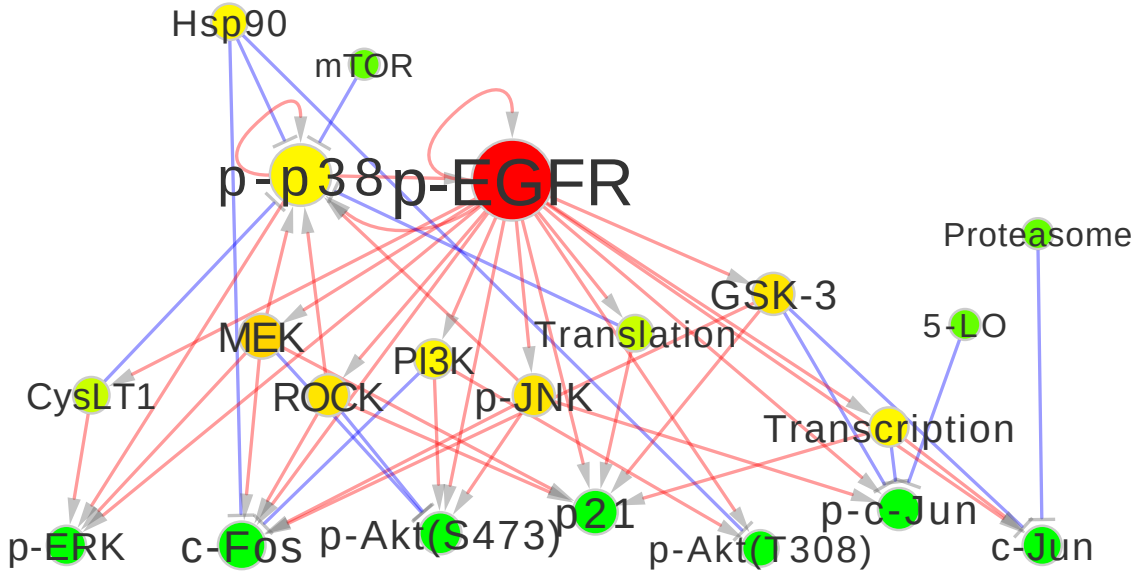


**Figure 4–6. EGF-induced migration signaling network in three cancer cell lines (*continued*).** EGF-induced migration signaling network in (**c**) TT cells. The threshold is set ± 50% from positive control. The edge color is decided based on the sign of edges; red means positive signaling, and blue means negative signaling. The size of node indicates the number of connecting edges. The color of node indicates the number of out of edges: a gradient color scale from green to red.

## 4.3 Discussion

In the present study, the author investigated some general and specific regulatory mechanisms of cell migration. To accomplish the objective, the author firstly examined which and when EGF-induced signaling pathways are activated among three cancer cell lines whose regulatory signaling for EGF-induced cell migration are different[107] (**chapter 3**). In fact, the activation patterns of signal transduction molecules are partially different between three cancer cell lines (**Figure 4–1**). While

(**a**) overlapped pathways

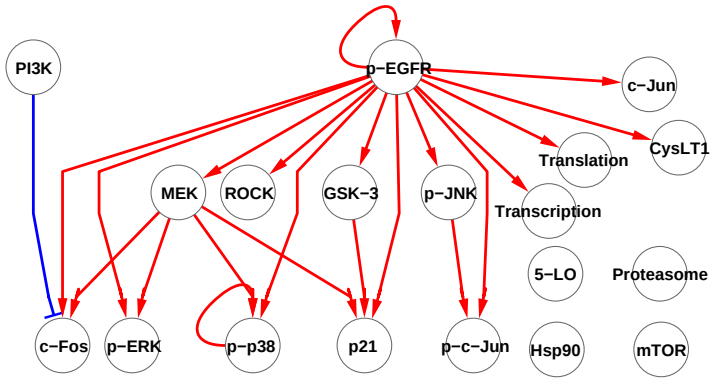


(**b**) A431 cells

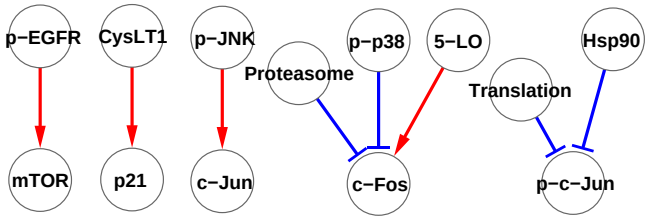


(**c**) EC109 cells

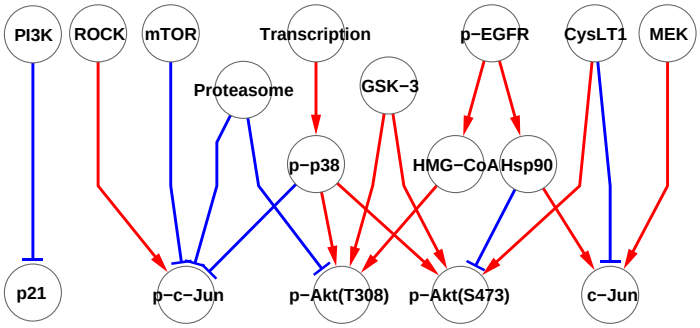


(**d**) TT cells

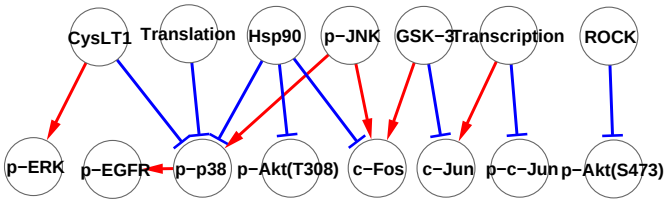


**Figure 4–7. Comparison of signaling network among three cancer cell lines.** (**a**) Common EGF-induced signaling network among three cancer cell lines. (**b**),(**c**), (**d**)Specific EGF-induced signaling network in (**b**) A431 cells, (**c**) EC109 cells, (**d**) TT cells.

(**a**) Common pathways in EC109 cells and TT cells

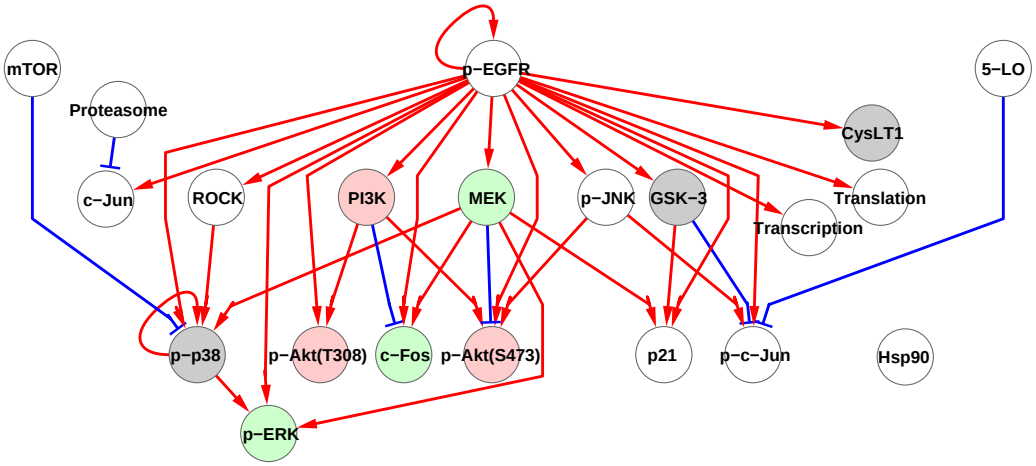


(**b**) Specific pathways in EC109 cells

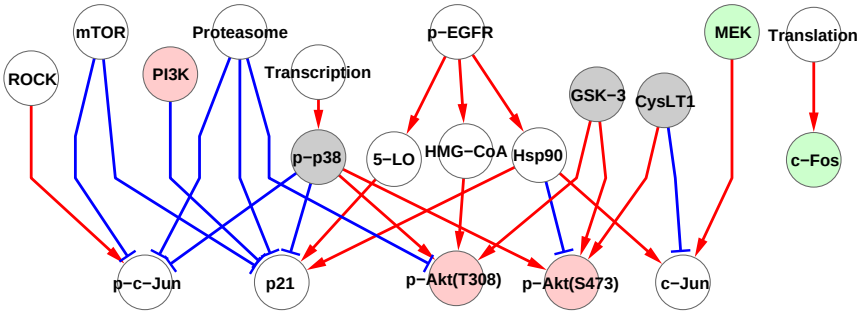


(**c**) Specific pathways in TT cells

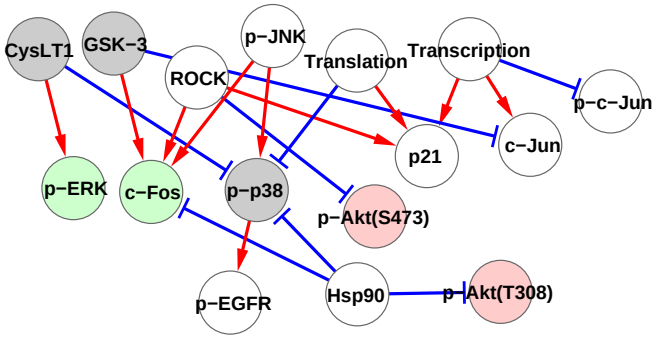


**Figure 4–8. Comparison of signaling network between EC109 cells and TT cells.** (**a**) Common signaling network between EC109 cells and TT cells. (**b**) Specific EGF-induced signaling network in EC109 cells. (**c**) Specific EGF-induced signaling network in TT cells. Green nodes; PI3K/Akt pathway components, Pink nodes; MAPK/c-Fos pathway components, Grey nodes; p38, GSK-3, and CysLT1.

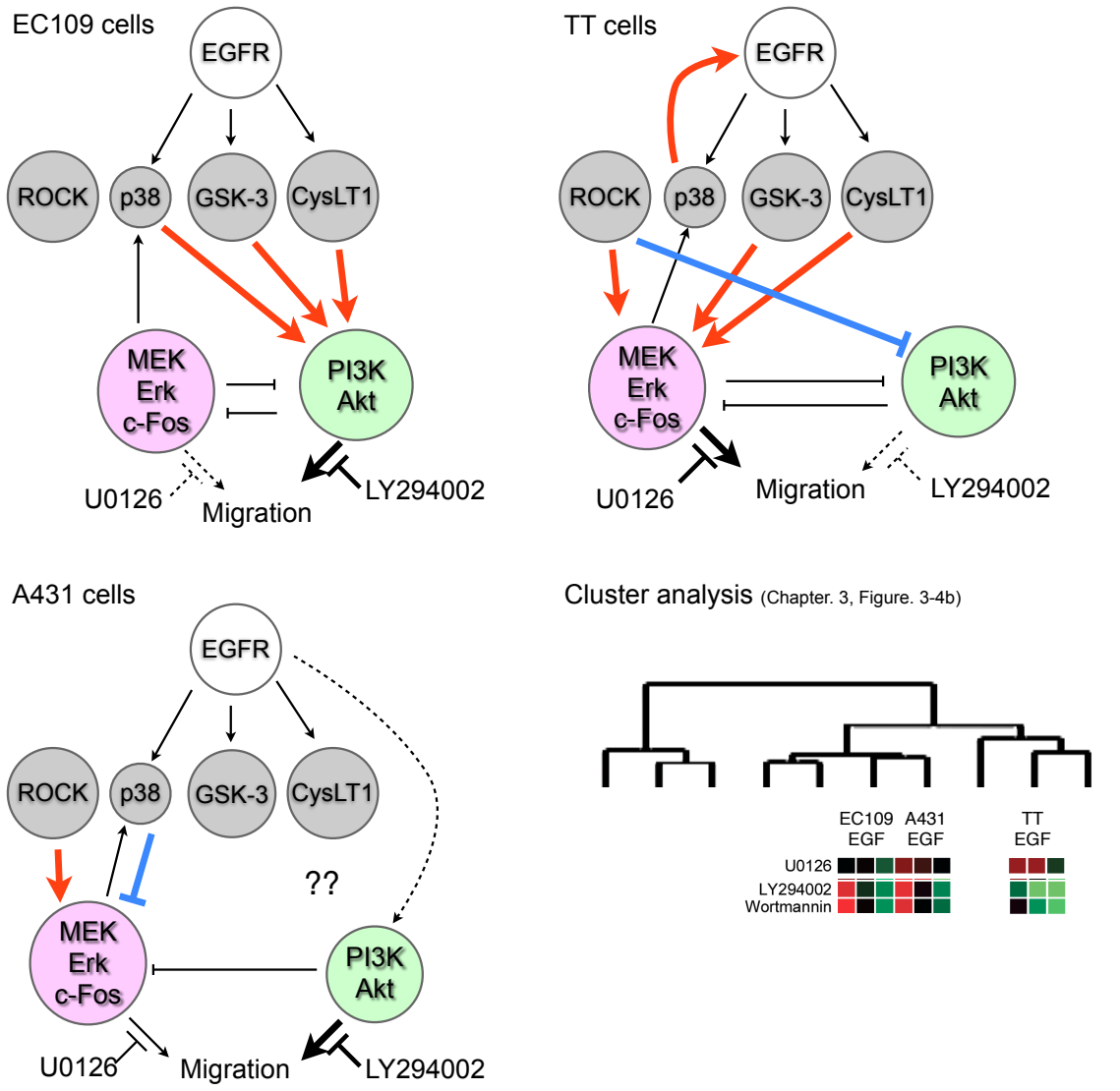


**Figure 4–9. Summary of variety of EGF-induced migration signaling between three cancer cell lines.** Characteristics of EGF-induced migration signaling in EC109 cells (upper left), TT cells (upper right), and A431 cells (lower left). Green nodes; PI3K/Akt pathway components, Pink nodes; MAPK/c-Fos pathway components, Grey nodes; p38, GSK-3, ROCK, and CysLT1. Lower right figure shows the Inhibitory pattern of MEK inhibitor and PI3K inhibitors on the three cancer cell lines presented in **chatper 3**, page 49.

the activation patterns of c-Fos or p-p38 are quite similar among three cancer cell lines, the pattern of p-Erk and p-c-Jun are especially different. The relative intensities of sustained p-Erk and p-c-Jun in TT cells are higher than those in A431 cells and EC109 cells. Interestingly, this difference is consistent with the classification of the chemosensitivity profile of these three cell lines[107] (**chapter 3**, **Figure 3–5b**, page 49), suggesting that sustained Erk and c-Jun phosphorylation are involved in the cell type-specific pathways for cell migration in TT cells. As a previous study revealed a positive feedback mechanism by which sustained JNK activity promote Erk signaling through IRS-2[103], these mechanism may also modulate cell migration in TT cells. By contrast, the phosphorylation of Akt was increased in EC109 cells and TT cells but not A431 cells. However, the author found that EGF-induced migration of A431 cells is suppressed by the addition of PI3K inhibitor (**chapter 3**, **Figure 3–3**, page 44), indicating that the activation of PI3K/Akt pathway is required for migration of A431 cells. At present, the author does not know why EGF-induced up-regulation of p-Akt is not detected in A431 cells. Another difference of time course data among three cancer cell line is shown in the protein expression level of EGFR. EGF stimulation decreased the protein expression level of EGFR in EC109 cells and TT cells, but it did not decrease in A431 cells. In addition, attenuation of the level of p-EGFR seems to be correlated with the protein expression level of EGFR in three cell lines. When EGF binds to

EGFR, EGFR is rapidly internalized from the cell surface via several pathways, including clathrin-coated pits[114,115]. Internalized receptors are either recycled to the cell surface or transported to lysosomes for degradation. It is well known that the fate of the receptors upon internalization is controlled by several protein, such as Cbl and LRRK1[116,117]. Thus, our results might indicate that the regulation of EGF-induced receptor degradation is different among three cancer cell lines, and this difference dictates the sustention of activation of downstream signaling.

Regulatory pathway for cell migration in each cancer cell lines was determined by examining the effect of cell migration inhibitors on signal transduction molecules (**Figure 4–6**). The overlapped pathway topology in all three cell lines includes JNK → p-c-Jun which is predicted as a common regulator in **chapter 3**, suggesting that regulatory signaling for cancer cell migration by JNK through the phosphorylation of c-Jun is actually common mechanisms in all types of cancer cells. Because the author could not detect significant up-regulation of p-Akt in A431 cells in this study, the pathway map in A431 cells did not include the regulation of p-Akt and thereby includes fewer nodes and edges than that in EC109 cells and TT cells. Therefore, an interpretation of the comparison among pathway maps among three cancer cell lines must be made with great caution.

To discuss and confirm the results of cluster analysis in **chapter 3**, the author finally compared the pathway map in EC109 cells to TT cells, and determined

the overlapped or cell type-specific topology (**Figure 4–8**). The author found that the network structures involved in PI3K/Akt pathway components (green nodes), MAPK pathway components (pink nodes) are substantially different. In EC109 cells, Akt phosphorylation wave is slower than TT cells (**Figure 4–1** and **Table 4–1**), suggesting that more intermediate proteins sustain Akt phosphorylation in EC109 cells than TT cells. In fact, the level of Akt phosphorylation was up-regulated by p38, GSK-3 and CysLT1 (gray nodes) in EC109 cells, while these pathways were not included in TT cells (**Figure 4–8b, c**). On the other hand, in TT cells, Erk phosphorylation wave is slower and more continuous than EC109 cells (**Figure 4–1** and **Table 4–1**), suggesting that more intermediate proteins sustain Erk phosphorylation in TT cells than EC109 cells. In fact, the MAPK pathway was affected by GSK-3 and CysLT1 in TT cells (GSK-3 → c-Fos, and CysLT1 → p-Erk), whereas these molecules did not regulate MAPK pathway in EC109 cells.

The findings of this study are summarized in **Figure 4–9**. The author found that CysLT1 and GSK-3 regulate MAPK pathway in TT cells, while these proteins regulate EC109 cells. In addition, ROCK regulates MAPK pathway in TT cells, but this regulation was not found in EC109 cells. The author considers that these differences of EGF-induced signaling pathway would determine the difference of mode of cell migration based on cell morphology. In previous study (**chapter 3**), the author found that A431 cells and EC109 cells moved keeping cell-cell contact

(collective migration), but TT cells moved as a single cell (individual migration). In light of above results, it is supposed that cancer cells moved as a single cell when CysLT1, GSK-3, and ROCK activates MAPK pathway, and these moved collective, keeping cell-cell adhesion when CysLT1 and GSK-3 activates PI3K/Akt pathway. The correlation of the balance of MAPK pathway and PI3K pathway and migration modes as indicated is supported by several other reports. MAPK activation consequently induces RhoA activation and epithelial-mesenchymal-transition, while PI3K activation suppresses RhoA activity in colon cancer[58]. In addition, PI3K are recruited to cell contacts during epithelial junction formation[118] where their activation via cadherin signaling has a clear impact on cadherin function and strengthening of cell—cell adhesion[119,120]. This could involve PI3K-induced Rac activation, as E-cadherin-stimulated actin cytoskeletal reorganization requires Rac activation and the PtdIns(3,4,5)P3-activated GEF Tiam1[121]. However, the reason why CysLT1- and GSK-3- regulated signaling are different between cell types remains unclear. The difference of downstream signaling of these molecules might be depend on i) balance of the amount of themselves and their substrates, ii) localization, iii) time-dependent activation pattern. In addition, because the regulation of p-Akt in A431 cells is also still unclear, these hypotheses should be further elucidated.

In summary, the author has shown novel consistency and variety of EGF-

induced regulatory signaling pathway for cancer cell migration by the combination approach of chemical biology with systems biology. This approach can be used for understanding the characteristics of cancer cell migration signaling, and opening up the potential for revealing novel molecular pathway as a target for cancer therapy.

## 4.4 Experimental Procedures

### Reagents

Rapamycin, and Y27632 were purchased from Calbiochem. MK571 was purchased from Cayman. Actinomycin D, cycloheximide, LY294002, mevastatin, MG132, SB203580, SB218078, SB415286, SP600125, U0126, and epidermal growth factor were purchased from Sigma. Herbimycin A was purified from cultures of *Streptomyces* sp. in our own laboratory.

### Cell culture

A431 cells, EC109 cells, and TT cells were cultured as indicated in **chapter 3**, page 58.

## Western blotting

Cells were seeded in 6-well plate or 60 mm dish and cultured overnight. After the culture supernatant was replaced with RPMI1640 supplemented with 1% fetal bovine serum, the cells were pretreated with drugs for 15 min and stimulated with 30 ng/ml EGF for indicated time. Cells were collected, lysed, and subjected to western blotting as indicated in **chapter 2**, page 33. Antibodies employed for immunoblotting include the following: anti-EGF Receptor antibody (#2232), anti-Akt antibody (#9272), anti-phospho-Akt (Thr308) antibody (#9275), anti-phospho-Akt (Ser473) antibody (#9271), anti-c-Jun antibody (#9165), anti-phospho-p38 antibody (#9211), anti-MAPK (Erk 1/2) antibody (#9102), anti-phospho-MAPK (Erk 1/2) antibody (#9101) (Cell Signaling); anti-c-Fos antibody (sc-7202), anti-p38 antibody (sc-7972), anti-p21 antibody (sc-397) (Santa Cruz Biotechnology); anti-phospho-tyrosine antibody (05-321) (upstate); anti-phospho-c-Jun antibody (558036) (BD Pharmingen); anti-$\beta$-actin antibody (A5316) (Sigma).

## Statistical analysis

One-way ANOVA was used to determine whether there are any significant differences in time series data sets. Pearson product-moment correlation coefficient was used to confirm reproducibility of the data. These statistical analyses were calculated by using the R project package (www.r-project.org/).

## Network deduction and comparison

The signed directed network was deduced from a difference of protein phosphorylation or expression level between mock-treated and inhibitor-treated data, according to the rule shown in **Figure 4–5**. This rule includes three simple assumptions that are commonly used in chemical biology.

a) There exists a positive regulation from molecule X to molecule Y when the level of molecule Y in the presence of both EGF and inhibitor of X is more than 50% lower than in EGF-treated condition.

b) There exists a negative regulation from molecule X to molecule Y when the level of molecule Y in the presence of both EGF and inhibitor of X is more than 50% higher than in EGF-treated condition.

c) There exists a negative regulation from molecule X to molecule Y when the level of molecule Y in the presence of inhibitor of X is higher than the half of the level in EGF-treated condition.

These data processing were done by using R. Signaling pathway maps were generated by using Cytoscape (www.cytoscape.org/). The comparison of pathway topology was also done by using Cytoscape.

# Chapter 5

# Conclusion

The elucidation of regulatory mechanisms of cell migration in tumor cells is required for the development of anti-metastatic research. Chemical biological methods which enable us to perturb protein function rapidly using small molecule compounds, on the other hand, systems biological methods which enable us to elucidate intracellular molecular interaction as a network systems. Therefore, combination of chemical biology and systems biology would have led to breakthrough in basic cancer research. In this thesis, the author researched a part of regulatory mechanism of cell migration from various angles based on chemical biology and systems biology. The results, significance and speculation about this study are summarized below.

In **chapter 2**, the author identified the novel derivatives of N-benzyl-ACM and

N-allyl-ACM as FTase inhibitors. The author concluded that these compounds suppressed cell migration through the inhibition of the farnesylation of H-Ras which is essential for the membrane localization of H-Ras. This conclusion is supported by following findings:

A) The inhibition concentration of FTase *in vitro*, H-Ras localization, and cell migration by these compounds are almost the same range.

B) C-10 epimers of these compounds, which did not inhibit FTase *in vitro*, also did not inhibit cell migration.

C) The phosphorylation level of Akt which acts downstream of H-Ras, but not p-Erk, was suppressed in the presence of N-benzyl-ACM and N-allyl-ACM.

D) The migration of A431 cells induced by EGF was suppressed by PI3K inhibitors (**chapter 3**), indicating that PI3K signaling regulates cell migration in A431 cells.

However, why C-10 epimers did not have inhibitory effect on FTase is not still unknown. Further study such as *in silico* docking study might be required for the elucidation of inhibitory mechanism of ACM derivatives on FTase.

In **chapter 3**, the author conducted a chemical genomic study to understand the general and specific principles of the regulatory pathways of cancer cell migration. The author first set up an analytical system to detect the effect of 34 kinds of chemical inhibitors on cell migration in a wound healing assay. The au-

thor obtained the chemosensitive migratory profile of ten types of cell migration, rather like a fingerprint. From the results of a subsequent cluster analysis on this dataset, the author classified the ten types of cell migration into three groups, and the 34 signal transduction inhibitors were clustered into four groups. The data showed that the compounds represented some diverse structures but targeted the same molecule (for example, LY294002 and wortmannin; PI3K inhibitors) were clustered into the same tree, indicating that this profiling is helpful in the identification of the molecular targets of compounds of unknown modes of action. A good example is MK571, CysLT1 antagonist. MK571 was classified the same group with UTKO1, which directly bound to 14-3-3ζ, and inhibited the interaction between the 14-3-3 proteins and Tiam1, a protein that has been reported to be a Rac-specific GEF. This resulted in the inhibition of Rac1. Based on these results, the author showed that CysLT1 signaling regulates Tiam1 expression and Rac1 activation in A431 cells. Now the author is preparing the paper about cell migration signaling regulated by CysLT1. Furthermore, the author's data indicated that JNK was a common regulator in all types of cell migration, whereas ROCK, GSK-3 and p38MAPK were involved in an EGF-stimulated mesenchymal type of cell migration. Thus, the author believe the results provided here have opened a broad avenue of mechanism study of the regulation of cell migration for continued progress in chemical genomic research.

In **chapter 4**, the author quantified the effect of the 15 inhibitors on the levels of expression or phosphorylation of nine proteins induced by EGF stimulation in three cancer cell lines in order to explore the diversity and consistency of EGF-induced cell migration pathway. Based on obtained data and chemical biological assumptions, the author deduced cell migration pathway in each cancer cell, and compared them. As a result, the author found that MEK/Erk-, and JNK/c-Jun-pathway are activated in migrating all three cells. Moreover, CysLT1 was found to regulate only MEK/Erk pathway in TT cells, whereas it regulates only PI3K/Akt pathway in EC109 cells. These results indicate that the CysLT1 signaling is related to the diversity of regulatory mechanisms in cancer cells. There are two major characteristics of the research. Firstly, this research is focused on the diversity and consistency of regulatory mechanism for cancer cell migration. The author's principal aim would be distinctly different from that of previous 'single cell / single protein' study. The second is that this study revealed signaling pathway for cell migration based on the combination methodology of chemical biology with systems biology. Despite chemical biological methodology successfully led the new aspect of regulatory mechanism of cell migration, the author should be aware of three primary challenges in using chemical biology to understand signaling networks[122]:

A) Lack of specificity of most kinase inhibitors limits their usefulness in research. Off-target effects must be considered when designing and interpreting experiments meant to provide mechanistic insights.

B) Even specific inhibition of a signaling node leads to complex downstream effects through largely uncharacterized interactions and feedback regulation.

C) Although many important signaling pathways have been mapped, most network topology is still uncharacterized. For example, this study cannot determine whether a pathway regulation is direct or indirect. Intermediate molecules must be considered if a novel pathway is found by the author's methodology.

For the indicated reasons, the novel findings such as the diversity of downstream signaling of CysLT1 should be further elucidated.

As just described, the author reported a study on the regulatory mechanism for cell migration based on the both of chemical biological approach and systems biological approach, at the same time, several limitations of this approach come within sight only after challenging this research. However, the author believe that these limitation will be overcome by further analytical method and the development of novel compounds which have few off-target effects. The author also believe that the combinatorial approach of chemical biology with systems biol-

ogy have a potential for not only uncovering the novel regulatory mechanism of cancer metastasis but also the development of novel anti-metastatic drug. Finally, the author hopes to close the thesis with a word from a scientist.

*"Once we accept our limits, we go beyond them." — Albert Einstein*

# References


1. Oppermann, H., Levinson, A. D., Varmus, H. E., Levintow, L. & Bishop, J. M. Uninfected vertebrate cells contain a protein that is closely related to the product of the avian sarcoma virus transforming gene (src). *Proc. Natl. Acad. Sci. USA* **76**, 1804–1808 (1979).

2. Cooper, G. M. Cellular transforming genes. *Science* **217**, 801–806 (1982).

3. Santos, E., Tronick, S. R., Aaronson, S. A., Pulciani, S. & Barbacid, M. T24 human bladder carcinoma oncogene is an activated form of the normal human homologue of BALB- and Harvey-MSV transforming genes. *Nature* **298**, 343–347 (1982).

4. Parada, L. F., Tabin, C. J., Shih, C. & Weinberg, R. A. Human EJ bladder carcinoma oncogene is homologue of Harvey sarcoma virus ras gene. *Nature* **297**, 474–478 (1982).

5. Bos, J. L. ras oncogenes in human cancer: a review. *Cancer Res.* **49**, 4682–4689 (1989).

6. Gupta, G. P. & Massagué, J. Cancer Metastasis: Building a Framework. *Cell* **127**, 679–695 (2006).

7. Chambers, A. F., Groom, A. C. & MacDonald, I. C. Dissemination and growth of cancer cells in metastatic sites. *Nat. Rev. Cancer* **2**, 563–572 (2002).

8. Fidler, I. J. The pathogenesis of cancer metastasis: the 'seed and soil' hypothesis revisited. *Nat. Rev. Cancer* **3**, 453–458 (2003).

9. Lauffenburger, D. A. & Horwitz, A. F. Cell migration: a physically integrated molecular process. *Cell* **84**, 359–369 (1996).

10. Kitano, H. Systems Biology: A Brief Overview. *Science* **295**, 1662–1664 (2002).

11. Jenssen, T. K., Laegreid, A., Komorowski, J. & Hovig, E. A literature network of human genes for high-throughput analysis of gene expression. *Nat. Genet.* **28**, 21–28 (2001).

12. Oda, K., Matsuoka, Y., Funahashi, A. & Kitano, H. A comprehensive pathway map of epidermal growth factor receptor signaling. *Mol. Syst. Biol.* **1**, E1–E17 (2005).

13. Ramani, A. K., Bunescu, R. C., Mooney, R. J. & Marcotte, E. M. Consolidating the set of known human protein-protein interactions in preparation for large-scale mapping of the human interactome. *Genome Biol.* **6**, R40 (2005).

14. Uetz, P. *et al.* A comprehensive analysis of protein-protein interactions in Saccharomyces cerevisiae. *Nature* **403**, 623–627 (2000).

15. Zou, M. & Conzen, S. D. A new dynamic Bayesian network (DBN) approach for identifying gene regulatory networks from time course microarray data. *Bioinformatics* **21**, 71–79 (2005).

16. Rual, J.-F. *et al.* Towards a proteome-scale map of the human protein-protein interaction network. *Nature* **437**, 1173–1178 (2005).

17. Ciriello, G. & Guerra, C. A review on models and algorithms for motif discovery in protein-protein interaction networks. *Brief. Funct. Genomic. Proteomic.* **7**, 147–156 (2008).

18. Yu, X., Lin, J., Zack, D. J., Mendell, J. T. & Qian, J. Analysis of regulatory network topology reveals functionally distinct classes of microRNAs. *Nucleic Acids Res.* **36**, 6494–6503 (2008).

19. Kanehisa, M. *et al.* From genomics to chemical genomics: new developments in KEGG. *Nucleic Acids Res.* **34**, D354–7 (2006).

20. Joshi-Tope, G. *et al.* Reactome: a knowledgebase of biological pathways. *Nucleic Acids Res.* **33**, D428–32 (2005).

21. Tomita, M. *et al.* E-CELL: software environment for whole-cell simulation. *Bioinformatics* **15**, 72–84 (1999).

22. Hatakeyama, M. *et al.* A computational model on the modulation of mitogen-activated protein kinase (MAPK) and Akt pathways in heregulin-induced ErbB signalling. *Biochem. J.* **373**, 451–463 (2003).

23. Sasagawa, S., Ozaki, Y., Fujita, K. & Kuroda, S. Prediction and validation of the distinct dynamics of transient and sustained ERK activation. *Nat. Cell Biol.* **7**, 365–373 (2005).

24. Busch, H. *et al.* Gene network dynamics controlling keratinocyte migration. *Mol. Syst. Biol.* **4** (2008).

25. Mani, K. M. *et al.* A systems biology approach to prediction of oncogenes and molecular perturbation targets in B-cell lymphomas. *Mol. Syst. Biol.* **4** (2008).

26. Chuang, H.-Y., Lee, E., Liu, Y.-T., Lee, D. & Ideker, T. Network-based classification of breast cancer metastasis. *Mol. Syst. Biol.* **3** (2007).

27. Liu, J. *et al.* Calcineurin is a common target of cyclophilin-cyclosporin A and FKBP-FK506 complexes. *Cell* **66**, 807–815 (1991).

28. Weiss, W. A., Taylor, S. S. & Shokat, K. M. Recognizing and exploiting differences between RNAi and small-molecule inhibitors. *Nat. Chem. Biol.* **3**, 739–744 (2007).

29. Peterson, R. T. Chemical biology and the limits of reductionism. *Nat. Chem. Biol.* **4**, 635–638 (2008).

30. Hughes, T. R. *et al.* Functional discovery via a compendium of expression profiles. *Cell* **102**, 109–126 (2000).

31. Lamb, J. *et al.* The Connectivity Map: using gene-expression signatures to connect small molecules, genes, and disease. *Science* **313**, 1929–1935 (2006).

32. Pan, C., Olsen, J. V., Daub, H. & Mann, M. Global effects of kinase inhibitors on signaling networks revealed by quantitative phosphoproteomics. *Mol. Cell Proteomics* **8**, 2796–2808 (2009).

33. Fox, P. L., Sa, G., Dobrowolski, S. F. & Stacey, D. W. The regulation of endothelial cell motility by p21 ras. *Oncogene* **9**, 3519–3526 (1994).

34. Ridley, A. J., Comoglio, P. M. & Hall, A. Regulation of scatter factor/hepatocyte growth factor responses by Ras, Rac, and Rho in MDCK cells. *Mol. Cell Biol.* **15**, 1110–1122 (1995).

35. Rowinsky, E. K., Windle, J. J. & Von Hoff, D. D. Ras protein farnesyltransferase: A strategic target for anticancer therapeutic development. *J. Clin. Oncol.* **17**, 3631–3652 (1999).

36. Takemoto, Y. *et al.* Chemistry and biology of moverastins, inhibitors of cancer cell migration, produced by Aspergillus. *Chem. Biol.* **12**, 1337–1347 (2005).

37. Oki, T., Matsuzawa, Y., Yoshimoto, A., Numata, K. & Kitamura, I. New antitumor antibiotics aclacinomycins A and B. *J. Antibiot.* **28**, 830–834 (1975).

38. Hori, S. *et al.* Antitumor activity of new anthracycline antibiotics, aclacinomycin-A and its analogs, and their toxicity. *Jpn. J. Cancer Res.* **68**, 685–690 (1977).

39. Sekizawa, R. *et al.* Isolation of novel saquayamycins as inhibitors of farnesyl-protein transferase. *J. Antibiot.* **49**, 487–490 (1996).

40. Kwon, B.-M. *et al.* Farnesyl protein transferase inhibitory components of Polygonum multiflorum. *Arch. Pharm. Res.* **32**, 495–499 (2009).

41. Sawada, M. *et al.* Synthesis and anti-migrative evaluation of moverastin derivatives. *Bioorg. Med. Chem. Lett.* **21**, 1385–1389 (2011).

42. Engelman, J. A. Targeting PI3K signalling in cancer: opportunities, challenges and limitations. *Nat. Rev. Cancer* **9**, 550–562 (2009).

43. Rodriguez-Viciana, P., Warne, P. H., Vanhaesebroeck, B., Waterfield, M. D. & Downward, J. Activation of phosphoinositide 3-kinase by interaction with Ras and by point mutation. *EMBO J.* **15**, 2442–2451 (1996).

44. Reszka, A. A., Halasy-Nagy, J. & Rodan, G. A. Nitrogen-bisphosphonates block retinoblastoma phosphorylation and cell growth by inhibiting the cholesterol biosynthetic pathway in a keratinocyte model for esophageal irritation. *Mol. Pharmacol.* **59**, 193–202 (2001).

45. Suri, S. *et al.* Nitrogen-containing bisphosphonates induce apoptosis of Caco-2 cells in vitro by inhibiting the mevalonate pathway: a model of bisphosphonate-induced gastrointestinal toxicity. *Bone* **29**, 336–343 (2001).

46. Staal, A. *et al.* The ability of statins to inhibit bone resorption is directly related to their inhibitory effect on HMG-CoA reductase activity. *J. Bone Miner. Res.* **18**, 88–96 (2003).

47. Marshall, C. J. Ras effectors. *Curr. Opin. Cell Biol.* **8**, 197–204 (1996).

48. Klemke, R. L. *et al.* Regulation of cell motility by mitogen-activated protein kinase. *J. Cell Biol.* **137**, 481–492 (1997).

49. Nguyen, D. H. *et al.* Myosin light chain kinase functions downstream of Ras/ERK to promote migration of urokinase-type plasminogen activator-stimulated cells in an integrin-selective manner. *J. Cell Biol.* **146**, 149–164 (1999).

50. Tanimura, S. *et al.* Prolonged nuclear retention of activated extracellular signal-regulated kinase 1/2 is required for hepatocyte growth factor-induced cell motility. *J. Biol. Chem.* **277**, 28256–28264 (2002).

51. Keely, P. J., Westwick, J. K., Whitehead, I. P., Der, C. J. & Parise, L. V. Cdc42 and Rac1 induce integrin-mediated cell motility and invasiveness through PI(3)K. *Nature* **390**, 632–636 (1997).

52. Gan, Y. *et al.* Differential roles of ERK and Akt pathways in regulation of EGFR-mediated signaling and motility in prostate cancer cells. *Oncogene* **29**, 4947–4958 (2010).

53. Huang, C., Rajfur, Z., Borchers, C., Schaller, M. D. & Jacobson, K. JNK phosphorylates paxillin and regulates cell migration. *Nature* **424**, 219–223 (2003).

54. Wagner, E. F. & Nebreda, A. R. Signal integration by JNK and p38 MAPK pathways in cancer development. *Nat. Rev. Cancer* **9**, 537–549 (2009).

55. Narumiya, S., Ishizaki, T. & Watanabe, N. Rho effectors and reorganization of actin cytoskeleton. *FEBS Lett.* **410**, 68–72 (1997).

56. Nobes, C. D. & Hall, A. Rho, rac, and cdc42 GTPases regulate the assembly of multimolecular focal complexes associated with actin stress fibers, lamellipodia, and filopodia. *Cell* **81**, 53–62 (1995).

57. Etienne-Manneville, S. & Hall, A. Rho GTPases in cell biology. *Nature* **420**, 629–635 (2002).

58. Makrodouli, E. *et al.* BRAF and RAS oncogenes regulate Rho GTPase pathways to mediate migration and invasion properties in human colon cancer cells: a comparative study. *Mol. Cancer* **10**, 118 (2011).

59. Yarrow, J. C., Totsukawa, G., Charras, G. T. & Mitchison, T. J. Screening for cell migration inhibitors via automated microscopy reveals a Rho-kinase inhibitor. *Chem. Biol.* **12**, 385–395 (2005).

60. Kakinuma, N., Roy, B. C., Zhu, Y., Wang, Y. & Kiyama, R. Kank regulates RhoA-dependent formation of actin stress fibers and cell migration via 14-3-3 in PI3K-Akt signaling. *J. Cell Biol.* **181**, 537–549 (2008).

61. Sanz-Moreno, V. *et al.* Rac activation and inactivation control plasticity of tumor cell movement. *Cell* **135**, 510–523 (2008).

62. Kurokawa, K. *et al.* Coactivation of Rac1 and Cdc42 at lamellipodia and membrane ruffles induced by epidermal growth factor. *Mol. Biol. Cell* **15**, 1003–1010 (2004).

63. Abbott, B. J. *et al.* Microbial transformation of A23187, a divalent cation ionophore antibiotic. *Antimicrob. Agents Chemother.* **16**, 808–812 (1979).

64. Yoshimoto, T. *et al.* 2,3,5-Trimethyl-6-(12-hydroxy-5,10-dodecadiynyl)-1,4-benzoquinone (AA861), a selective inhibitor of the 5-lipoxygenase reaction and the biosynthesis of slow-reacting substance of anaphylaxis. *Biochim. Biophys. Acta.* **713**, 470–473 (1982).

65. Osherov, N. & Levitzki, A. Epidermal-growth-factor-dependent activation of the src-family kinases. *Eur. J. Biochem.* **225**, 1047–1053 (1994).

66. van Beek, E., Pieterman, E., Cohen, L., Löwik, C. & Papapoulos, S. Farnesyl pyrophosphate synthase is the molecular target of nitrogen-containing bisphosphonates. *Biochem. Biophys. Res. Commun.* **264**, 108–111 (1999).

67. Inoue, S., Bar-Nun, S., Roitelman, J. & Simoni, R. D. Inhibition of degradation of 3-hydroxy-3-methylglutaryl-coenzyme A reductase in vivo by cysteine protease inhibitors. *J. Biol. Chem.* **266**, 13311–13317 (1991).

68. Bowman, E. J., Siebers, A. & Altendorf, K. Bafilomycins: a class of inhibitors of membrane ATPases from microorganisms, animal cells, and plant cells. *Proc. Natl. Acad. Sci. USA* **85**, 7972–7976 (1988).

69. Cooper, J. A. Effects of cytochalasin and phalloidin on actin. *J. Cell Biol.* **105**, 1473–1478 (1987).

70. Whitesell, L., Mimnaugh, E. G., De Costa, B., Myers, C. E. & Neckers, L. M. Inhibition of heat shock protein HSP90-pp60v-src heteroprotein complex formation by benzoquinone ansamycins: essential role for stress proteins in oncogenic transformation. *Proc. Natl. Acad. Sci. USA* **91**, 8324–8328 (1994).

71. Nishi, K. *et al.* Leptomycin B targets a regulatory cascade of crm1, a fission yeast nuclear protein, involved in control of higher order chromosome structure and gene expression. *J. Biol. Chem.* **269**, 6320–6324 (1994).

72. Vlahos, C. J., Matter, W. F., Hui, K. Y. & Brown, R. F. A specific inhibitor of phosphatidylinositol 3-kinase, 2-(4-morpholinyl)-8-phenyl-4H-1-benzopyran-4-one (LY294002). *J. Biol. Chem.* **269**, 5241–5248 (1994).

73. Endo, A., Kuroda, M. & Tanzawa, K. Competitive inhibition of 3-hydroxy-3-methylglutaryl coenzyme A reductase by ML-236A and ML-236B fungal metabolites, having hypocholesterolemic activity. *FEBS Lett.* **72**, 323–326 (1976).

74. Lee, D. H. & Goldberg, A. L. Proteasome inhibitors: valuable new tools for cell biologists. *Trends Cell Biol.* **8**, 397–403 (1998).

75. Woszczek, G. *et al.* Functional characterization of human cysteinyl leukotriene 1 receptor gene structure. *J. Immunol.* **175**, 5152–5159 (2005).

76. Ford-Hutchinson, A. W. FLAP: a novel drug target for inhibiting the synthesis of leukotrienes. *Trends Pharmacol. Sci.* **12**, 68–70 (1991).

77. Bialojan, C. & Takai, A. Inhibitory effect of a marine-sponge toxin, okadaic acid, on protein phosphatases. Specificity and kinetics. *Biochem. J.* **256**, 283–290 (1988).

78. Schiff, P. B. & Horwitz, S. B. Taxol stabilizes microtubules in mouse fibroblast cells. *Proc. Natl. Acad. Sci. USA* **77**, 1561–1565 (1980).

79. Kummer, J. L., Rao, P. K. & Heidenreich, K. A. Apoptosis induced by withdrawal of trophic factors is mediated by p38 mitogen-activated protein kinase. *J. Biol. Chem.* **272**, 20490–20494 (1997).

80. Schulte, T. W. *et al.* Antibiotic radicicol binds to the N-terminal domain of Hsp90 and shares important biologic activities with geldanamycin. *Cell Stress Chaperones* **3**, 100–108 (1998).

81. Brown, E. J. *et al.* A mammalian protein targeted by G1-arresting rapamycin-receptor complex. *Nature* **369**, 756–758 (1994).

82. Gould, G. W., Cuenda, A., Thomson, F. J. & Cohen, P. The activation of distinct mitogen-activated protein kinase cascades is required for the stimulation of 2-deoxyglucose uptake by interleukin-1 and insulin-like growth factor-1 in KB cells. *Biochem. J.* **311 ( Pt 3)**, 735–738 (1995).

83. Zhao, B. *et al.* Structural basis for Chk1 inhibition by UCN-01. *J. Biol. Chem.* **277**, 46609–46615 (2002).

84. Coghlan, M. P. *et al.* Selective small molecule inhibitors of glycogen synthase kinase-3 modulate glycogen metabolism and gene transcription. *Chem. Biol.* **7**, 793–803 (2000).

85. Han, Z. *et al.* c-Jun N-terminal kinase is required for metalloproteinase expression and joint destruction in inflammatory arthritis. *J. Clin. Invest.* **108**, 73–81 (2001).

86. Thastrup, O., Foder, B. & Scharff, O. The calcium mobilizing tumor promoting agent, thapsigargin elevates the platelet cytoplasmic free calcium concentration to a higher steady state level. A possible mechanism of action for the tumor promotion. *Biochem. Biophys. Res. Commun.* **142**, 654–660 (1987).

87. Yoshida, M., Kijima, M., Akita, M. & Beppu, T. Potent and specific inhibition of mammalian histone deacetylase both in vivo and in vitro by trichostatin A. *J. Biol. Chem.* **265**, 17174–17179 (1990).

88. Takatsuki, A., Arima, K. & Tamura, G. Tunicamycin, a new antibiotic. I. Isolation and characterization of tunicamycin. *J. Antibiot.* **24**, 215–223 (1971).

89. DeSilva, D. R. *et al.* Inhibition of mitogen-activated protein kinase kinase blocks T cell proliferation but does not induce or prevent anergy. *J. Immunol.* **160**, 4175–4181 (1998).

90. Kobayashi, H. *et al.* Involvement of 14-3-3 proteins in the second epidermal growth factor-induced wave of Rac1 activation in the process of cell migration. *J. Biol. Chem.* **286**, 39259–39268 (2011).

91. Owellen, R. J., Owens, A. H. & Donigian, D. W. The binding of vincristine, vinblastine and colchicine to tubulin. *Biochem. Biophys. Res. Commun.* **47**, 685–691 (1972).

92. Arcaro, A. & Wymann, M. P. Wortmannin is a potent phosphatidylinositol 3-kinase inhibitor: the role of phosphatidylinositol 3,4,5-trisphosphate in neutrophil responses. *Biochem. J.* **296 ( Pt 2)**, 297–301 (1993).

93. Sasazawa, Y. *et al.* Xanthohumol impairs autophagosome maturation through direct inhibition of valosin-containing protein. *ACS Chem. Biol.* (2012).

94. Uehata, M. *et al.* Calcium sensitization of smooth muscle mediated by a Rho-associated protein kinase in hypertension. *Nature* **389**, 990–994 (1997).

95. Scherf, U. *et al.* A gene expression database for the molecular pharmacology of cancer. *Nat. Genet.* **24**, 236–244 (2000).

96. Nakatsu, N. *et al.* Chemosensitivity profile of cancer cell lines and identification of genes determining chemosensitivity by an integrated bioinformatical approach using cDNA arrays. *Mol. Cancer Ther.* **4**, 399–412 (2005).

97. Muroi, M. *et al.* Application of proteomic profiling based on 2D-DIGE for classification of compounds according to the mechanism of action. *Chem. Biol.* **17**, 460–470 (2010).

98. Werno, C., Zhou, J. & Brüne, B. A23187, ionomycin and thapsigargin upregulate mRNA of HIF-1alpha via endoplasmic reticulum stress rather than a rise in intracellular calcium. *J. Cell Physiol.* **215**, 708–714 (2008).

99. Yamazaki, M., Chiba, K. & Yoshikawa, C. Genipin suppresses A23187-induced cytotoxicity in neuro2a cells. *Biol. Pharm. Bull.* **32**, 1043–1046 (2009).

100. Huang, C., Jacobson, K. & Schaller, M. D. A role for JNK-paxillin signaling in cell migration. *Cell Cycle* **3**, 4–6 (2004).

101. Sun, Y., Yang, T. & Xu, Z. The JNK pathway and neuronal migration. *J. Genet. Genomics* **34**, 957–965 (2007).

102. Ching, Y. P. *et al.* P21-activated protein kinase is overexpressed in hepatocellular carcinoma and enhances cancer metastasis involving c-Jun NH2-terminal kinase activation and paxillin phosphorylation. *Cancer Res.* **67**, 3601–3608 (2007).

103. Wang, J. *et al.* Sustained c-Jun-NH2-kinase activity promotes epithelial-mesenchymal transition, invasion, and survival of breast cancer cells by regulating extracellular signal-regulated kinase activation. *Mol. Cancer Res.* **8**, 266–277 (2010).

104. Pollard, T. D. & Borisy, G. G. Cellular motility driven by assembly and disassembly of actin filaments. *Cell* **112**, 453–465 (2003).

105. Jiang, W. *et al.* p190A RhoGAP is a glycogen synthase kinase-3-beta substrate required for polarized cell migration. *J. Biol. Chem.* **283**, 20978–20988 (2008).

106. Harwood, A. J. Signal transduction in development: holding the key. *Dev. Cell* **2**, 384–385 (2002).

107. Magi, S., Tashiro, E. & Imoto, M. A chemical genomic study identifying diversity in cell migration signaling in cancer cells. *Sci. Rep.* **2**, 823 (2012).

108. Balciunaite, E., Jones, S., Toker, A. & Kazlauskas, A. PDGF initiates two distinct phases of protein kinase C activity that make unequal contributions to the G0 to S transition. *Curr. Biol.* **10**, 261–267 (2000).

109. Nagashima, T. *et al.* Quantitative transcriptional control of ErbB receptor signaling undergoes graded to biphasic response for cell differentiation. *J. Biol. Chem.* **282**, 4045–4056 (2007).

110. Chen, J.-Y., Lin, J.-R., Cimprich, K. A. & Meyer, T. A two-dimensional ERK-AKT signaling code for an NGF-triggered cell-fate decision. *Mol. Cell* **45**, 196–209 (2012).

111. Goldenberg, I. H. & Rabinowitz, M. Actionmycin D inhibition of deoxyribonucleic acid-dependent synthesis of ribonucleic acid. *Science* **136**, 315–316 (1962).

112. Pestka, S. Inhibitors of ribosome functions. *Annu. Rev. Microbiol.* **25**, 487–562 (1971).

113. Katz, M., Amit, I. & Yarden, Y. Regulation of MAPKs by growth factors and receptor tyrosine kinases. *Biochim. Biophys. Acta.* **1773**, 1161–1176 (2007).

114. Kurten, R. C. Sorting motifs in receptor trafficking. *Adv. Drug Deliv. Rev.* **55**, 1405–1419 (2003).

115. Dikic, I. Mechanisms controlling EGF receptor endocytosis and degradation. *Biochem. Soc. Trans.* **31**, 1178–1181 (2003).

116. Visser Smit, G. D. *et al.* Cbl controls EGFR fate by regulating early endosome fusion. *Sci. Signal.* **2**, ra86 (2009).

117. Ishikawa, K., Nara, A., Matsumoto, K. & Hanafusa, H. EGFR-dependent phosphorylation of leucine-rich repeat kinase LRRK1 is important for proper endosomal trafficking of EGFR. *Mol. Biol. Cell* **23**, 1294–1306 (2012).

118. Pece, S., Chiariello, M., Murga, C. & Gutkind, J. S. Activation of the protein kinase Akt/PKB by the formation of E-cadherin-mediated cell-cell junctions. Evidence for the association of phosphatidylinositol 3-kinase with the E-cadherin adhesion complex. *J. Biol. Chem.* **274**, 19347–19351 (1999).

119. Kovacs, E. M., Ali, R. G., McCormack, A. J. & Yap, A. S. E-cadherin homophilic ligation directly signals through Rac and phosphatidylinositol 3-kinase to regulate adhesive contacts. *J. Biol. Chem.* **277**, 6708–6718 (2002).

120. Gavard, J. *et al.* Lamellipodium extension and cadherin adhesion: two cell responses to cadherin activation relying on distinct signalling pathways. *J. Cell Sci.* **117**, 257–270 (2004).

121. Kraemer, A., Goodwin, M., Verma, S., Yap, A. S. & Ali, R. G. Rac is a dominant regulator of cadherin-directed actin assembly that is activated by adhesive ligation independently of Tiam1. *Am. J. Physiol., Cell Physiol.* **292**, C1061–9 (2007).

122. Carlson, S. M. & White, F. M. Using small molecules and chemical genetics to interrogate signaling networks. *ACS Chem. Biol.* **6**, 75–85 (2011).

# Acknowledgement

本研究は慶應義塾大学理工学部教授 井本正哉博士のご指導の下行いました。終始親身に熱く御指導御高配賜りましたこと、研究者としての生き様を示して頂きましたことに謹んで感謝の意を表します。

また、本研究を遂行するにあたり、多くの御指導、御助言を頂きました慶應義塾大学理工学部専任講師 田代悦博士に深く感謝の意を表します。

本論文の執筆にあたり、御指導、御助言を頂きました慶應義塾大学理工学部教授 佐藤智典博士、慶應義塾大学理工学部教授 榊原康文博士、慶應義塾大学理工学部准教授 舟橋啓博士に厚く御礼申し上げます。

本研究に際し多くの御教示賜りました慶應義塾大学理工学部生命情報学科の全ての先生方に深く感謝致します。先生方の御講義や直接の御指導によって、実験生物学と情報生物学を組み合わせる研究の大切さと難しさを学んだことを感謝致します。

Aclacinomycin A およびその類縁体を合成して頂きました微生物化学研究所 設楽哲夫博士および高橋良和博士に深く御礼申し上げます。

本研究で使用した FTase 阻害剤の探索源および標準阻害剤キットは、癌研究会 矢守隆夫博士および微生物化学研究所 川田学博士をはじめ、文部科学省新学術領域研究『がん研究の特性等を踏まえた支援活動』 化学療法基盤支援活動班 （旧 文部科学省がん研究に係わる特定領域研究・統合がん 化学療法基盤情報支援班）の先生方から御供与頂きました。厚く御礼申し上げます。

UTKO1 を御供与頂きました東京大学大学院農学生命科学研究科教授 渡邉秀典博士に感謝の意を表します。

Leptomycin B および Trichostatin A を御供与頂きました理化学研究所 吉田稔博士に感謝の意を表します。

本研究を行うにあたり、終始一から親身の御指導、御鞭撻により研究を導いて頂きました慶應義塾大学理工学部ケミカルバイオロジー研究室（旧応用細胞生物学研究室）卒業生、理化学研究所吉田化学遺伝学研究室博士研究員 竹本靖博士および名古屋市立大学大学院医学研究科再生医学分野博士研究員 澤田雅人博士に深く御礼申し上げます。御指導頂いた学部生の間の濃密な一年間の中で、お二方の勤勉さ、きめ細かい実験計画、サイエンスに対する哲学の全てに感銘を受けました。研究者として最高のスタート地点をお二方の親身な御指導によって作って頂いたことを感謝致します。

本研究を行うにあたり、多くの御助言を頂きましたケミカルバイオロジー研究室卒業生、理化学研究所吉田化学遺伝学研究室博士研究員 小林大貴博士に深く御礼申し上げます。細かい実験やパソコンに関する技術から研究に対する心構え、後輩を指導する姿勢に至るまで、学部生時代から博士課程の間まで長きに渡り手本となり御指導頂けたことが今の私を支える大きな柱となっていることを感謝致します。

ケミカルシステムバイオロジーの研究に際し、ケミカルバイオロジー研究室 佐伯雄也君に 3 年間に渡りご協力頂きました。心より感謝致します。彼を指導し、共に研究をしてこれた経験は研究者としての私を大きく成長させたと感じています。

本研究室の研究生活の中で言わば「博士課程時代の第二の同期」として様々な場面で苦労を共にし、支えあってきたケミカルバイオロジー研究室 藤巻貴宏君に御礼申し上げます。

また、特別研究員奨励費の管理や旅費の手続きなど様々な面でサポートして頂いたケミカルバイオロジー研究室秘書 梅崎秀香さんに厚く御礼申し上げます。

学部修士時代の研究室生活の苦楽を共にした同期の揖場郷君、小田一成君、白川峰征君、高野圭君、三澤茉由子君に感謝申し上げます。また、ケミカルバイオロジー研究室の諸先輩方ならびに卒業生の皆様、加藤直裕君、笠松誠人君、重倉桃子君をはじめ後輩の皆様に感謝致します。

また、本研究を発表した学会および研究会で出会い、議論し、酒を酌み交わす中で刺激を受けた全ての方々に感謝致します。現在も各々の学術研究や仕事の世界で頑張っているモチベーションの高い友人たちに良い刺激を受けたことを感謝します。特に開成高校時代の同級生には、「腐っても開成卒」というプライドを会う度に呼び起こしてもらったことを感謝します。肉体的にも精神的にも厳しかった博士課程３年の最後の時期に気兼ねなくテニスに誘ってくれた慶應義塾大学理工学部天然物合成化学研究室 外山智久君をはじめ、SLC ソフトテニス部の後輩たちに感謝します。

特別研究員として３年間採用して頂きました日本学術振興会に感謝の意を表します。育英奨学生として奨学金を賜りました慶應工学会に感謝の意を表します。研究員として半年間雇用して頂きました慶應義塾大学の文部科学省グローバル COE プログラム「*In vivo* ヒト代謝システム生物学拠点」に感謝の意を表します。国際学会発表の際に旅費および滞在費を支援して頂きました東京大学の文部科学省グローバル COE プログラム「ゲノム情報ビッグバンから読み解く生命圏」に感謝の意を表します。

最後に、私の研究生活を暖かく見守り、どんな時も常に私の味方となって背中を押してくれた家族に心より感謝致します。